2009

Effect of Thermal Treatment on Tensile Properties of a Vacuum Die Cast Hypoeutectic Al-Si Alloy

Kazi Ahmmed
University of Windsor

EFFECT OF THERMAL TREATMENT ON TENSILE PROPERTIES OF A VACUUM DIE CAST HYPOEUTECTIC Al-Si ALLOY

By
Kazi Foyez Ahmmed

A Thesis
Submitted to the Faculty of Graduate Studies
Through the Department of Mechanical, Automotive and Materials Engineering in Partial Fulfillment of the Requirements for the Degree of Master of Applied Science at the University of Windsor

Windsor, Ontario, Canada
2009

AUTHOR'S DECLARATION OF ORIGINALITY

I hereby certify that I am the sole author of this thesis and that no part of this thesis has been published or submitted for publication.

I certify that, to the best of my knowledge, my thesis does not infringe upon anyone's copyright nor violate any proprietary rights and that any ideas, techniques, quotations, or any other material from the work of other people included in my thesis, published or otherwise, are fully acknowledged in accordance with the standard referencing practices. Furthermore, to the extent that I have included copyrighted material that surpasses the bounds of fair dealing within the meaning of the Canada Copyright Act, I certify that I have obtained a written permission from the copyright owner(s) to include such material(s) in my thesis and have included copies of such copyright clearances to my appendix.

I declare that this is a true copy of my thesis, including any final revisions, as approved by my thesis committee and the Graduate Studies office, and that this thesis has not been submitted for a higher degree to any other University or Institution.

ABSTRACT

Vacuum assisted high pressure die casting processes appear to gain popularity in automotive industry. A number of thermal treatment schemes have been experimented in an effort to understand the effect of thermal treatment on tensile properties of vacuum die cast modified AA365 alloy. The results of tensile testing indicate that, high temperature treatments have an observable effect on tensile properties. The average ultimate tensile strength of about 286 MPa is achieved at 200˚C thermal treatment for 90 minutes. However, the ductility has reduced to 7.8% from 10.7% in as-cast condition. The morphology of eutectic silicon and magnesium-based phase has sound effect on the tensile properties of the tested alloy. The reduction in the strengths of the alloy treated at 350˚C for 120 minutes should be at least attributed partly to the absence of the magnesium-based phase and change of eutectic Si morphology.

To
My Parents
Kazi Kalim Ullah
And
Fatema Begum

ACKNOWLEDGEMENTS

The author wish to express his sincere gratitude to Dr.H.Hu for his diligent supervision, patience and guidance throughout the study at the University of Windsor.

He would also like to thanks Dr.X.Nie and Dr. T.Bolisetti for being the committee members and for their valuable suggestions to improve this research work and finally make it to much more meaningful.

Special thanks goes to Mr.P.Seguin, Mr.A.Jenner, Mr.J.Robinson and all the members of the technical support center for their precious technical assistance. He is also grateful to Dr. L.Han, Q.Zhang, J.Burns and S.Bhowmick for their informative directions and suggestions.

Finally the authors expressed his acknowledgements to Ryobi Die Casting (USA) Inc. for supplying the die casting components to run this research work successfully. Specially thanks to Mr. Yeou-li Chu and Mr.Patrick Cheng for their great suggestions and information regarding this research work.

TABLE OF CONTENTS

LIST OF FIGURES

Figure **Page No.**

LIST OF TABLES

Chapter-I
Introduction

1.1 Background

Aluminum alloys with silicon as a major alloying element consist of a class of alloys, which provides the most significant part of all shaped casting manufactured, especially in the aerospace and automotive industries. This is mainly due to the outstanding effect of silicon in the improvement of casting characteristics, combined with other physical properties, such as mechanical properties and corrosion resistance. Casting processes are among the oldest methods for manufacturing metal goods. Aluminum based products are successfully cast in any kind of casting process. Silicon facilitate aluminum alloy with different casting process. In general, an optimum range of silicon content can be assigned to casting process. For slow cooling rate processes (sand, plaster, investment) the range is 5-7 wt%, for permanent moulds 7-9% and for die castings 8-12%. Advances in die casting technology, especially the development of the cold chamber die casting process and improvement in die materials have made the die casting process the most commonly used method for producing aluminum castings.

Among all die casting process, high-pressure die casting (HPDC) is a popular and cost-effective method for massively producing metal components where physical dimensions must be accurately replicated and surface finish is important. Approximately half of all castings worldwide that are made from aluminum alloys are manufactured by HPDC processes. They are used for a wide range of automotive parts and other consumer goods.

Although in HPDC process, high velocity allows for the production of thin-walled castings, the associated turbulent conditions remain the major source of interior and surface casting defects, which may have deleterious effects on the mechanical properties. Because of this, castings usually contain internal pores in which gases, such as air, hydrogen or vapours formed by the decomposition of organic die wall lubricants are entrapped. The formation of porosity may also result from metal shrinkage during solidification. Defect-containing regions in a tensile sample reduce the load-bearing area and, therefore, produce a concentration of the strain.

Whereas it is normal to accept some level of porosity in die-castings, the presence of internal gas-filled pores does have the major disadvantage that components made from aluminum alloys which have the capacity to respond to age hardening cannot be heat treated at high temperatures. Heat treatment cannot be used because, during solution treatment (e.g., 8 h at 540˚C), gas pressure in the pores causes them to expand, resulting in unacceptable surface blistering. Moreover, the dimensions of die-cast parts may change due to swelling, and mechanical properties are adversely affected. It was found that the volume of gas porosity and the pore sizes in the castings were significantly reduced by using vacuum assistance during die casting. As a result, the density and the mechanical properties, particularly the tensile strength and ductility, were improved markedly. An optimum injection speed was also identified for producing high performance castings. However, with vacuum assistance system it is not always possible to eliminate the possibility of air entrapment on casting, especially when a high velocity is incorporate into the system to fill very thin area of casting. Therefore, high temperature heat treatment may also cause blistering problem with these types of castings.

In Al-Si alloys system, the morphology of silicon has a vital impact on microstructure which in turns affect on their mechanical properties. Strontium modification facilitates the microstructure to change the morphology of silicon from needle-like form to globular shape. Moreover, high pressure die casting with assistance of vacuum provides relatively homogenous microstructure due to severe chill rate and ultra-fine grain size in die castings. Low silicon, strontium modified pro-eutectic aluminum alloy offers a homogenous microstructure with an acceptable morphology of silicon in HPDC process. Thus, they become increasingly promising in automotive sectors recently. Their "as-cast" structure approaches that of the solution heat-treated condition. Therefore a low temperature heat treatment like T4 and T5 temper results in properties quite similar to those which might be obtained if given a full T6 temper [1].

Although a vacuum assistance system can facilitate the casting to somewhat reduce gas porosity, die castings are usually made of complex irregular shapes and cooling of these sections is often uneven. Additionally, due to the high degree of restraint imposed by the die, die castings may be ejected with residual stresses, a key factor that plays a major role in post-ejection casting distortion. Residual stress often arises due to these reasons and creates a negative impact on dimensional stability during machining. To release residual stresses it is essential to apply a thermal treatment to as-cast components. However, studies on effect of thermal treatments for residual stress relief on the variation of microstructure and tensile properties are limited in the open literature. In the present study a low silicon, strontium-modified pro-eutectic aluminum alloy was prepared by a vacuum high pressure die casting process. A number of thermal treatment schemes for the as-cast alloy over a wide range of temperatures between 120˚C to 350˚C have been experimented in an effort to optimize the properties.

For understanding their strengthening mechanisms, the microstructure of the treated alloys were analyzed. The outcome of the present work is expected to enhance the current knowledge of the HPDC aluminum-silicon alloys and provides novel information for optimizing their component design.

1.2 Thesis Layout

This thesis is a partial fulfillment of the requirement for the degree of Masters of Applied Science. It is divided into six chapters. Chapter 1 presents a general background conducted in this study as an introduction with vacuum assistance high pressure die casting process applied in low silicon content and modified AA-365 alloy. The necessity of low temperature heat treatment rather than high temperature heat treatment has also included in this introductory chapter.

Chapter 2 represents a comprehensive description on vacuum assistance high pressure die casting system under several literature surveys, where it was shown the superiority of vacuum assisted HPDC system over conventional die casting processes was shown. The fundamental classification of Al-Si alloy is also described. Moreover, the advantages of heat treatments on die cast components are discussed.

Chapter 3 outlines the methodology of the overall experiments. A systematic experimental procedure is described for evaluation of mechanical properties and microstructural characterization.

In chapter 4 the effect of thermal treatment at different temperatures and times is presented. Mechanical properties are evaluated at the corresponding temperatures and times. Moreover, microstructures at different heat treating conditions were analyzed with

the optical and scanning electron microscopy. The establishment of the relation between the properties and microstructure is attempted.

Finally the conclusions of this study are summarized in chapter five and the future work is proposed in chapter 6.

CHAPTER-II

Literature Review

2.1 Economical Importance of Aluminum-Silicon Die Casting Alloys

Al-Si alloys are some of the most widely used alloys for cast domestic, military, automotive and aerospace components. The use of aluminum components in the automotive industry has increased considerably during the past ten years due to their lightweight and reduced fuel energy consumption advantages. Another advantage, which is equally important from an environmental point of view, is the fact that aluminum components may be recycled at relatively low energy costs. Among aluminum alloys, aluminum-silicon (Al-Si) alloys are known for their good castability, resistance to hot tearing, reasonable mechanical properties and excellent corrosion resistance. In addition, as silicon increases in volume during solidification, the susceptibility of casting to shrinkage defects is reduced. The addition of Mg, Cu, and Zn makes the alloys heat-treatable, providing the means to enhance their properties with the use of appropriate heat treatments. The increasing demands for light weight components with uniform properties necessary for mass production of parts for the transportation, construction and electronics industries and also the excellent die casting characteristics of aluminum alloys has made the die casting process the predominant method for producing aluminum alloy castings, which is reflected in the tonnage of die castings produced in the United States and Japan in recent years. In 1992, Japan produced 63.5% of its total aluminum alloy castings via the die casting

process [2]. Moreover, among all the various different alloys that may be die cast such as magnesium and zinc, the production tonnage of the aluminum alloys are the highest ones. In 1992, 367,000 t of Aluminum were die cast in the United States, in contrast with only 16,700 t of Magnesium and 106,000 t of Zinc [2]. In 1994, the shipments of aluminum die castings in the United States reached 984, 000 t, which represented about 58% of the total shipments of aluminum alloy castings [3]. In 2001, the value of U.S. shipments of aluminum die castings totalled $3.8 billion [4]. And in 2006, the demand of aluminum casting in US was 2.6 million tons. Among them, 1.5 million tons was made by high pressure die casting [5].

2.2 Possible Reasons for Al-Si Alloys Suitability

The most attractive reasons for which Al-Si alloys are widely used due to its inexpensiveness and availability. The silicon phase can also form with different morphologies, e.g. rod, flake, fibre and therefore depending upon solidification conditions and impurity elements such as sodium, strontium or phosphorous a range of properties can in theory be achieved from a specific alloy composition [6]. The mechanical properties of an Al-Si cast alloy are mainly characteristics such as the grain size, dendrite arm spacing (DAS), the size, shape and distribution of the eutectic silicon particles, as well as the morphologies and amounts of intermetallic phases present. Moreover the level of aluminum dendrites in hypoeutectic Al-Si alloys is consequently dependant on solidification parameters like cooling rate, casting process etc., and its control can improve mechanical properties of the finished products. The presence of impurity and alloying elements, such as Fe, Mn, Cu, Zn and Mg creates more complications in microstructure of Al-Si alloys due to the formation different inter

metallic phases [7]. Each impurity element in combination with others may promote the formation of a particular inter metallic micro constituent provided that its relative concentration is compatible with the expected inter metallic compound [8]. All these variables (amount of silicon, DAS, amounts of alloying elements, amounts of intermetallic phases and casting process) cause significant change after proper heat treatment, which, in turn, influences the resultant mechanical properties.

2.3 Classification of Aluminum Alloys

According to the classifications used by the industry in general and specifically the Aluminum Association of the United States, there is a distinction between wrought alloys and foundry alloys. Wrought alloys are those obtained by working on ingots of particular forms. This work can be affected by rolling, extruding, drawing or forging. Foundry alloys are those for which the ingots are melted and poured into mould having the shape of the final product. The main difference between the two classes of alloys lies in the elements added to the aluminum base. In foundry alloys, the elements are usually present in more important quantities, primarily to facilitate the casting process.

2.3.1 Alloy Designation of Foundry Alloy

In the classification used by the Aluminum association of the United states for wrought alloy in the 1× ×.× Series, the second and third number indicate the purity of the aluminum. Thus 150.× signifies at least 99.5% of aluminum [9].

Table 2-1 Alloy designation of Aluminum Alloys [9]

Major Aluminum Alloys	Wrought Alloys	Cast Alloys
Aluminum	1XX.1	1XX.0
Aluminum-Copper	2XX.1	2XX.0
Aluminum-Manganese	3XX.1	
Aluminum-Silicon	4XX.1	4XX.0
Aluminum-Magnesium	5XX.1	5XX.0
Aluminum-Magnesium & Silicon	6XX.1	6XX.0
Aluminum-Zinc	7XX.1	7XX.0
Aluminum-Lithium	8XX.1	
Unused		9XX.0

The last digit, after the decimal point, indicates the form of the product: 0 for a cast part and 1 for an ingot.

2.3.2 Aluminum Heat-Treatable Alloys

Heat-treatable alloys are alloys that can achieve higher strength by heat-treatment. Alloys in this group contain one or more elements chosen to give higher strength by precipitation hardening (age hardening). Of the above, aluminium alloys, the most commonly used ones use copper, magnesium and silicon, or zinc. Copper is used because of its high strength, relatively low corrosion resistance, and excellent machinability and heat treatability. The combination of magnesium and silicon is the most popular extrusion alloy, due to its good extrudability, strength, corrosion resistance,

machinability, weldability, formability, and heat treatability. Zinc is used because of its very high strength, good machinability, and heat treatability.

Table 2.2 Heat Treatable Aluminum Alloys [10]

Major Alloying Element	Wrought Alloys	Cast Alloys	Characteristics
Copper	2XXX	2XX.0	High strength-to-weight ratio, low corrosion resistance, heat treatable
Magnesium & Silicon	6XXX	6XX.0	Medium strength; good formability, machinability, and weldability
Zinc	7XXX	7XX.0	Moderate to very high strength, heat treatable, prone to fatigue

A product's performance is determined by the composition and heat treatment approach that is selected to produce the alloy.

2.4 Aluminum-Silicon System

Aluminum-Silicon alloys are popular for their unique combination of desirable characteristics including excellent castability, low density and good mechanical properties. They are one of the dominant groups of aluminum foundry alloys. In general,

Aluminum alloys with 5-20% silicon are in common use. The characteristic feature of these alloys is that they consist of a primary phase, aluminum or silicon and a eutectic mixture of these two elements [11]. Depending on the purity of the base material, the Al-Si alloys contain varying amount of impurity elements like iron, manganese, copper and zinc. Also, copper and magnesium are often added as alloying elements to increase the strength and hardenability of the materials being cast. The impurities and alloying elements partly go into solid solution in the matrix and partly form inter-metallic particles during the solidification process [12]. The eutectic composition is close to 12% Si. Below this concentration (Hypoeutectic alloys), aluminum precipitates from the liquid as the primary phase in the form of dendrites; above this concentration (Hypereutectic alloys) primary silicon particles form from the liquid upon cooling (Figure 2.1) [11].

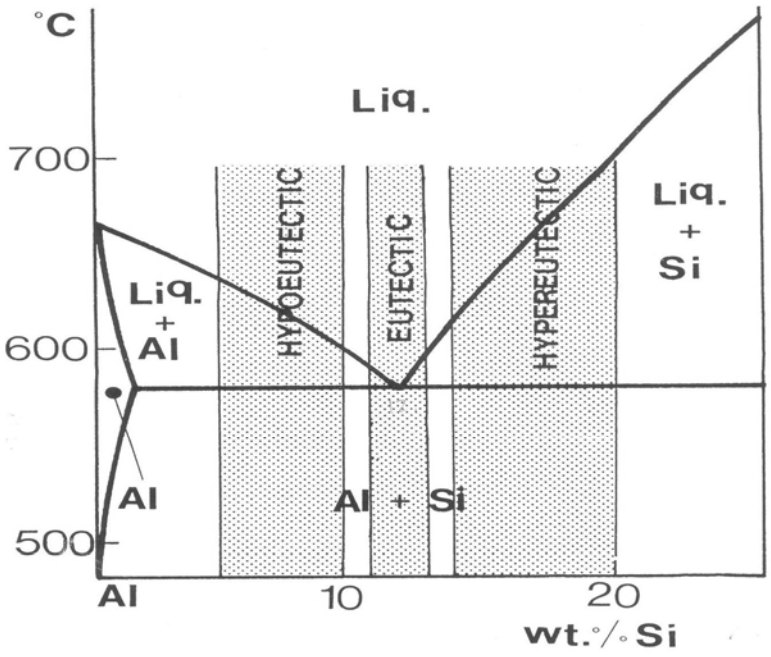

Figure 2.1 Part of the Al-Si phase diagram showing composition ranges of various alloy types [11].

The solubility of silicon in aluminum reaches a maximum 1.5% at the eutectic temperature, and the solubility of silicon decreases to 0.05 at % at 300°C. The only invariant reaction in the system, other than the melting of pure Al and pure Si, is a eutectic transformation of liquid solution to solid solution Al and nearly pure Si [11], namely:

$$L \longrightarrow Al_{eut} + Si_{eut}$$

It is widely accepted that this eutectic reaction occurs at 577.6°C and at 12.6% silicon. However it has recently been shown by Cantor and coworkers et al. [13-16] that binary Al-Si alloys prepared from pure materials (99.999% purity Al and 99.9999% purity Si) can have up to 50 ppm iron. This level of iron is normally considered a trace level impurity of little consequence but experimentally proved it has significant role in the formation of the Al-Si eutectic**.** It can be seen that iron, except when present in exceedingly low amounts (0.0015%), results in the formation of iron containing β-(Al, Si, Fe) phase that plays an important role in the nucleation of the eutectic phases. Therefore the system should be considered as essentially an Al-Si-Fe system rather than binary Al-Si system [12].

Table 2- 3 Typical levels of iron in "high-purity" Al-Si alloys [12]

Purity of Al-Si alloy (wt %)	**Fe (wt %)**
99.99	0.0050
99.999	0.0025-0.0030
99.9999	≤0.0015

Hypoeutectic alloys usually follow the following main sequence of phase precipitation:

1. Dendritic network of α-Al formation.
2. Eutectic reaction among Aluminum and Silicon and
3. Other secondary eutectic phase like Mg_2Si and Al_2Cu formation (Depending upon the alloy contents).

A eutectic alloy doesn't show the pre-eutectic reactions and in hyper-eutectic alloys, the primary reaction involves precipitation of silicon particles until the eutectic composition is reached.

Moreover precipitations of iron and manganese-containing phases will also take place as well as with the main reactions. The most common of such phase in foundry alloys are Al_5FeSi and $Al_{15}(Mn, Fe)_3Si_2$ and at the end of the solidification process Mg_2Si, Al_2Cu and other more complex phases will precipitate from the remaining liquid [11].

2.4.1. Primary Silicon Refinement

The number and size of primary silicon particles in hypereutectic alloys can be controlled by the addition of particles that facilitate the nucleation of silicon crystals. AlP (Aluminum phosphide) which is naturally present in the most aluminum-silicon alloys is one of the most efficient substrates on which silicon may nucleate. Additional amount of phosphorus may be introduced into the melt before casting for further improve the nucleating effect which in increase the number of AlP particles [11].

2.4.2 Modification of Eutectic Silicon

Silicon crystals in the eutectic mixture grow in faceted manner in Al-Si alloy which is shown in below (Figure 2.2):

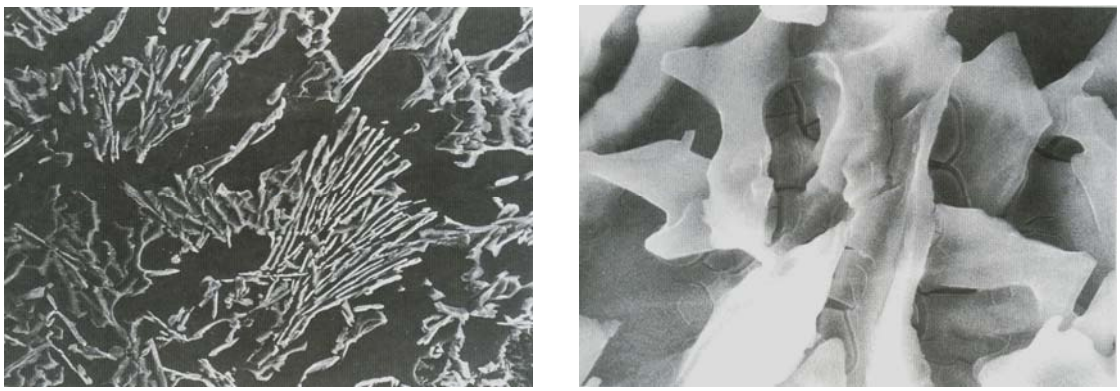

(a) (b)

Figure 2.2 Silicon crystals in an unmodified sample of alloy 356 (SEM pictures after deep etching): a) at X100; b) at X1000 [11].

The growth of the silicon is favoured in certain crystallographic directions and some twin planes (Figure 2.3) forms “re-entrant edges” which promotes the effective growth.

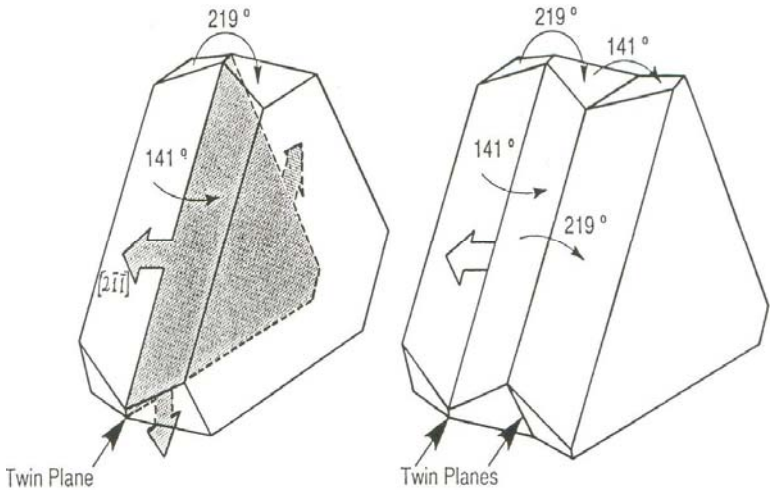

Figure 2.3 Location of twin planes and re-entrant edge in a silicon crystal [11].

Silicon crystals, in directional solidification develop ahead of the aluminum phase and the morphology of the silicon crystals looks fan-shaped in metallographic sections (Figure 2.2-b) and they consist of silicon flakes, which seem to grow out from a few nucleation sites. Thus this kind of eutectic structure gives rather poor mechanical properties to the casting and the material becomes brittle [11].

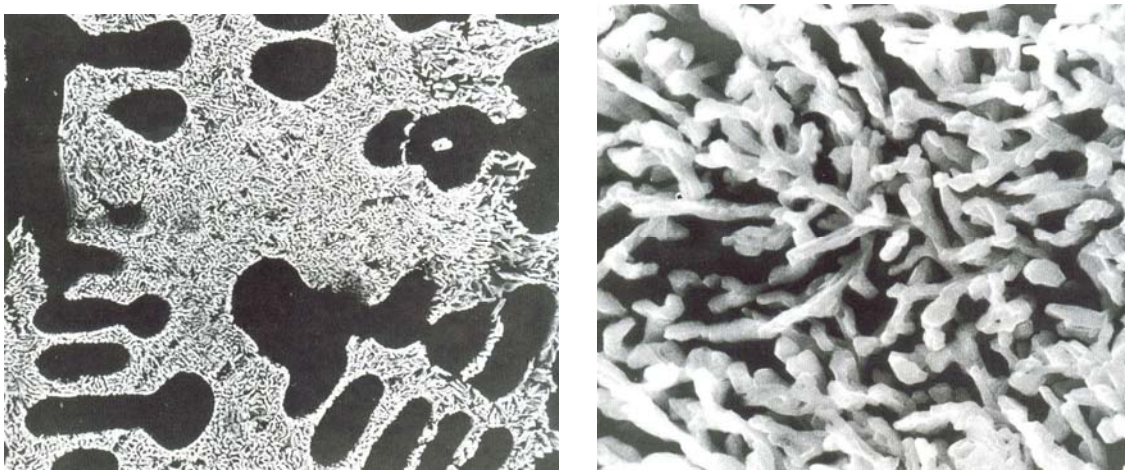

(a) (b)

Figure 2.4 Silicon crystals in a modified sample of alloy 356. SEM pictures after deep etching. Note the seaweed-like morphology, a) X100; b) X1000 [11].

It is experienced that addition of electropositive elements like Na, Ca or Sr will completely change the morphology of the eutectic silicon crystals from large flakes into a fibrous structure resembling a seaweed type of morphology (Figure 2.4.) This morphological change influence on the nucleation and growth process of eutectic silicon and the reaction temperature lowered by around 10˚C, in relation to the untreated material [11].

2.4.3 Addition of Sodium

Sodium is a classical additive to promote the modification of the silicon crystals. They influence the structure in several ways. Mondolfo et al. [17] states that:

1. Sodium forms the compound Na_3P by reacting with phosphorous (presents naturally), which is not a good nucleant for silicon crystals. This makes nucleation much difficult at close to the equilibrium temperatures.
2. Addition of Sodium makes the TPRE (Twin Plane Re-Entrant Edge) growth mechanism almost impossible by poisoning the re-entrant edge growth step in the silicon crystals which hindered the effective growth mechanism and a higher degree of undercooling is needed to drive an alternative growth process.
3. Sodium changes the interfacial surface energy between aluminum and silicon by reducing the surface tension of, which in turn may influence nucleation as well as growth processes.
4. Excess sodium leads to formation of an AlNaSi compound which may nucleate silicon at low degrees of undercooling and thereby counteract the modification process, which is called over modification.
5. Moreover sodium has a high vapour pressure and high affinity to oxygen and thus it readily burns off and its modification efficiency is lost within rather short time.

2.4.4 Modification by Strontium addition

Strontium becomes very popular as an additive for silicon modification in foundry. The effect of Strontium addition was studied [11] by the following manner, a sample of alloy 356 was melted in a resistance furnace and held at 750C for 6 hours to burn off any possible remainders from earlier modifying additions. An untreated sample

was also taken for reference after which an addition of Al 3.5% Sr master alloy in rod form was made to varying Sr. levels in a series of experiments.

For thermal analysis and metallographic examination different time interval, varying from 5 minutes to 6 hours were found in this study [11]. Typical series of curves and corresponding microstructures are shown in Figures 2.5 and 2.6. Only the first part of the eutectic reaction is shown for each sample, the nucleation temperature indicated by a dot (.).

Following features were concluded from the associated study:

1. Strontium addition has lowered the nucleation as well as the growth temperature on the order of 10˚C.
2. After an incubation period (1/2-2 hr), nucleation temperature shows a minimum.
3. When optimum modification is achieved, the evolving curves show a horizontal or slightly declining plateau without previous undercooling (no recalescence).
4. However as soon as a fade in modification is observed, the nucleation and growth temperatures start to increase and a reclascence effect becomes more and more noticeable.

It was also studied that during the time period when the modification effect is optimum, the cooling curves show the following features:

1. A low nucleation temperature, < 565˚C.
2. A growth temperature < 562˚C.
3. Absence of a reclescence function (TG-TMin < 1˚C) [13].

All these criteria seem to be necessary to define a fully modified structure. Moreover it was also experimentally found that the degree of modification does not change markedly between addition levels of 0.005-0.05% Sr. However low additions fade rapidly which is show in Figure 2.5.

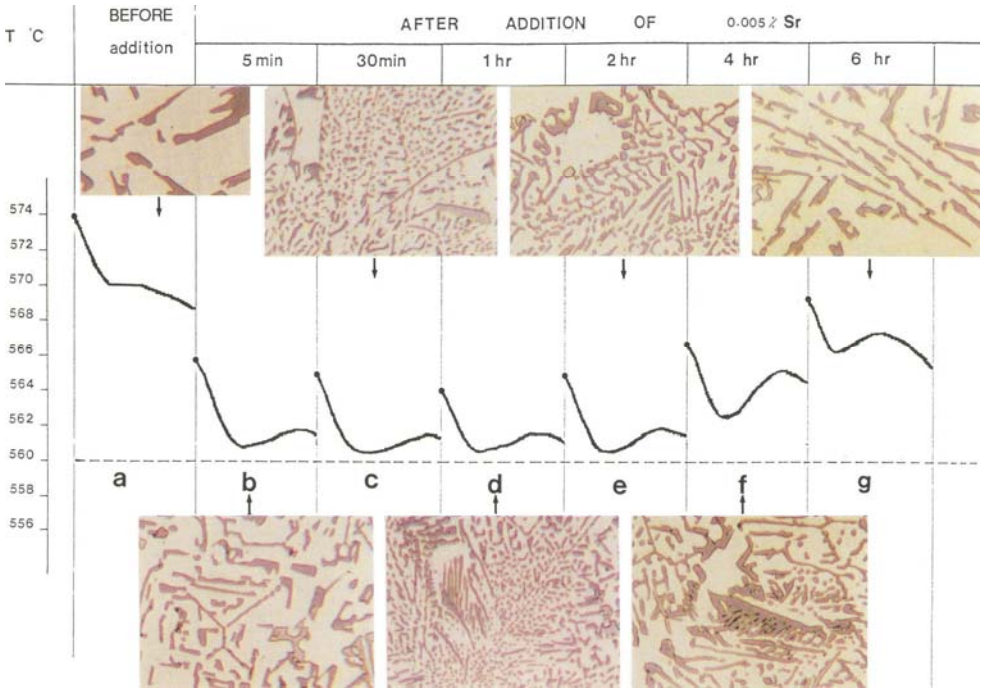

Figure 2.5 Part of cooling curves around the eutectic reaction from a sample of alloy 356 to which 0.005% Sr was added (X560) [11].

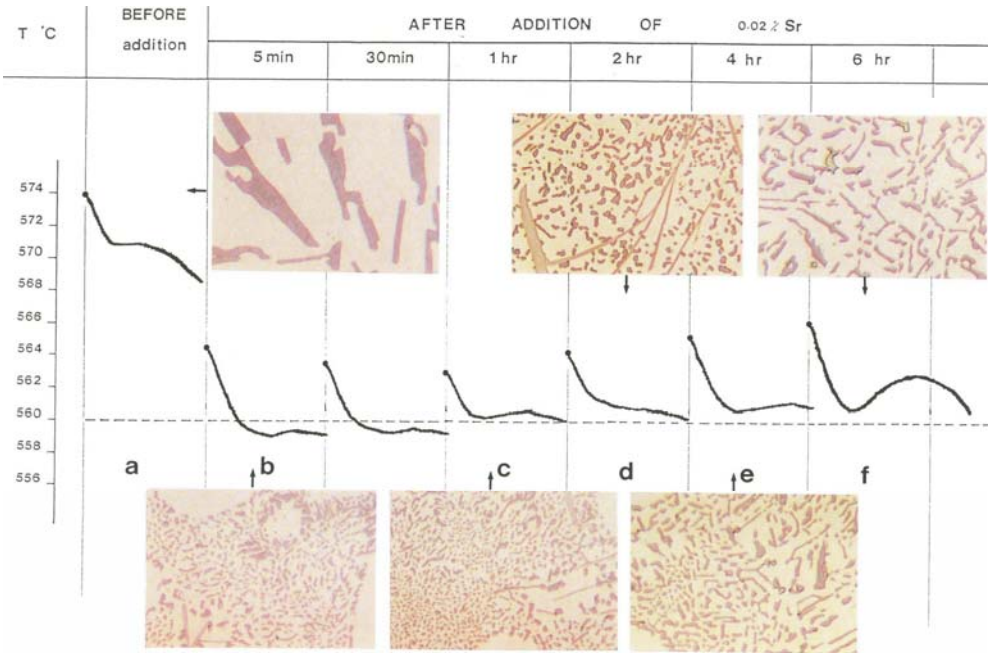

Figure 2.6 Same as Figure 2.5, but with an addition of 0.02% Sr, X560 [11].

2.5 Solidification fundamentals of Al-Si Hypoeutectic Alloys

Understanding the nucleation and growth mechanism together with some knowledge on the kinetics of the phases form during solidification are the key parameters to optimize microstructure of engineering alloys and to ensure superior properties for the as cast-finished products. Eutectic reaction where the morphology of eutectic Si can easily be altered is mostly depends on these factors (nucleation and growth mechanism). Nucleation and growth mechanisms can be manipulated through changes in impurity concentration or kinetics of the eutectic reaction which in turns influence the microstructure as well as the mechanical properties [18]. Evolution of the eutectic structure during their final stages of solidification and hence controls the efficiency of liquid metal feeding into die cavities**.** Feeding efficiency in turn affects on shrinkage,

which may cause porosity and chemical segregation in cast parts. Moreover, upon addition of trace quantities of certain elements, such as Na or Sr, to a hypoeutectic Al-Si alloy, the structure of the eutectic Si phase transforms from a plate-like structure to a fine fibrous (coral-like) structure. All These morphological transformation significantly changes the mechanical properties and overall performance of cast components.

2.5.1 Nucleation Mechanism

In past 80 years much of the fundamental research in the Al-Si alloy system has been directed towards understanding the mechanism and modification of the eutectic Si phase morphology by different trace element additions (Na or Sr). In spite of many hypotheses proposed to explain the modification of the eutectic structure in hypoeutectic Al–Si alloys, the genesis of this factor (nucleation mechanism) technologically remains uncertain which is mainly due to the lack of conclusive evidence. It was believed that the eutectic silicon phase nucleates on the primary aluminum dendrites during solidification of the hypoeutectic alloys which in turn inhibit the growth of the eutectic silicon phase and thus transforming the morphology of the Si phase from plate-like to fibrous [19-20]. Shankar et al. [12]observed that in most of the cases they cannot explain many observed phenomena that are associated with chemical modification, particularly: (1) the relatively large undercooling during solidification that is observed with the evolution of the eutectic phases when modifying elements are present and (2) the occurrence of eutectic modification, and even over modification, without chemical additives, but rather due to an increased superheat and/or a relatively fast solidification rate.

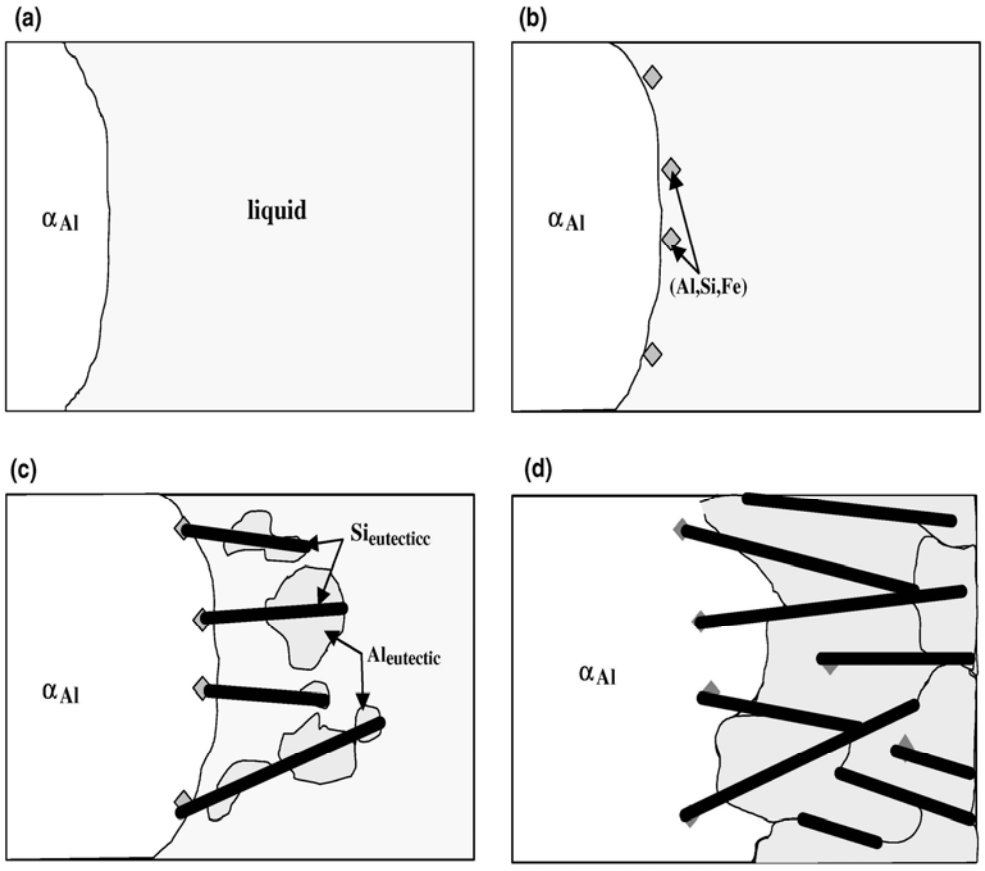

Figure 2.7 Sequence of events during nucleation of eutectic phases in Al–Si hypoeutectic alloy [12].

Shankar et al. [12] proposed that nucleation of the eutectic phases in Al–Si hypoeutectic alloys proceeds as illustrated schematically in Figures 2.7 (a)–(d). From the figure it can be seen that during solidification, the primary aluminum phase forms as dendrites at the liquidus temperature of the alloy which is followed by the evolution of a secondary β-(Al, Si, Fe) phase at some temperature between the liquidus temperature and the eutectic temperature of the alloy depending on the concentration of Fe in the alloy.

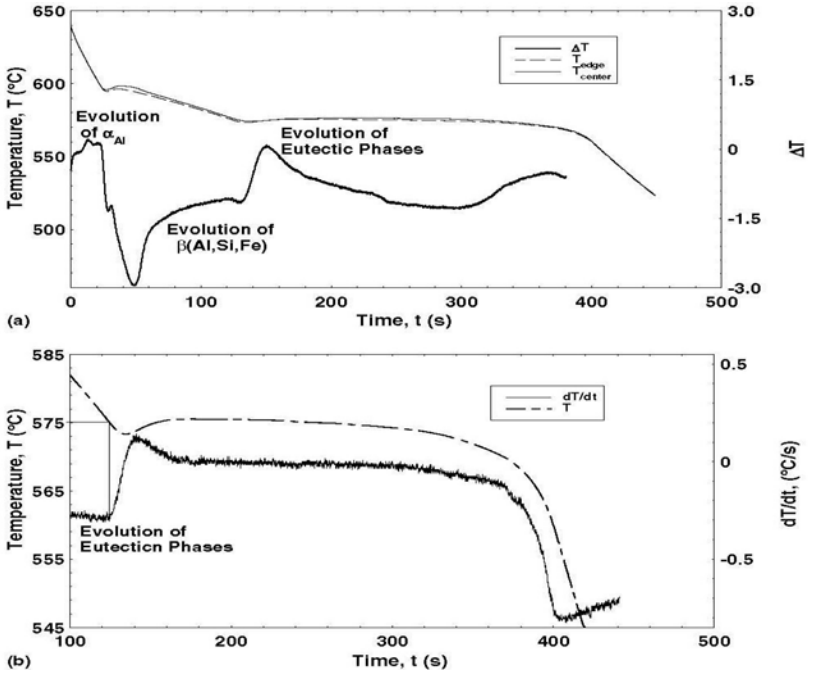

Figure 2.8 Solidification curve a) shows the sequence of phase evolution during solidification. b) is a "zoom in" on (a) with ðT/ðt also plotted in order to clearly show the nucleation temperature of the eutectic phases in this alloy [12].

According to Shankar et al. [12] at the eutectic temperature, and at an undercooling of 0.4C–0.8 ˚C, eutectic silicon (Si_{eut}) nucleates on the secondary β -(Al, Si, Fe) phase in the solute field ahead of the growing aluminum dendrites (Figure 2.7-c). After nucleation, the eutectic silicon grows as flakes into the eutectic liquid and thus liquid surrounding the eutectic silicon flakes become enriched with aluminum as it is being depleted of silicon. Eutectic aluminum (Al_{eut}) then starts to nucleate and grows on the edges and tips of the eutectic silicon flakes and finally the aluminum dendrites stop growing upon impingement with the growing eutectic aluminum grains (Figure 2.7-d).

It is also shown in Shankar et al. [12] works by thermal analysis (Figure 2.8) that the first solid to form is α-Al dendrites followed by β (Al, Si, Fe) particles. Moreover he has also predicated the relationship among α-Al and β-(Al, Si, Fe) in his work which is shown in Figure 2.9.

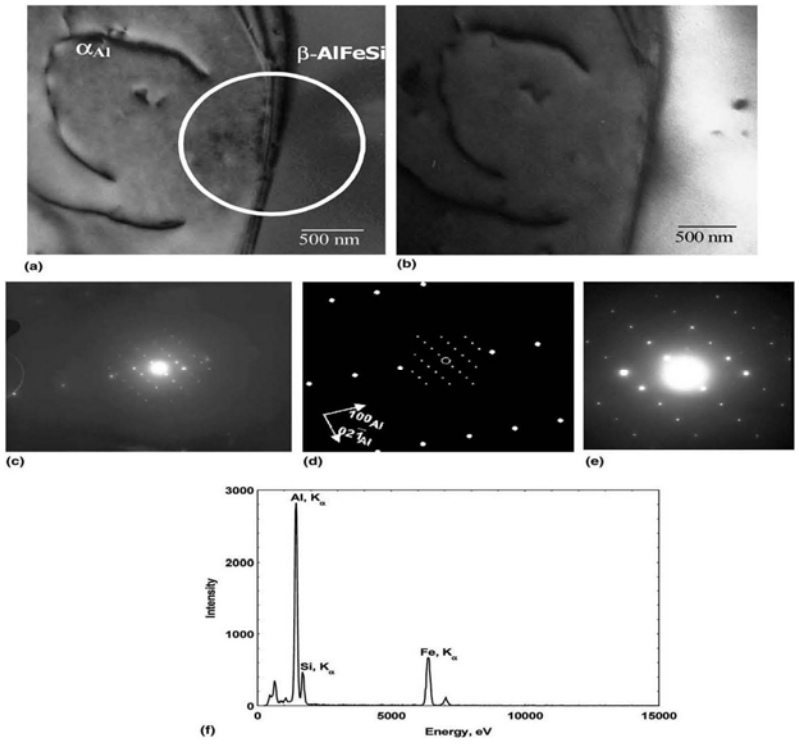

Figure 2.9 (a) Bright field TEM image; (b) centered dark field image showing the β-Al9Si2Fe2 phase; (c) SAD pattern taken in the encircled region in (a); (d) digital replication of (c) for better visualization; (e) SAD pattern from the b-Al9Si2Fe2 phase brought to a zone axis and (f) EDS spectrum obtained from the b-Al9Si2Fe2 particle [12].

Figure 2.9(a) is a bright field TEM image of the interface between an α-Al dendrite and a β-(Al, Si, Fe) particle with the β-(Al, Si, Fe) particle oriented on a zone

axis. Figure 2.9 (b) shows centered dark field image for β- (Al, Si, Fe) phase. Fig. 2.9(c) is a SAD pattern obtained from the encircled region in Figure 2.9(a) and which shows a preferred crystallographic relationship between α-Al dendrites and the β-(Al, Si, Fe) particles. For clarity a digital replication for diffraction pattern is shown in Figure 2.9 (d). The SAD pattern shown in Figure 2.9 depicts that β-(Al, Si, Fe) is oriented on a zone axis. An EDS spectrum obtained from the β phase is also shown in Figure 2.9 (f). All these figures and analysis strongly suggest that the β(Al, Si, Fe) phase has nucleated on the α-Al dendrites.

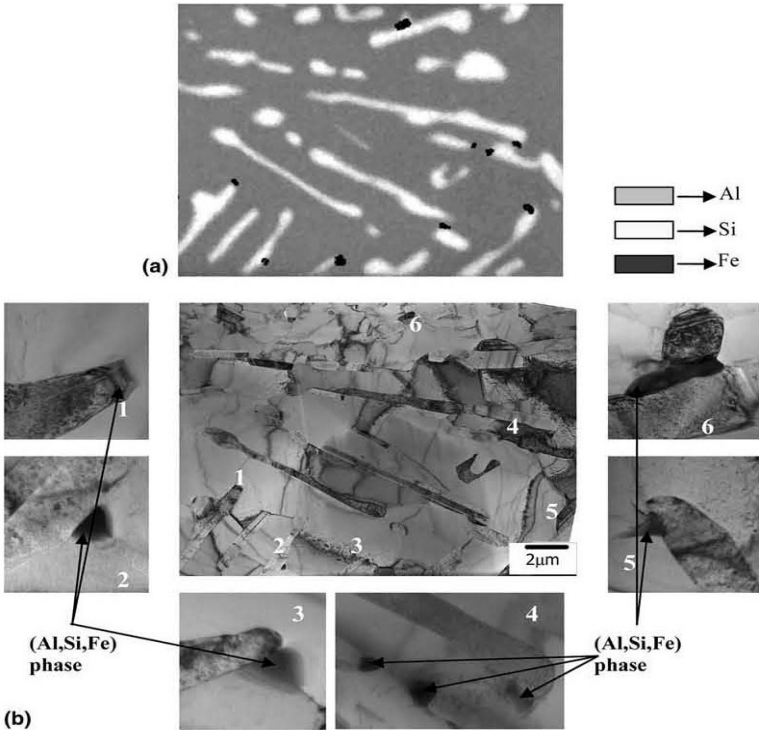

Figure 2.10 (a) Composite elemental map of Al, Si and Fe (key given) obtained from the image shown in (b) and (b) TEM bright field image showing locations where β-(Al, Si, Fe) phases were found [12].

Shankar et al. [12] also evaluate the corresponding relation with β-phase with eutectic silicon in hypoeutectic Al-Si alloys which is shown in Fig. 2.10. Fig. 2.10 (a) is an elemental mapping for Al, Si and Fe, from the TEM bright field image shown in Fig. 2.10 (b). It is observed from this analysis that almost every eutectic silicon flake in the microstructure has a β-(Al, Si, Fe) particle attached to its edge. Another interesting feature was found in his work that several β-(Al, Si, Fe) particles are attached to more than one eutectic silicon flake that show differing crystallographic orientations from one another.

Nogita et al. [21] proposed a model for eutectic nucleation based on the presence of impurities in the melt which is shown in Fig. 2.11. They proposed that during the first stage of solidification, α-Al dendrites grow and phosphorus and silicon will segregate at the dendrite-liquid interface due to their low solubility in solid aluminum. When sufficient phosphorus presents, AlP particles format the interface to act as nucleants for silicon crystals, and eutectic solidification begins from each growing crystals.

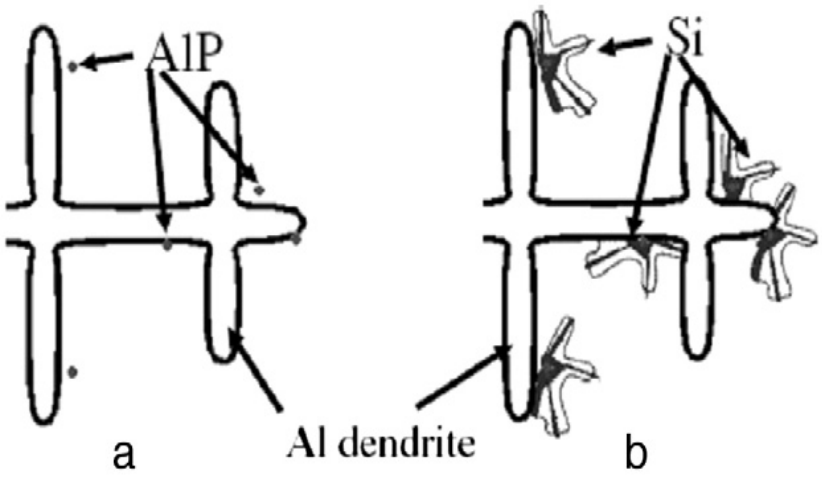

Figure 2.11 (a) Segregation of AlP during the growth of Al dendrites; (b) AlP particles as nucleation sites for polyhedral silicon crystals [18].

Nafisi et al. [18] also proposed a mechanism for the formation of eutectic Si in hypoeutectic Al-Si alloys which is shown in the schematic diagram given in Figure 2.12. It should be emphasized in his work that small number of these tiny silicon particles could act as nucleation sites for the eutectic flakes or fibrous silicon.

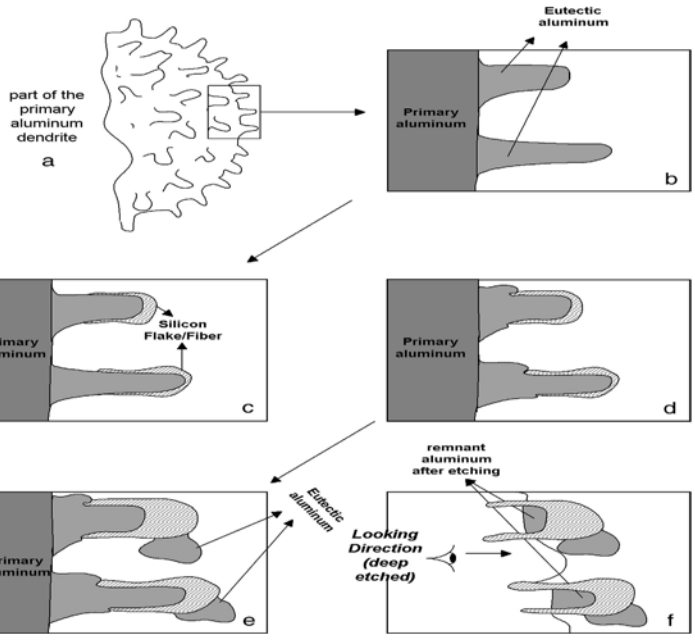

Figure 2.12 Simple schematic presentation for the proposed hypothesis; (a) 3D view of the eutectic spike forming on the primary α-Al, (b) 2D view of the identified segment, (c) Formation of silicon particles, (d) Growth of eutectic compounds, (e) Formation of new eutectic aluminum and silicon and (f) Schematic of the deep etched structure [18].

Figure 2.12 (a) and (b) showing that once the eutectic Al spikes form, the liquid at the vicinity of these spikes becomes enriched in Si which eventually leads to the formation of dome/doughnut-shaped Si particles resembling a sleeve for the spikes and then the further solidification leads to over grow the Si particle by the eutectic Al, while

the rejected Si due to the formation of eutectic Al nucleates simultaneously on these Si particles (Fig. 2.12 -e and f).

2.6 Introduction with Die Casting Process

2.6.1 Origins of Die Casting Process

Metal goods manufacturing is an ancient method and among them casting process are the oldest one. In early periods of casting processes (many of which are still used today), the mold or form used must be destroyed in order to remove the product after solidification. Therefore for endless quantities production a permanent mold was the obvious alternative to save time and make the process more feasible in economically. In the Middle ages of casting process craftsmen started to use of iron molds in the manufacture of pewter ware. The first information revolution occurred in casting when Johannes Gutenberg developed (c. 1439) a method to manufacture movable type in mass quantities using a permanent metal mold. After that over the centuries, the permanent metal mold processes continued to evolve. An injection method was developed in the late 19th century where metal was injected into metal dies under pressure to manufacture print type. In 1884 Ottamar Mergenthaler culminated this development by creating linotype machine that could easily and quickly set movable type. However, all these techniques still had some constraint for mass production of metal component. Therefore several efforts have been continuing for the development of casting process. Finally in 1910 Doehler et al. [22] developed such a process, which can produce a high volume of metal components within a very short period of time. Figure 2.13 is a diagram filed with patent 973,483 for his first production die casting machine. Initially low melting alloy like zinc alloys were used in die casting and with an increasing demand for other metals drove the

development of new die materials and process variants. Aluminum alloys were being die cast by 1915 in large quantities [23].

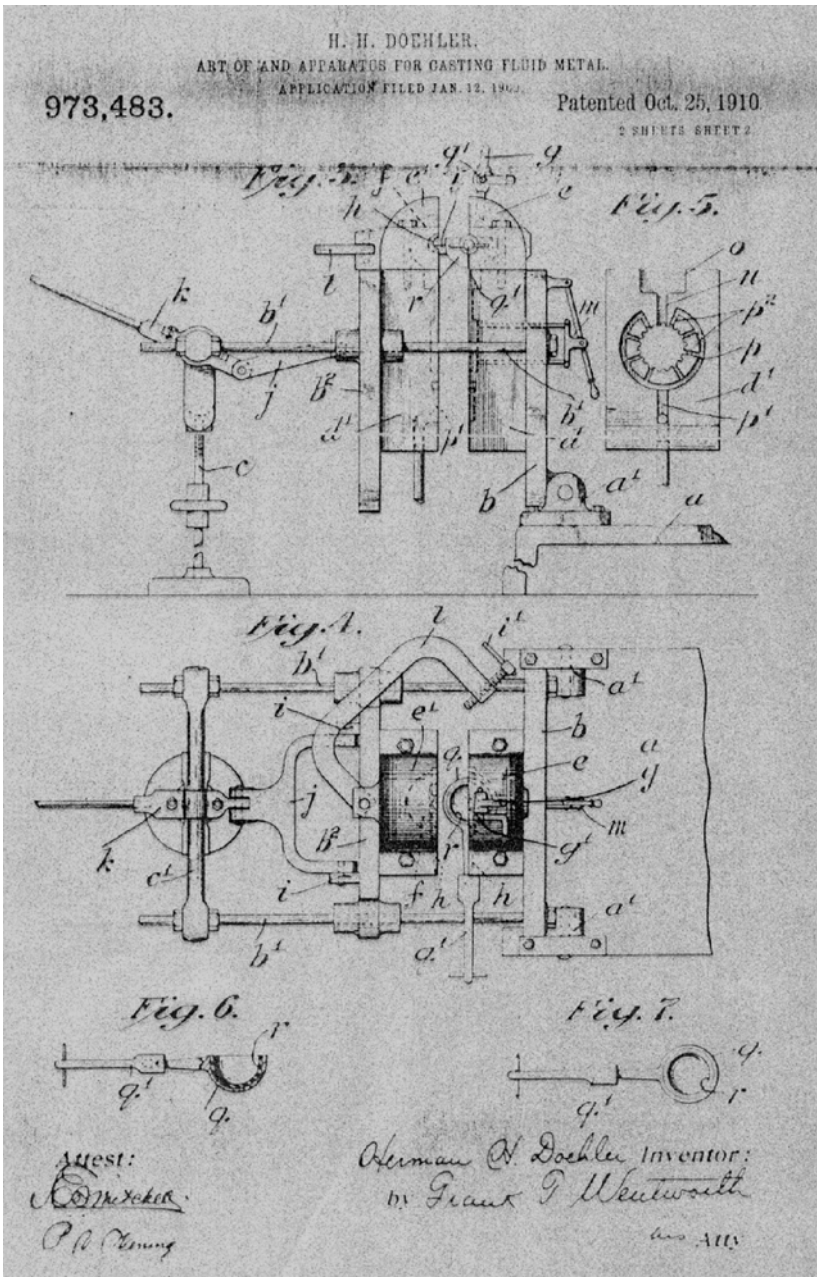

Figure 2.13 Doehler's patent for a production die casting machine [22].

Much progress has been made in the development of die casting technologies over the last century and this development continue to be made driving the capabilities of the process to new levels and increasing the integrity of die cast components [24].

2.6.2 Introduction of High Pressure Die Casting (HPDC) Process

Die casting is a versatile process for producing engineered metal parts where the molten metal is being forced under high pressure into reusable steel molds. These molds can be designed to produce intricate shapes with a high degree of accuracy and repeatability. Casting parts, using high pressure can be sharply defined with smooth or textured surfaces and are suitable for a wide variety of attractive and serviceable finishes. Die casting are among the highest volume, mass-produced items manufactured by the metal-working industry, and they can be found in thousands of consumer, commercial and industrial products. Now a days die cast parts becomes so popular that they are using widely from automobiles industry to toys successfully.

2.6.2.1 Classification of High Pressure Die Casting Process

High pressure die casting process generally divided into two groups, named as (1) Conventional die casting process and (2) High integrity die casting process. These are also divided into some sub groups which are shown in Figure 2.14 [25].

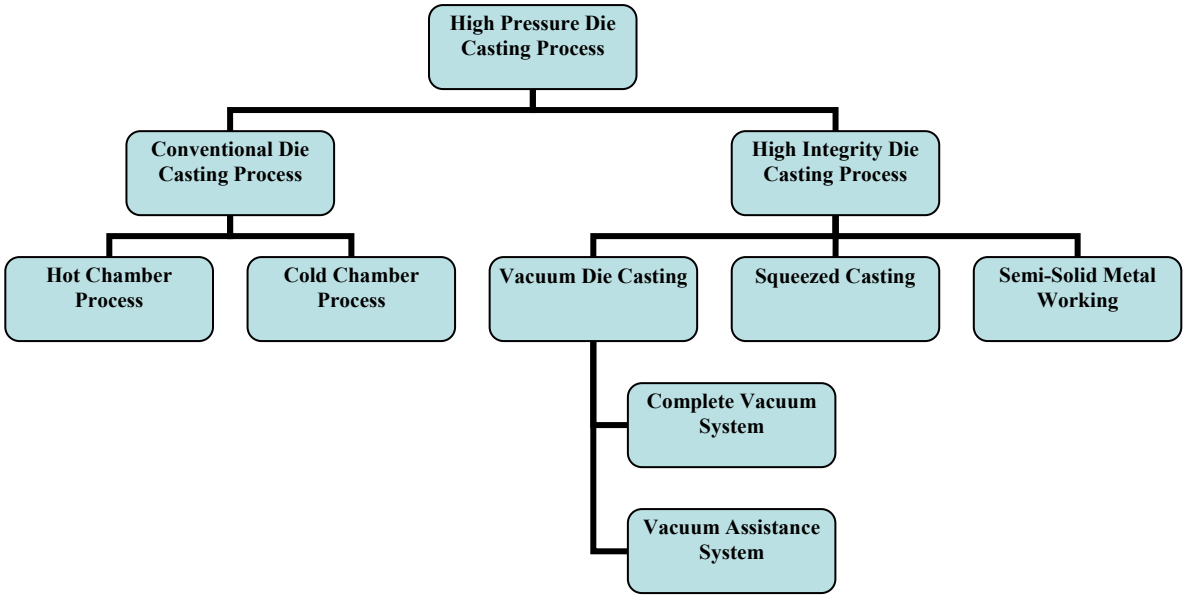

Figure 2.14 Classification of Die Casting [25].

2.6.2.2 Conventional Die Casting Process

Conventional die casting (CDC) is a net-shape manufacturing process where a permanent metal die use that produces components ranging in weight from a few ounces to nearly 25 kg quickly and economically [25]. Traditionally, die casting is not used to produce large products however, past studies have shown that very large products such as a car door frame or transmission housing, can also be produced using die casting technologies. Conventional die cast process can be used in a wide range of alloy systems, including aluminum, zinc, magnesium, lead, and brass. There are two basic conventional die casting processes exist: the hot chamber process and the cold-chamber process which are described from the design of the metal injection systems utilized. A schematic of a hot-chamber die casting machine is shown in Figure 2.15.

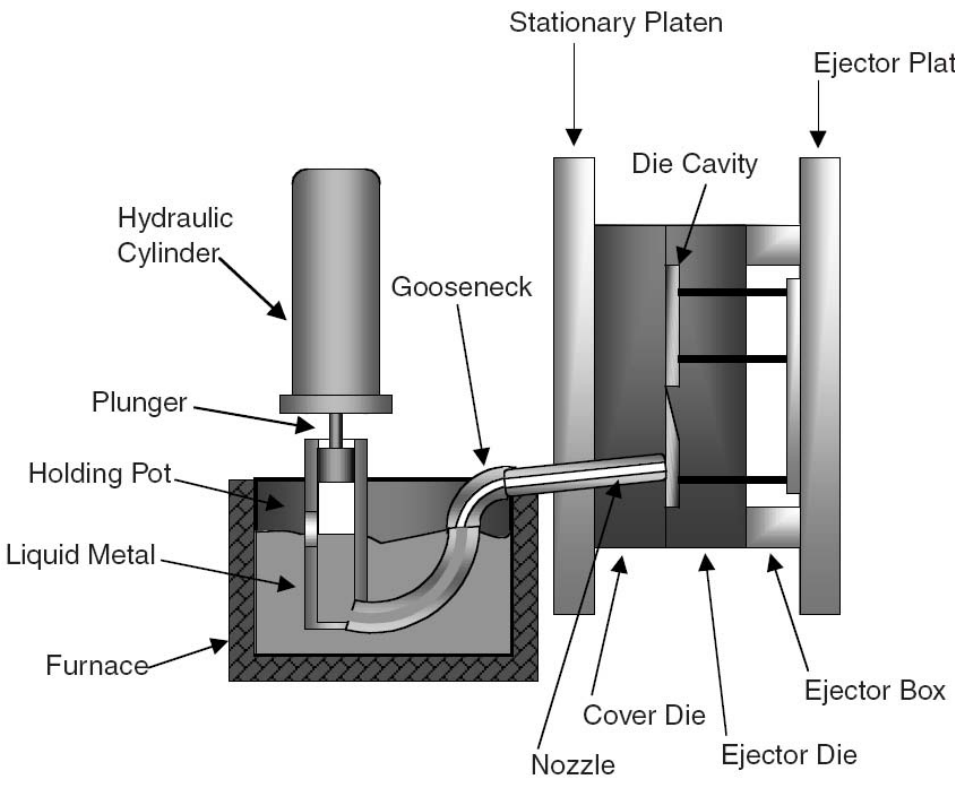

Figure 2.15 Graphical illustration of hot chamber die casting process [25].

Molten metal needs to travel only a very short distance for each cycle therefore the cycle time should be minimum and hot chamber die casting provides this facility by immerging the injection system in molten metal. Hot-chamber die casting process is a very rapid process with cycle times varying from less than 1 sec for small components weighing less than a few grams to 30 sec for castings of several kilograms where dies are normally filled between 5 and 40 m/sec [25]. This process traditionally used for low melting point metals and alloys such as lead or zinc alloys. Higher melting point metals and alloys generally not practiced with hot chamber die casting as they cause rapid degradation of the metal injection system. Cold-chamber die casting machines are typically used for high melting point alloys like aluminum or brass. An illustration of a

cold-chamber die casting machine is presented in Figure 2.16. Unlike the hot-chamber machine, the metal injection system is only in contact with the molten metal for a short period of time. This process starts with ladling the liquid metal into the shot sleeve for each cycle. Die cavity and plunger tip normally are sprayed with an oil or lubricant to provide further protection from severe degradation. This increases the die materials life and reduces the adhesion of the solidified component. Figure 2.16(b) is an illustration of the cycle using the cold-chamber die casting process as a model. As said before, liquid metal is ladled into an injection system (*a*), which is then immediately pushed (*b*) through a runner system (*c*) into a die cavity (*d*) high pressure applied for intensification. High pressures are maintained on the alloy during solidification. After complete solidification, the die opens (*e*) and finally the component is ejected (*f*) [25].

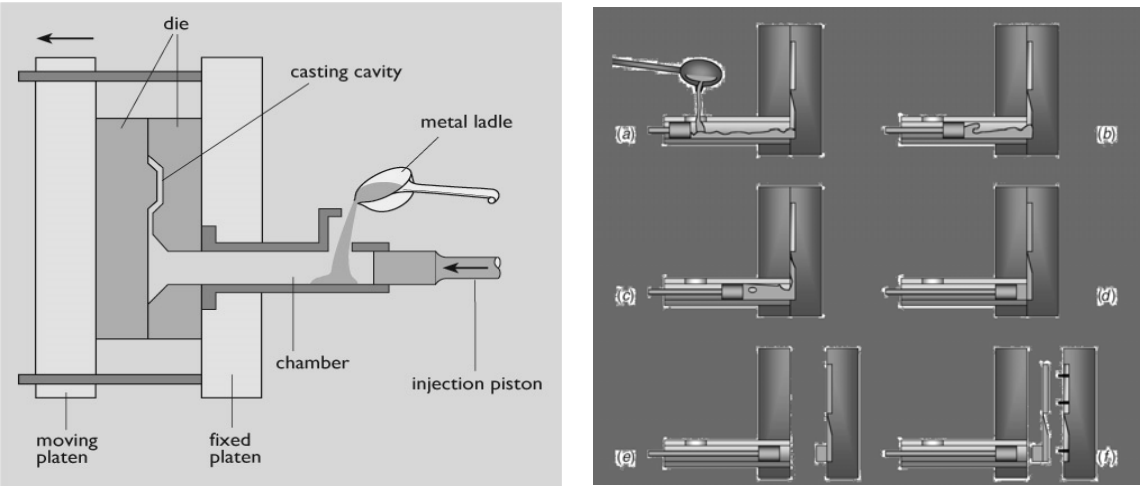

(a) (b)

Figure 2.16 a) Schematic of Cold chamber die casting process, b) Casting cycle for cold chamber die casting process [25].

2.6.2.3 Problems with Conventional Die Casting Process

Although conventional die casting is utilized to produce many products in the current global market, unfortunately this process has a major limitation that prevents it to use on a broader scale. Porosity is the potential defect in conventional die cast components which often limits the use of the conventional die casting process in favour of products fabricated by other means. Conventional die castings often are unable to tight leak arise from pressure vessel and this is one of the prime source for gas entrance as well as for porosity creation. Moreover, the detection of porosity in conventional die casting process is also very difficult because of their size and amount. However when this kind of casting component goes into application they often shows premature failure which is always unexpected. Subsequent machining, however, cuts into porosity hidden within the component, compromising the integrity of the product and thus in some cases an "as-produced" is acceptable. Porosity is usually attributed to two main sources: solidification shrinkage and gas entrapment. Most alloys have a higher density in their solid state as compared to their density in the liquid state and thus shrinkage porosity often forms during solidification. Due to turbulence when liquid metal enters and fills into the die cavity, gas often becomes entrapped in the solidified metal and results porosity in finished product. Porosity also acts as a stress concentrator by creating crack initiation site for cracks, when use in structural purposes. Therefore it is always expected to quantify the porosity in components as well as to take some steps to prevent the severity of porosity. Recently numerous studies have documented how porosity in die castings varies with several operating conditions [26-31]. Gordon et al. [32] has developed a method for

quantifying the porosity in die cast components where he described the total porosity in a component by the following equations:

$$\%P = \text{(solidification shrinkage)} + \text{(gas contribution)} \quad \text{(2.1)}$$

which can be further defined as

$$\%P = \beta V^*/Vc + \Phi\,[T\rho L/(237k)P]\,(v - v^*) \quad \text{(2.2)}$$

where,

- %P = Percent Porosity
- β = Solidification shrinkage factor in percent
- V* = Volume of liquid in casting cavity that is not supplied liquid during solidification in cubic meters.
- Vc = Volume of the casting cavity in cubic meters.
- T = Temperature of the gas in the casting cavity in degrees Kelvin.
- P = Pressure applied to the gas during solidification in atmosphere.
- Φ = Fraction of the gas that doesn't report to the solidification shrinkage pores.
- ρ = Liquid alloy density at the melting temperature in grams per cubic centimetre.
- v = Quantity of gas contained in the casting at standard temperature and pressure conditions (273 K at 1 atm) in cubic centimetres per 100 g of alloy, and
- v* = Solubility limit of gas in the solid at the solidus temperature at standard temperature and pressure conditions in cubic centimetres per 100 g of alloy.

The first portion of Equation 2.1 expresses the relationship for porosity due to solidification shrinkage and the second portion describes the porosity due to gas entrapment. According to Gordon et al. [32] the total gas contained in the casting includes

gas from physical entrapment, gas from lubricant decomposition, and gas dissolved in the alloy which can also be described mathematically as,

$$V = V_{Entrained} + V_{Lubricant} + V_{Soluble\ gas} \quad \ldots\ldots\ldots\ldots\ldots\ldots\ldots\ldots \quad (2.3)$$

Each of the gas contributions in Equation 2.3 are expressed in cubic centimetres at standard temperature and pressure conditions per 100 g of alloy.

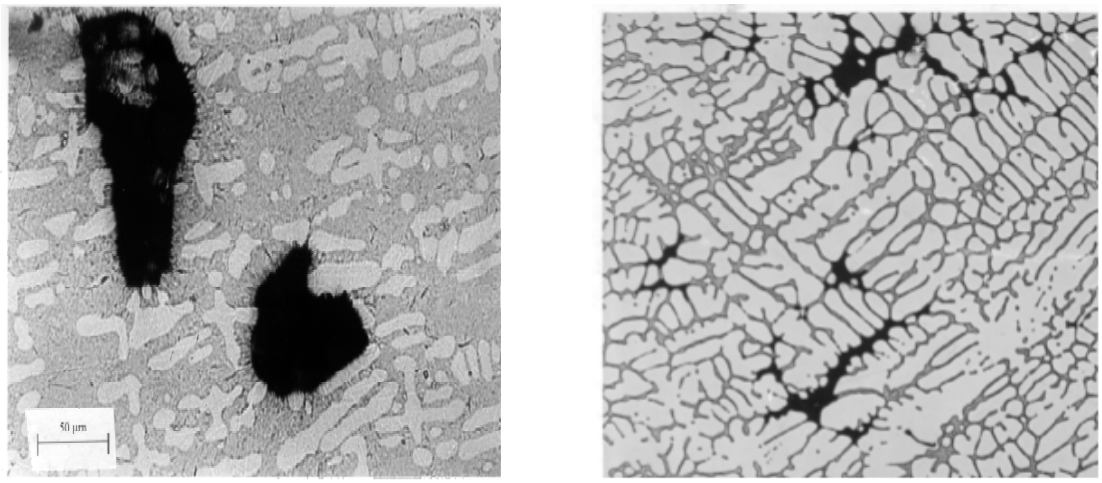

(a) (b)

Figure 2.17 (a) Blistering effect, (b) gas porosity in an Al-10%Cu alloy [33].

In addition to porosity, the microstructures inherent with the conventional die casting cannot meet the mechanical requirements needed for many applications and thus limits their use. Subsequent heat treating, which can alter the microstructure to improve the mechanical properties, is rarely possible due to defects that emerge during thermal processing, such as blistering (Figure 2.17).

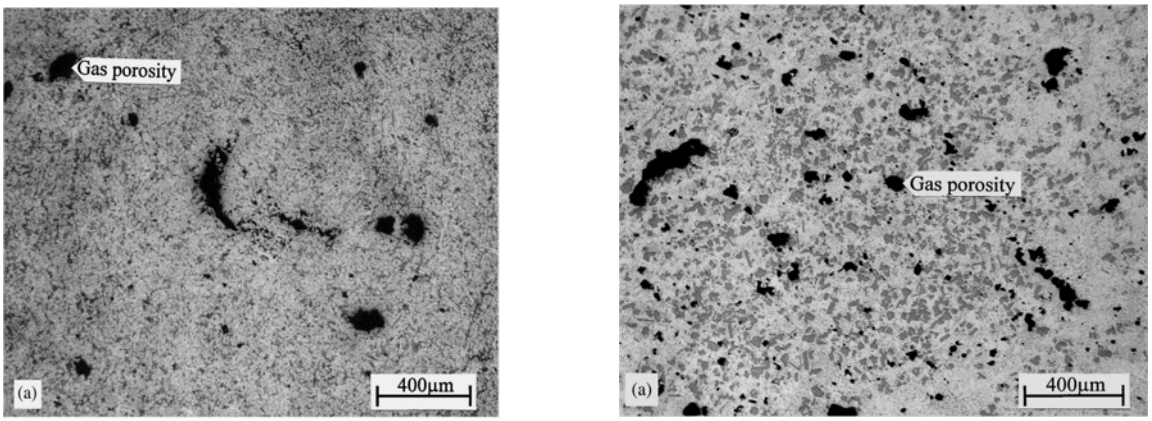

(a) (b)

Figure 2.18 Light optical micrographs of castings in the Al 8% (a) and 18% (b) Si alloy, showing the porosity distribution in conventional [26].

Figure 2.18 shows the occurrence of gas porosity in either hypo or hyper eutectic aluminum silicon alloys by approaching conventional die casting process. These types of microstructures are always unexpected in casting components as they have negative influence in mechanical properties as mentioned before.

Regardless of the limitations found in conventional die cast components, demands still exist for high integrity products. In many cases, product engineers and designers turn to investment casting, forging, injection molding, and assembled fabrications to meet necessary requirements as these processes are more costly than conventional die casting in both processing time and raw material costs [25].

2.6.2.4 Improving Die Casting

Several successful efforts have been made in last few decades in stretching the capabilities of conventional die casting while preserving short cycle times and providing

dimensional stability and other beneficial characteristics. Edward et al. [25] figured out the following three strategies which have successfully extended the capabilities of the die casting process, which are as follows:

1. Eliminating or reducing the amount of entrapped gases,
2. Eliminating or reducing the amount of solidification shrinkage, and
3. Altering the microstructure of the metal.

In the first two strategies he prescribed the affect of each of the major quantities that contribute to porosity as defined in equation 2.1 and in the third strategy, co-relation of mechanical properties with microstructure is explained.

2.6.2.5 High Integrity Die Casting Process

Now a day's high integrity die casting process becoming the most attractive method due to the restrictions in conventional die casting process for production of versatile components with different kind alloys. Generally, three high integrity die casting processes namely vacuum die casting, squeeze casting and semi-solid metalworking (SSM) have been successfully developed and deployed for commercial use in high volume production.

In vacuum die casting method a controlled vacuum system is used to extract gases from the die cavities and runner system during metal injection. By using such a vacuum system in this process they minimizes the gas content from physical entrapment ($V_{Entrained}$) and gas content due to decomposition of lubricant (V_{Lube}) as defined in Equation 2.3 [25].

Squeeze casting is characterized by the use of a large gate area and planar filling of the metal front within the die cavity to minimize the gas content. The mechanism,

however, is much different than vacuum die casting process. In squeeze casting no vacuum system is incorporated in the process rather the planar filling allows gases to escape from the die, as vents remain open throughout metal injection. Furthermore, the large gate area allows metal intensification pressure to be maintained throughout solidification and thus reduce the magnitude of V^* (Volume of liquid in casting cavity that is not supplied liquid during solidification in cubic meters) as defined in Equation 2.2. Both porosity from entrapped gas and solidification shrinkage are reduced by using squeeze casting [25].

During semi-solid metalworking a partially liquid–partially solid metal mixture is injected into the die cavity where the fill front is planar in order to minimize gas entrapment, as in squeeze casting. Solidification shrinkage is also greatly reduced in this process, as a significant portion of the metal injected into the die cavity is already solid. Moreover a unique microstructure is generated during semi-solid metalworking and thus the mechanical properties inherent to this microstructure are superior to those created in conventionally die cast components.

Porosity problems are greatly minimized in high integrity die casting process. Moreover, the microstructures as well as the mechanical properties are also improved in comparison to conventional de cast components. This is due to reduction of porosity level and thus the viability of subsequent heat treatment [25].

2.7 Introducing Vacuum Die Casting Process

So far it is shown that entrapped gas is a major source of porosity in conventional die castings and minimization of this problem can improve the mechanical properties in some extent. A vacuum system in die casting process is thus a logical necessity to extract

the gases from the die cavities, runner system and shot sleeve during processing [34]. Vacuum die casting is such a process which meets this logical requirement and thus makes die casting process much more meaningful.

2.7.1 Advantage of Vacuum Die Casting

Although high pressure die casting provides near-net shape casting however this process, creates inherent defects, typified by gas porosity in the produced castings due mainly to the entrapment of air in the molten metal as a consequence of the high speed injection of the molten metal into the die cavity. Mechanical properties and pressure tightness are adversely affected by the presence of gas porosity in castings. Moreover porosity which particularly located adjacent to the casting surface, tend to expand in size and leading to the formation of blisters at the casting surface during heat treatment for further improvement of properties. Therefore, the applications of aluminum die castings are normally limited to non-structural components that do not require such a heat treatment.

In order to minimize this gaseous problem from casting component, numerous metal casting processes namely permanent mold casting, lost-foam casting, plaster mold casting and investment casting have utilized vacuum systems. The prime constraint in the evolution of vacuum die casting has been the development of a reliable vacuum shut-off valve which properly minimizes the leaking of gas in the die cavity. Vacuum die casting is such a method of casting in which a vacuum system is incorporated with a reliable shut-off valve and thus virtually eliminated gas from the die. In addition vacuum die casting is also compatible with other high integrity processes, including squeeze casting and semi-solid metalworking [25]. Attempts to develop methods of vacuum die casting

were first introduced into hot chamber die casting machines [35]. More recent developments have led to the application of vacuum die casting in the field of cold chamber aluminum production [35, 36]. This use of vacuum system in the die casting process is an innovative development in casting industry. The working principle is the same as low-pressure die casting. Vacuum pump decrease the inside pressure in the die and thus the pressure difference forces the liquid metal to enter the die. This transfer of liquid metal through the die is less turbulent than by other casting techniques so that gas inclusions can be very limited.

This innovative technique generally aimed to those components which require subsequent heat treatment for further improvement of properties. By creating a pressure lower than atmospheric pressure in the injection chamber and die cavity, the relative absence of air results in casting of better quality [37]. Moreover back pressures encountered by metal trying to the entire die cavity are also reduced which facilitate to produce large casting areas with thin wall sections [24].

Vacuum die casting process have proven successful in stretching the capabilities of conventional die casting while preserving short cycle times, and providing dimensional stability and other beneficial characteristics. According to Paul Robbins et al. [38], they are:

- Rejections due to porosity are virtually eliminated,
- Rejections after secondary processing are virtually eliminated,
- Excellent surface quality is ensured,
- Product density and strength are increased,
- Larger, thinner, and more complex, casting are made possible,

- Less casting pressure is required,
- Tool life and mold life are extended,
- Better de closure, and
- Flash is reduced or eliminated.

Figure 2.18 schematically illustrates a vacuum die casting machine. The molten metal is kept in a holding furnace (11 in Figure 2.19) and is fed to the casting chamber (2 in Figure 2.19) through the inlet pipe (10 in Figure 2.19). Then the casting plunger (1in Figure 2.19) advances forward forcing the metal into the closed die cavities while a vacuum is being run on the mould. The vacuum eliminates the gas which could be trapped with the cast. The mould is allowed to cool in the mould halves. Once initial cooling is complete, one half of the mould retracts and the part is cooled through a water jet. The part is retracted and transferred to a finishing line [39].

Vacuum die casting utilizes a controlled vacuum (about 5×10^{-1} KPa [37]) to extract gases from the die cavities and runner system during metal injection. With this much of applied vacuum, porosity due to entrapped gases is virtually eliminated [23].

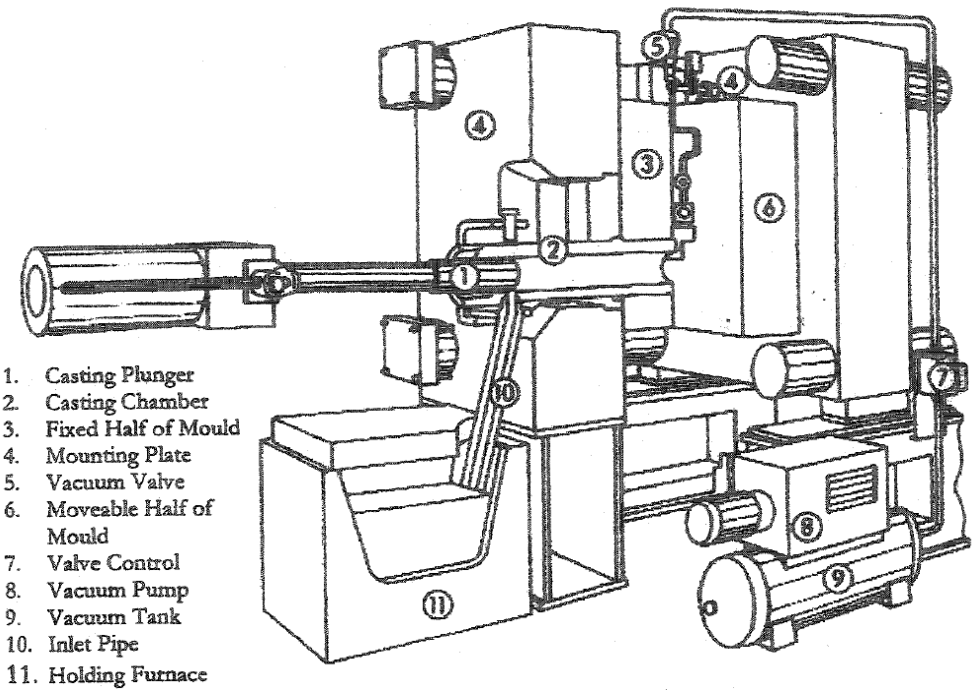

Figure 2.19 Schematic view of vacuum die casting process [39].

2.7.2 Types of Vacuum Die Casting

According to the vacuum system arrangement vacuum die casting process can be classified into two types namely; (1) A complete vacuum system: where the whole die casting system, including the die, injection chamber and furnace are completely sealed and evacuated during casting and (2) A vacuum assistance system: where a vacuum valve is incorporated into a die to evacuate the entrapped air in the cavity. In complete vacuum system molten metal is transferred from the furnace to the injection chamber via a vacuum feed tube. A high level of vacuum is able to achieve in this kind of arrangement however, it is relatively complex with stringent requirements in the system sealing. Vacuum assistance system is relatively cheap and simple arrangement rather than complete vacuum system. Although the vacuum level is not that much high in this kind of

arrangement nevertheless more attention has been focused on this system recently because of their simplicity and requires little or no machine modification as it is a stand alone system.

Figure 2.20 schematically illustrates casting process in a vacuum die casting machine. The molten metal is kept in a holding furnace and is fed to the casting chamber through the inlet pipe (step 1 in Figure 2.20) .The casting plunger advances forward forcing the metal into the closed die cavities while a vacuum is being run on the mould (step 2 in Figure 2.20). The vacuum eliminates the porosity of the part to be cast, drawing out almost all the pores (depending upon the vacuum level applied in the process). At this stage the mould is allowed to cool in the mould halves. When the initial cooling is complete, one half of the mould retracts and part is cooled through a water jet. The part is retracted and transferred to a finishing line [39].

Vacuum assisted die casting differs from the conventional HPDC process only in one point, here in this process; an external vacuum pump is connected to the HPDC die. Vacuum system starts operating shortly after the plunger has sealed off the sleeve inlet and pulls the vacuum either until the shot is finished or until just before that. In die casting plunger speed maintain in two phase to avoid liquid metal splashing as well as to reduce excessive turbulence in molten metal. Generally the normal plunger speeds in the first phase of the shot is 0.1-0.6 m/s and the usual die filling times, only about 1.5 to 2.5 seconds are available for evacuation. Therefore a high level of vacuum cannot be expected within this short time. Various levels of achievable die pressure can be found in literature, ranging from 150 mbar (= 1.5×10^{-2} MPa), 1810^{-3} to 28×10^{-3} MPa, 100 mbar (= 1.0×10^{-2} MPa) and 200 mm Hg (= 26.10×10^{-3} MPa) [40].

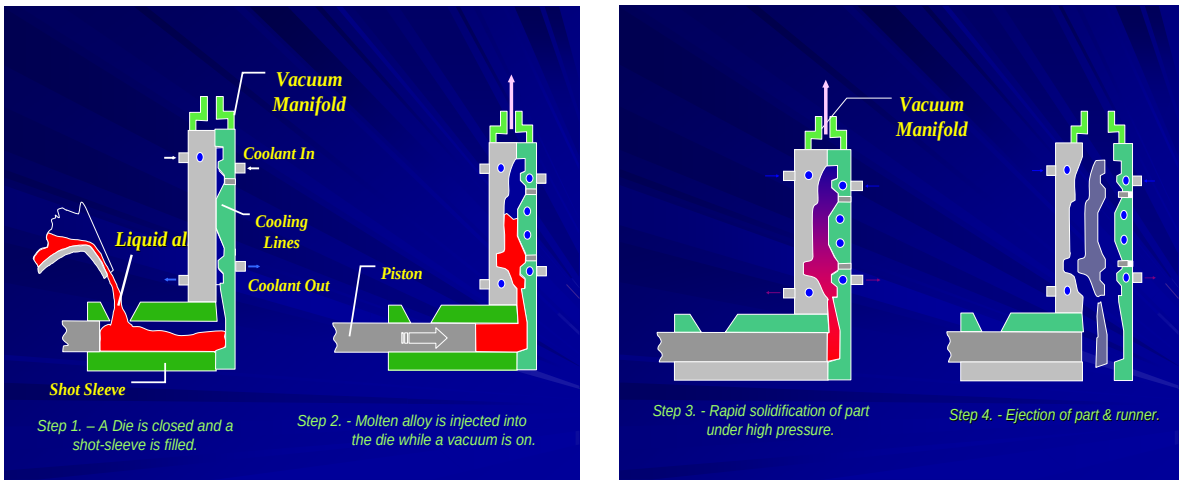

(a) Steps 1 to 2 (b) Steps 3 to 4

Figure 2.20 Schematic views of different steps in vacuum die casting process [41].

Nevertheless, useful vacuum assistance can be applied during die filling of thin walled castings by reducing the back-pressure of compressed air as mentioned before and can be helpful in reducing entrapment of air and lubricant-related gas reaction products. Industry experts mention that it is possible to fill thin-walled cavities at a reduced filling speed compared to that of conventional HPDC, which is evidence of reduced back-pressure.

It is expected to understand the working principal of vacuum pump during the casting process to have a better knowledge. In the following paragraphs some important components of vacuum system are described to have a better look on it.

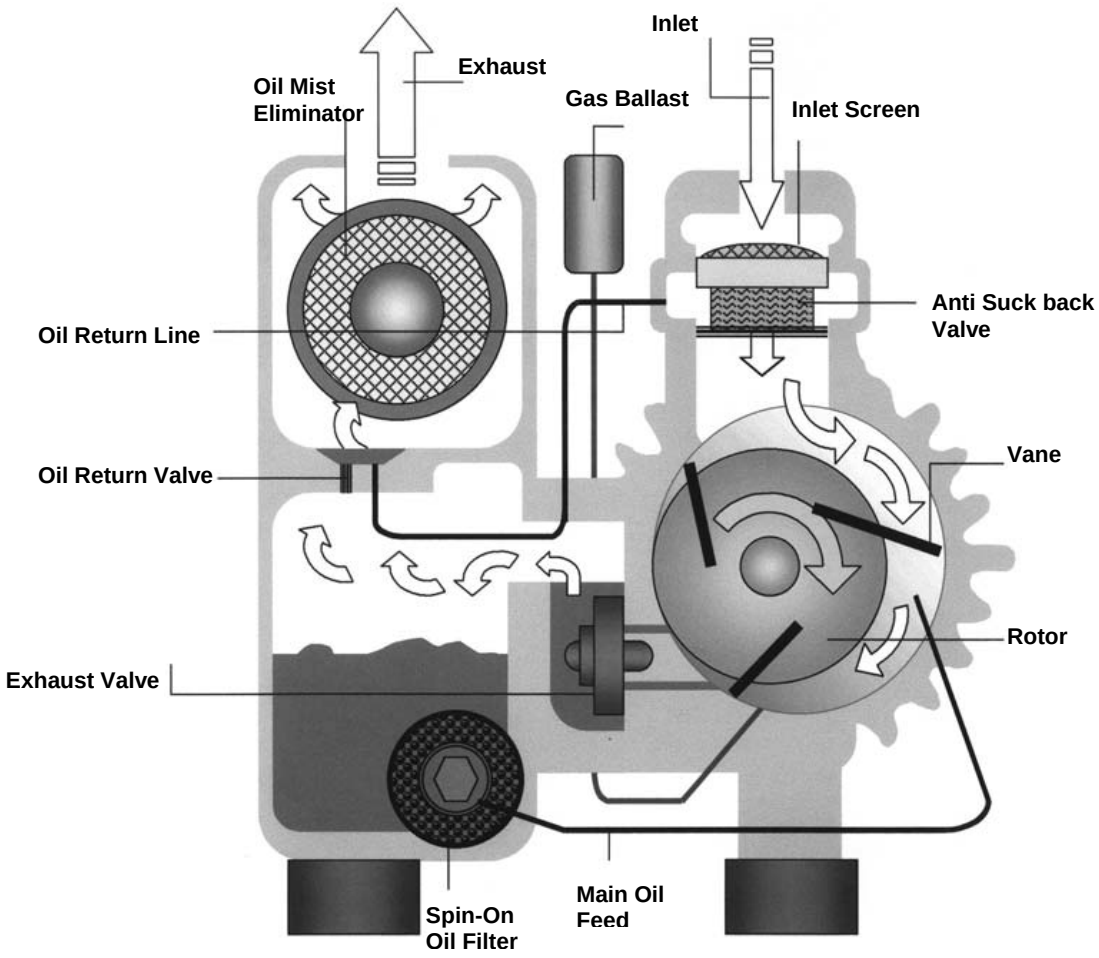

Figure 2.21 Illustration of a rotary vane vacuum pump [25].

In vacuum die casting process usually a rotary vane vacuum pumps are commonly used. Figure 2.21 is an illustration of such a pump. There is an eccentric rotor presents within the pump cylinder that pulls the vacuum. As the rotor turns, gases are trapped and compressed between several vanes and the walls of the pump cylinder and thus the compressed gases are discharged into the exhaust box. Then the gases pass through an oil eliminator that extracts oil vapours from the exhaust gases prior to discharging them to the environment [25]. A numerous number of vacuum pumps are

commercially available, as shown in Figure 2.22. Often they are portable for easy placement within the die casting facility [25].

A proper vacuum valve is required to prevent metal flow into it which is usually connected to the plunger stroke. For security the valve may be closed shortly, which shortens the effective evacuation time even further. Kim et al. [42] approached a very elegant method in using the well-known chill blocks to automatically seal the vacuum channel. In this method, when the melt reaches the chill block it eventually solidifiers and seals the channel by itself, thus ensuring that the vacuum pump can suck air until the casting stroke has been completed.

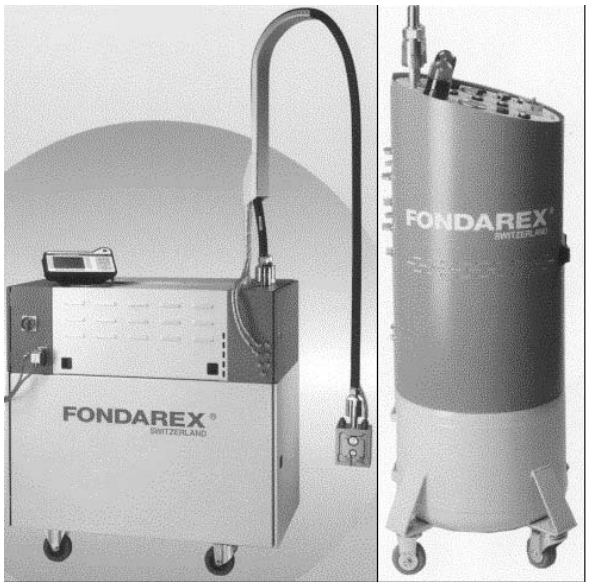

Figure 2.22 Examples of portable vacuum systems for use in vacuum die casting [40].

2.7.3 Managing Gas in Die during a Vacuum Die Casting Process

According to Edward et al. [25] products which are manufactured using high integrity vacuum die casting processes have little porosity. Moreover approaching this kind of technique, the mechanical properties are much improved in comparison to

conventional die cast components. This is due to reduction of porosity levels and the viability of subsequent heat-treating that are not generally possible with conventional die casting process.

Nevertheless in real casting, porosity still arises in HPDC process even with a vacuum assistance system, which may affect the mechanical properties of a casting component. As mentioned in the preceding section that there are three main contributing factors to the formation of gas porosity in die castings which are entrapped injection chamber and die cavity air, gases due to combustion or volatilisation of die or plunger lubricants and gas (mostly hydrogen) dissolved in the melt. Dissolve hydrogen in molten metal is always difficult to evacuate and thus the application of vacuum will have a major influence only on the entrapped air or gases during injection. Figure 2.23 provides an overview of the possible sources of gas pick-up in the HPDC process.

Although in conventional die casting, gases are vented from the die, the amount of gas that must vent from the dies is much greater than that of just the die cavity. This is expected that all gases in the runner system must be vented as well as any volume of the shot sleeve not filled with metal. This is virtually impossible for all gases to exit the die before die fill is complete due to short cycle times. Usually, the time to fill a die is measured in milliseconds. Therefore it is virtually impossible to expel all gases from the die cavity through the vents. In most cases experimentally found that gases are entrapped in the die and compressed into the metal even when the gases are compressed and thus the porosity can manifest as blisters at a later time. This is often occurs during heat treatment [25].

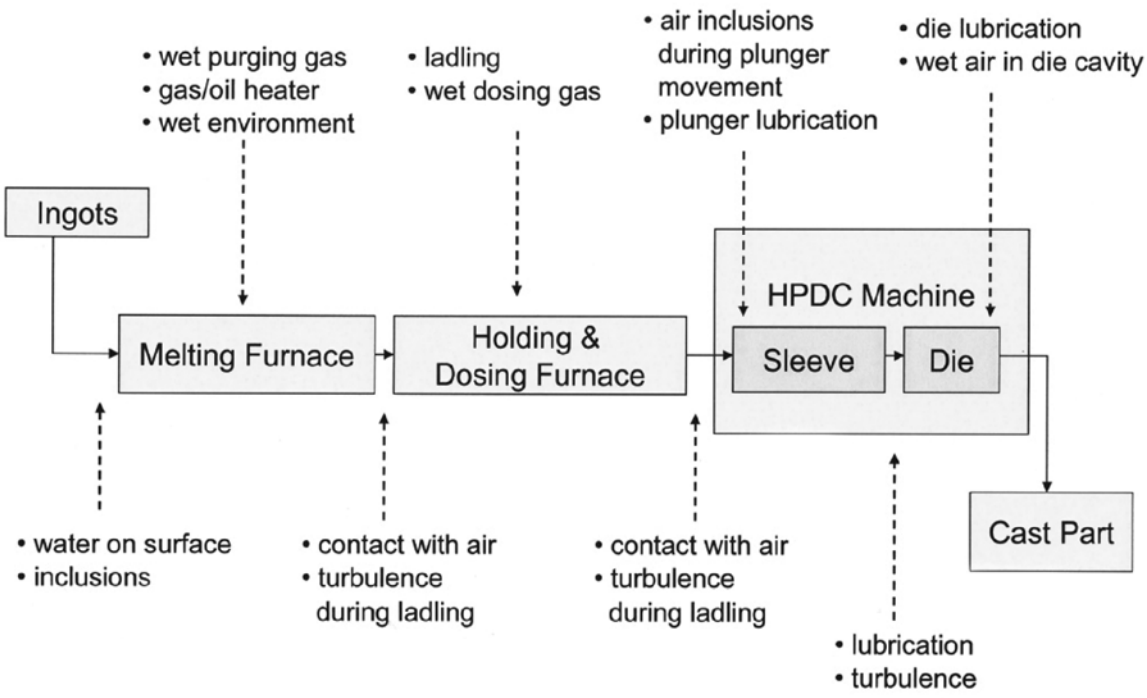

Figure 2.23 Sources of gas in HPDC [43].

In some special cases, conventional die casters do not choose to vent gases from the die at all. Therefore in such cases, all gases must be compressed into the component. For certain application this type of component might be acceptable, specifically in non-structural purposes but such practices do not produce high integrity products. With an appropriate vacuum system, 95% of all gases in the die cavity can be removed at 750 mm Hg pressure.

In die casting hydrogen (H_2) is the only gas capable of dissolving to a significant extent in molten aluminum [44]. It is experimentally found that hydrogen solubility is considerably greater in the liquid than in the solid state. However a dramatic decrease in its solubility occurs at the solidification point of aluminum (650˚C) which is shown in Figure 2.24. From the figure it can be seen that the actual liquid and solid solubilities of hydrogen in pure aluminum just above and below the solidus are 0.65 and 0.034 ml/ 100g

and thus the difference results in out gassing and consequently leads to the formation of porosity during solidification [44].

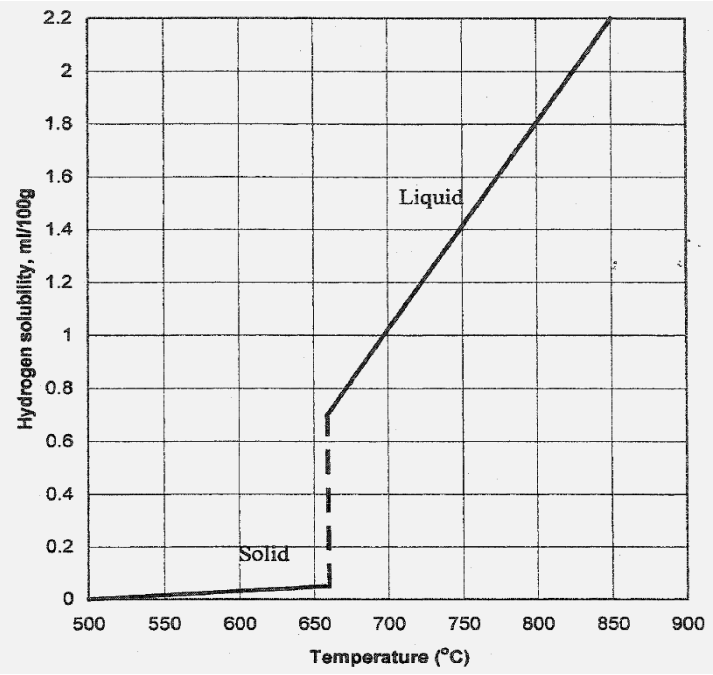

Figure 2.24 Solubility of Hydrogen in Aluminum at 1 atmospheric hydrogen pressure [44].

Hydrogen porosity often causes diffusion-controlled nucleation and growth by decreasing the hydrogen concentration and increasing the rate of solidification which acts to suppress void formation and growth [44]. Hydrogen can pick up into the molten metal by several ways among them, wet spots from remaining lubricants and CH groups in the lubricants may be considered the most dangerous. During ladling and die filling nitrogen trapped in casting component. It is experimentally found that for wieldable castings for WIG/MIG welding the gas content should be below 10 ml/100 g, while conventional HPDC parts often show more than 30 ml/100 g. However a lower consumption of

lubricant helps to achieve the target value, but requires improved thermal management inside the die to avoid degradation by higher melting point alloys [25].

During welding of HPDC parts nitrogen inclusions and hybrids cause major problems. According to Wiesner et al. [43] dissolved hydrogen is generally no problem in welding, because the partial pressure is below 10 bars and usually below 5 to 7 bar due to diffusion of hydrogen in the solid aluminum casting but on the other hand nitrogen does not dissolve in aluminum and is therefore entrapped under solidification pressure which quickly release a high amount of pressure of about 500 to 1000 bar and leads to explosion like splashing [25]. The same is also true for hydrogen, when they presents as hydrides. Fortunately aluminum does not form hydrides, but some of the usual alloying elements do such as Titanium and magnesium. Wiesner et al. [43] found that at temperatures below 600˚ c the capacity for hydrogen storage of hydrides is about 1000 times larger than solubility of hydrogen in aluminum. This is why hydrogen-related porosity is hardly visible in castings component. Again according to Wang et al. [45], the influence of hydrogen on porosity formation is much less effective, which is negligible when compared to the gas from other sources such as air entrapment.

Die casting alloys are solidified in a very high cooling rate at about 50-100˚C/Sec, which does not allow sufficient time for hydrogen to diffuse away, thus a supersaturated hydrogen solid solution is formed in casting component. Therefore porosity problem is the most important factor that normal die casting alloy can not be subjected to heat treatment [25].

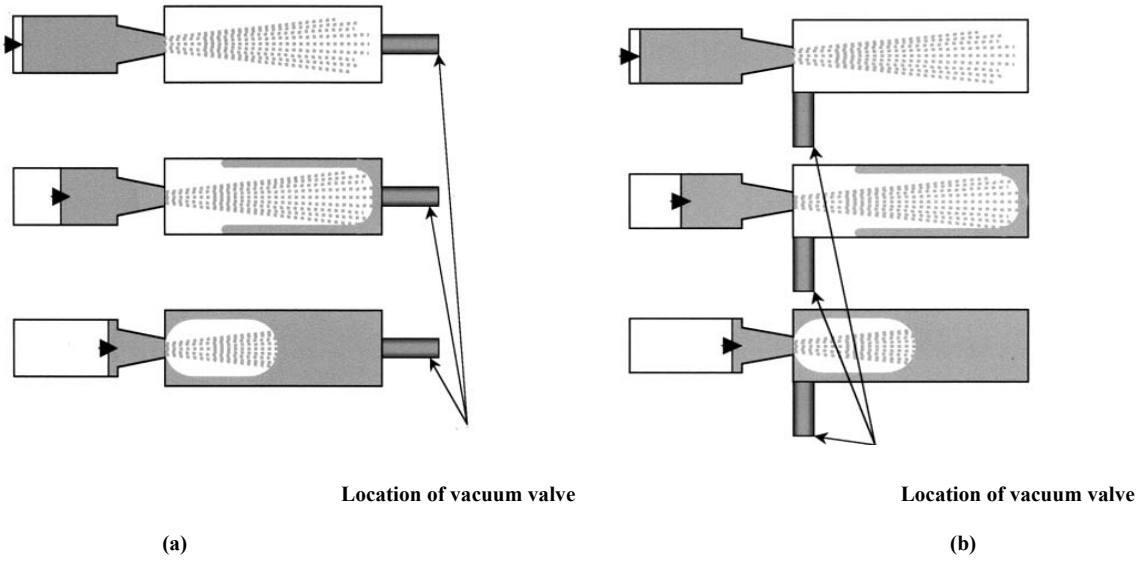

Figure 2.25 Graphical illustrations showing the progression of a die cavity filling with (a) improper vacuum valve placement; (b) proper vacuum valve placement [25].

During die casting process, the vacuum should be applied to the die as long as possible to extract as much gas as possible. Vacuum shut-off valve should be located at the last location to fill in the die. A wrong placement of vacuum shut-off valve (for example placement at the furthest point from the gate as shown in Figure 2.25) may close the valve quickly during the filling process. Simulation or computer modeling may be utilized to identify proper vacuum valve placement [25].

The starting time for vacuum is also critical in vacuum die casting. It is recommended that the vacuum should be applied just after the plunger tip closes the pour hole otherwise if the vacuum is applied before the pour hole is closed, air from outside of the machine will be pulled through the system. Moreover if the vacuum is not applied immediately after the pour hole is closed, gases may be entrapped in the metal as waves crest and roll over within the shot sleeve. This phenomenon is illustrated in Figure 2.26 [25].

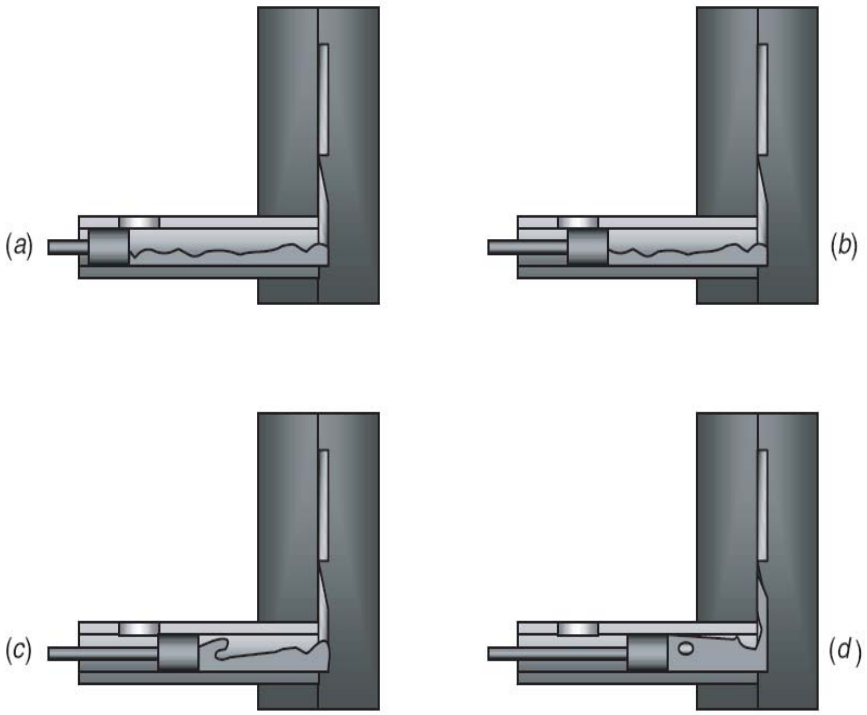

Figure 2.26 Graphical progression showing liquid metal wave cresting and gas entrapment in the shot sleeve: (a) pour hole open; (b) pour hole closed; (c) wave cresting and (d) gases trapped [25].

As stated in preceding section, gas porosity can also originate from gases dissolved in the molten metal. Although due to the short cycle times and high solidification rate in both conventional and vacuum die casting, this form of porosity rarely occurs as the dissolved gases do not have sufficient time to coalesce and form porosity. However, subsequent heat treatment can create conditions for such porosity to form into blisters which can be minimized following good melting and holding practices [25].

2.7.4 Managing Shrinkage in a Die

Normally in die casting process high metal intensification pressures are often maintained throughout solidification to minimize solidification shrinkage porosity. However when small gates (typically used in CDC) used for pouring the liquid metal in casting chamber, the liquid metal freeze quickly and thus creates a barrier, which inhibits pressurization within the die cavity [25]. Therefore a proper gate design and appropriate utilization of intensification pressure can only resolve this kind of problem. Vacuum die casting offers no additional benefits with regards to solidification shrinkage porosity, in comparison to conventional die casting.

2.7.5 Advantages of Vacuum Assistance System in Vacuum Die Casting

According to Niu et al. [24] vacuum assistance die casting improves the mechanical properties and increases the density of the alloys when compared to conventional die casting. He performed several experiments on aluminum alloys with and without using vacuum system to analysis the advantage of vacuum assistance system.

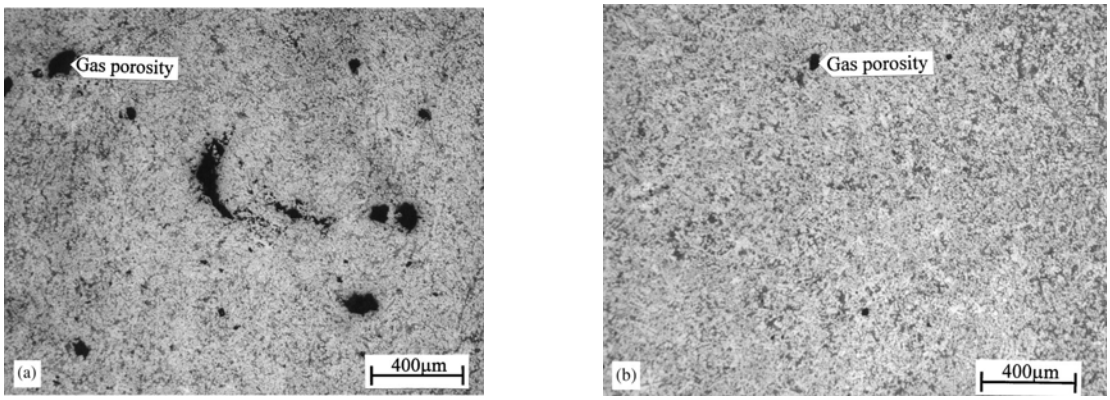

(a) (b)

Figure 2.27 Light optical micrographs of castings in the Al-8%Si alloy, showing the porosity distribution in: (a) conventional, (b) vacuum assisted die castings [24].

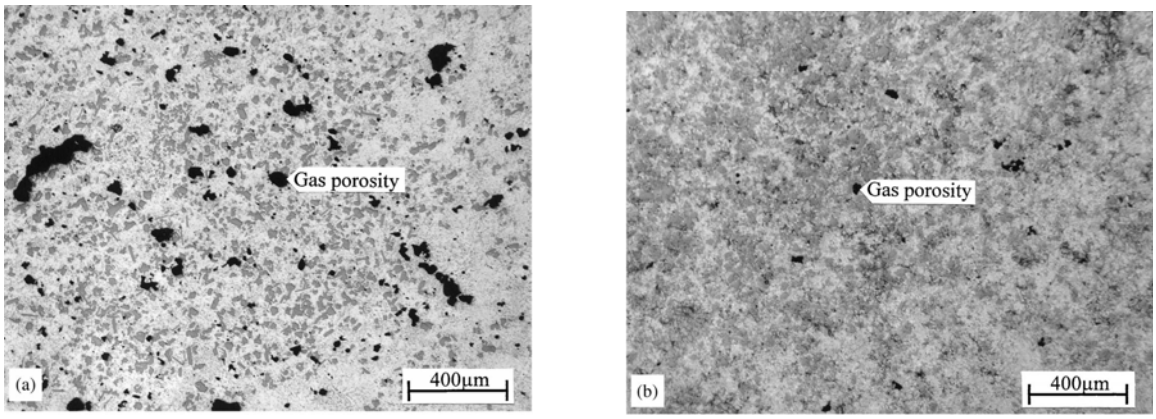

(a) (b)

Figure 2.28 Light optical micrographs of castings in the Al-18%Si alloy, showing the porosity distribution in: (a) conventional, (b) vacuum assisted die castings [24].

Figure 2.27 and 2.38 shows the micrographs of the Al-8%Si and Al-18%Si alloys, respectively which were die cast using both conventional and vacuum system. It can be seen that a great number of gas pores were produced during conventional die casting (Figs. 2.27a and 2.28a). In contrast, the size and the number of the gas pores were significantly reduced and showed a uniform distribution in the vacuum assisted die castings (Figs. 2.27b and 2.28b). This result indicates that the vacuum assistance indeed benefits to reduce gas porosity in casting component.

Porosity plays an important role in fracture mechanism. As mentioned before porosity acts as a stress concentrator and thus crack initiate as well as propagate through those weak sites. Therefore the cast product fails at very low deformation. Niu et al. [24] studied this fracture mechanism in conventional and vacuum assisted die casting product and a significant improvement in fracture behaviour was observed when the cast product prevents from porosity formation. They are shown in Figures 2.29 and 2.30.

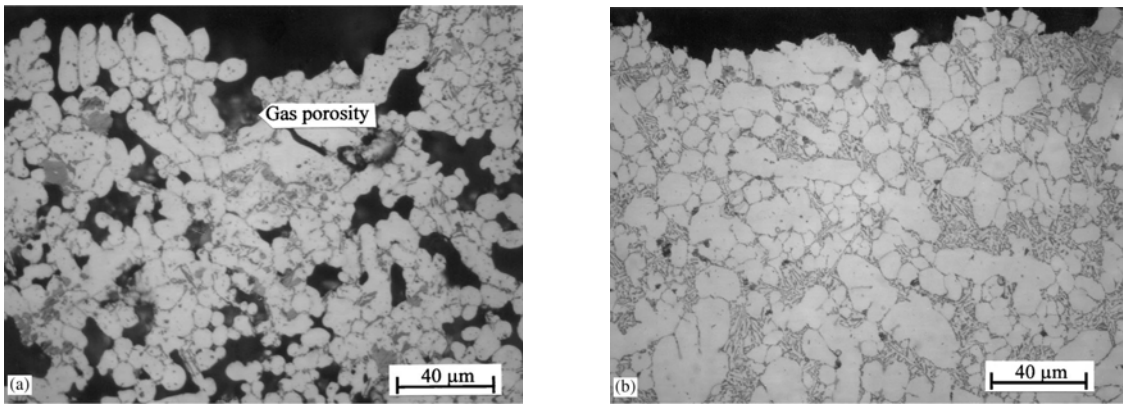

(a) (b)

Figure 2.29 Light optical micrographs of a longitudinal section of the fractured castings for the Al-8%Si alloy: (a) conventional die casting; (b) vacuum assisted die casting [24].

Figure 2.29 (a) shows the fracture in conventional die cast component where it is seen that a significant amount of porosity arises with this type of process and cracks are easily formed in the porosity because of high stress concentration due to the reduced effective area. Fracture path is therefore along the interconnection of the porosity thus the deformation should be very low and fracture should proceeds in brittle manner [24].

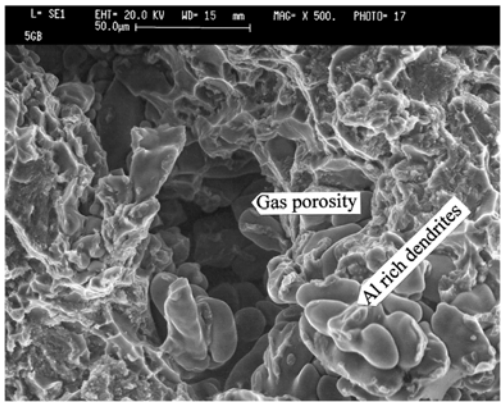

Figure 2.30 SEM micrograph of the fracture surface around a gas pore for the Al-8%Si alloy [24].

To observe the deformation pattern Niu also observed the fractured (longitudinal) surface along the porosity in scanning electron microscope (SEM) which is shown in Figure 2.30. In this analysis it can be seen that smooth α-Al grains can be observed ever after the fracture which indicates relatively low deformation occurring in the region near a pore. Therefore, the specimen fractured under lower stress and strain. However using vacuum system significantly reduce the porosity level and thus the fractured surface revealed ductile fracture behaviour with a large degree of deformation occurring before fracture which is shown in Figure 2.29 (b). Here in this case Fracture was found to originate from the eutectic silicon plates and the fracture path is mainly along the boundary between the a-Al grains and the eutectic mixture [24]. This analysis proved successfully that the strength and ductility were improved by vacuum assistance due to the reduction of porosity in the castings.

2.8 Die Casting Alloys

Now a day's high pressure die casting (HPDC) is widely used as a cost-effective way to mass-produce metal components that are required to have close dimensional tolerances and smooth surface finishes. However standard HPDC components cannot conventionally heat treated to improve mechanical properties as mentioned before in the preceding sections because the castings are relatively porous. It is experimentally found that during conventional solution treatment (e.g. at 500˚C for 8h), the pores expand, resulting in the unacceptable surface blisters (Figure 2.17), distortion and lower mechanical properties [46].

Recently, CSIRO Light Metals Flagship in Australia has revealed a heat treatment cycle for HPDC aluminum alloys that avoids these problems. Exploiting age hardening, large improvements in tensile properties have been achieved as compared with the as-cast condition. Usually the 0.2% proof stress may be approximately doubled when compared to the as-cast condition, although the actual properties that result depend on the alloy, the part geometry, wall thickness its quality and the exact procedures utilized [46]. However vacuum assistance system is becoming very popular in die casting industry which eliminates gas porosity in a satisfactory level and enables the most common engineering alloys to be heat treated for adequate mechanical properties. It is shown in heat treatment sections (section 2.9.5) of this chapter, how vacuum assistance system facilitates heat treatment to improve mechanical properties.

NADCA accumulated some HPDC aluminum alloys from various countries or regions which are capable of responding to heat treatment are shown in table 2-5 [46]. It is found that several of these alloys also have corresponding equivalents in other regions. For example, A380 is also equivalent to the British standard alloy LM24.

Table 2-4 Heat treatable HPDC alloys from different world regions [46]

Alloy/ w% (Al bal)	Si	Fe	Cu	Mn	Mg	Ni	Zn	Pb	Sn	Ti	Others
CA313(Aus)	7.5-9.5	Max 1.3	3.0-4.0	Max 0.5	Max 0.3	Max 0.5	Max 3	Max 0.35	Max 0.25	Max 0.2	Max 0.2
A380 (US)	7.5-9.5	Max 1.3	3.0-4.0	Max 0.5	Max 0.1	Max 0.5	Max 3		Max 0.35		Max 0.5
C380(US)	7.5-9.5	Max 1.3	3.0-4.0	Max 0.5	0.1-0.3	Max 0.5	Max 3		Max 0.35		Max 0.5
A383(US)	9.5-11.5	Max 1.3	2.0-3.0	Max 0.5	0.1-0.3	Max 0.5	Max 3		Max 0.15		Max 0.5
383(US)	9.5-11.5	Max 1.3	2.0-3.0	Max 0.5	Max 0.1	Max 0.5	Max 3		Max 0.15		Max 0.5
A384(US)	10.5-12	Max 1.3	3.0-4.5	Max 0.5	Max 0.1	Max 0.5	Max 1		Max 0.35		Max 0.5
B384(US)	10.5-12	Max 1.3	3.0-4.5	Max 0.5	0.1-0.3	Max 0.5	Max 1		Max 0.35		Max 0.5
390(US)	16-18	Max 1.3	4.0-5.0	Max 0.5	0.45-0.65	Max 0.1	Max 1.5			Max 0.1	Max 0.2
ADC10 (JIS)	7.5-9.5	Max 1.3	2.0-4.0	Max 0.5	Max 0.3	Max 0.5	Max 1		Max 0.3		
ADC12 (JIS)	10.5-12	Max 1.3	1.5-3.5	Max 0.5	Max 0.3	Max 0.5	Max 1		Max 0.3		
AlSi8Cu3 (Fe)(0(ISO)	7.5-9.5	Max 1.3	2.5-4.0	Max 0.6	Max 0.3	Max 0.5	Max 1.2	Max 0.3	Max 0.2	Max 0.2	Max 0.5
AlSi9Cu3(Fe) (DIN226)	8.0-11.0	Max 1.2	2.0-3.5	0.1-0.5	0.1-0.5	Max 0.3	Max 1.2	Max 0.2	Max 0.1	Max 0.15	Max 0.15
SC84R (Canada)	7.5-9.5	0.7-1.2	3.0-4.0	Max 0.5	0.45-0.75		0.7-1.2			Max 0.1	Max 0.15
LM2(UK)	9.0-11.5	Max 1.0	0.7-2.5	Max 0.5	Max 0.3	Max 0.5	Max 2	Max 0.3	Max 0.2	Max 0.2	Max 0.05
A360(US)	9.0-10.0	Max 1.3	Max 0.6	Max 0.35	0.4-0.6	Max 0.5	Max 0.5		Max 0.15		Max 0.25
AlSi10Mg (DIN 239B)	9-11	Max 0.8	Max 0.8	Max 0.4	0.2-0.5		Max 0.1			Max 0.15	Max 0.15

2.8.1 Introduction of Silafont-36 (AA365)

Silafont-36 or AA365 alloy is one of the predominant aluminum alloy used in automotive industry because of its ease of handling in the cast house, excellent castability, outstanding mechanical properties and good welding characteristics with all standard processes.

In Table 2-5, the standard chemical composition is listed. Silicon content about 9.5% offers good castability and excellent die-filling capabilities for this kind of alloy. This is important when large parts are cast or when complicated die designs have to be filled. Since silicon expands during solidification, lower shrinkage behaviour and hot tearing tendencies are avoided compared to other alloys systems. Eutectic silicon is modified by strontium in silafont-36 which is very important for ductility because strontium additions change the silicon morphology from a blocky or lamellar type into a more coral like form. However, strontium will enhance hydrogen pick-up in the melt which requires an efficient melt cleaning device such as impeller technique. This helps to keep hydrogen content at a lower level and thus minimizes porosity formation and provides good weldability. Moreover strontium modified structure usually provides higher elongation instead of higher cooling rate in die casting process [47]. This is shown in Figure 2.31 where the samples were taken from 4 mm die-cast plates. Experimentally found that by adding Strontium in the range of approximately 100 ppm to 200 ppm, the elongation was increased from 5% to 10% [48].

Table 2-5 Chemical composition of Silafont-36 (AA 365) [47]

Alloy	Element (wt%)							
	Si	**Fe**	**Mn**	**Mg**	**Cu**	**Ti**	**Sr**	**Al**
Silafont-36	9.51	0.12	0.65	0.13	0.02	0.04	0.023	Balance

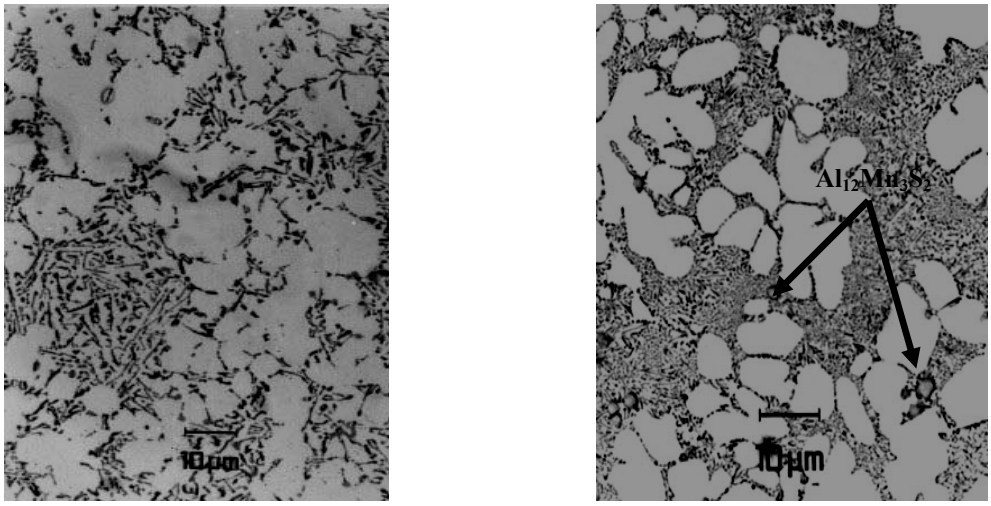

(a) (b)

Figure 2.31 (a) Micro structure of AlSi10Mg alloy, 5% elongation; (b)Micro structure of Silafont-36, 10% elongation (Temper F, not etched Test plate 4 mm wall thickness) [48].

In Silafont-36, Iron content usually kept below 0.12% (wt %) to minimize the formation of AlFeSi-phases that appear as needle-like shapes in the cast microstructure. Because of their acicular morphology, they deteriorate strength, elongation and fatigue behaviour of the overall alloy [48]. However Manganese is used in place of Iron to provide good ejection behaviour and reduced die soldering. Manganese forms $Al_{12}Mn_3Si_2$ type phases in Silafont-36 which appear as globulitic particles in the microstructure, as

seen in Figure 2.31(b). Furthermore the amount of Magnesium content determines the mechanical properties and aging behaviour [48].

2.8.1.1 Influence of Manganese

It was established in the literature [49] that Manganese will lower ductility in an AlSiMg alloy when its content exceeds 0.2%. Therefore Manganese was not recommended as an addition to high pressure die casting alloys to substitute Iron or as a combination with Iron.

According to Zovi et al. [50] Manganese content has very negligible effect on ultimate tensile strength and yield strength which is illustrated in Figure 2.32. Figure 2.33 also shows almost same behaviour with the T6 treated samples. However samples with no Manganese showed a different behaviour which might be caused by the very poor ejection behaviour as described above. Because of this poor ejection behaviour the casting parts had cracks or marks on the surface and the heat treatment may have caused surface damage leading to poor results [50].

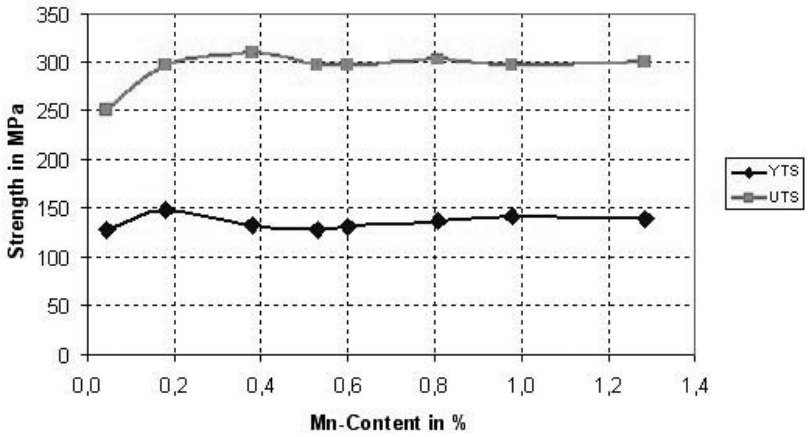

Figure 2.32 Mechanical properties as a function of Manganese content in As Cast Condition (F) [50].

Moreover the elongation, as seen in Figure 2.34 for both as cast (F) and solution treated (T6) conditions shows a different behaviour. However, in both cases without any Manganese there are poor values of elongation due to poor ejection behaviour. It can be seen that in as cast state there is a steady elongation exist with a manganese content of >0.4%. Even with using high Manganese content, the elongation is still above 8% but the optimum content was found to be between 0.5% and 0.8%. In contrast at heat treated condition, elongation value is found different.

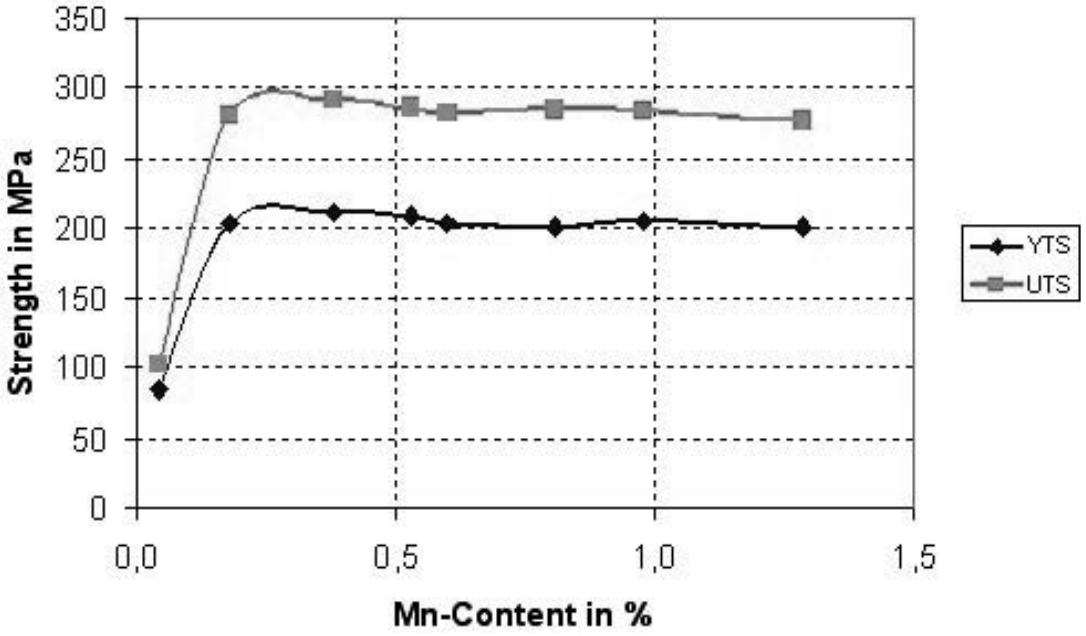

Figure 2.33 Mechanical properties as a function of Manganese content (at T6 Temper) [50].

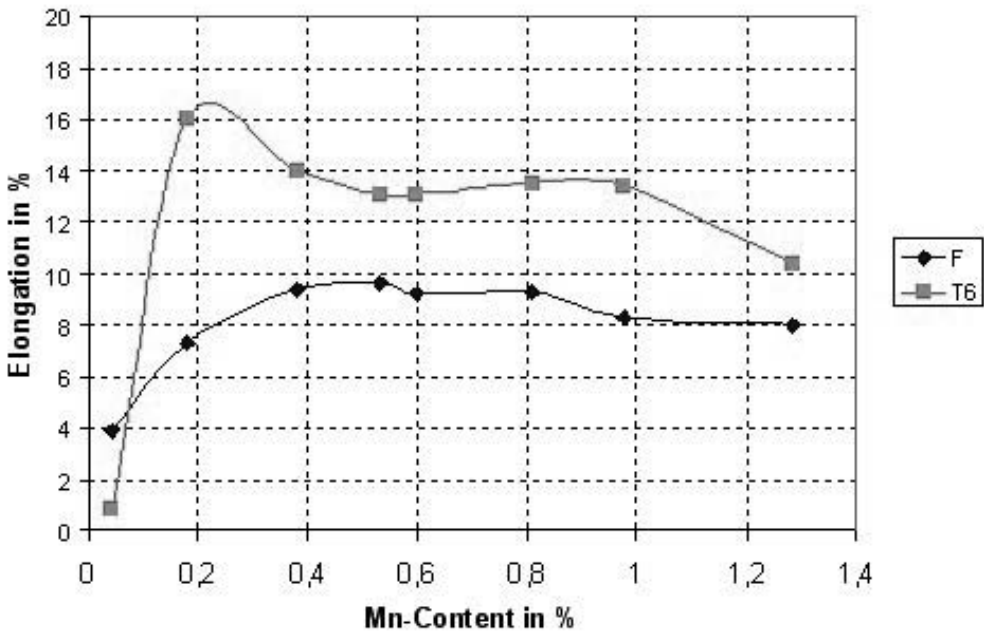

Figure 2.34 Elongation as a function of Manganese content, Temper F and Temper T6 [50].

The highest value of Manganes was measured in Zovi's work is about 0.2%, which provides a constant elongation of 12% to 14% over a range of 0.4 to 1.0%. Therefore, the optimum range for stable condition is between 0.5% and 0.8% Manganese. Solution treatment might be caused the differences in elongation where the intermetallic phase of Manganese forms globular particles as they have a higher impact on ductility than in the as cast state [50].

2.8.1.2 Influence of Magnesium on the Mechanical Properties of Silafont-36

Currently, there are four versions of Silafont-36 used in automotive sectors. They are as follows:

0.13 – 0.19 wt% Magnesium

This amount of Mg generally used for crash relevant parts and connecting techniques such as flanging. The parts were heat treated for increasing ductility or to

avoid long term natural aging. Examples include nodes or damping parts where the damping insert is fixed using flanging technique [50].

0.18 – 0.24 wt % Magnesium

Safety parts with medium requirements on yield strength, good fatigue properties and crash relevant properties are made with this much of Mg. An example would be the engine cradles. Proper heat treatments are required to meet the desired requirements [50].

0.24 – 0.35 wt % Magnesium

For parts where high yield strength is required in combination with good impact properties such as steering racks or end plates. High screw forces should be possible for mounting parts together [50].

0.28 – 0.35 wt % Magnesium

This amount of Mg is generally used for structural components requiring heat treatments with air quenching after solutionizing [50].

2.8.1.3 Applications of Silafont-36

Magnesium content around 0.15% is used for making damping part which is shown in Figure 2.35. The edge is flanged and had to withstand all the forces during lifetime of the part. A sound grain structure expected in the flanged area as the oxide skins or pre-solidifications will lead to poor results during the deformation process.

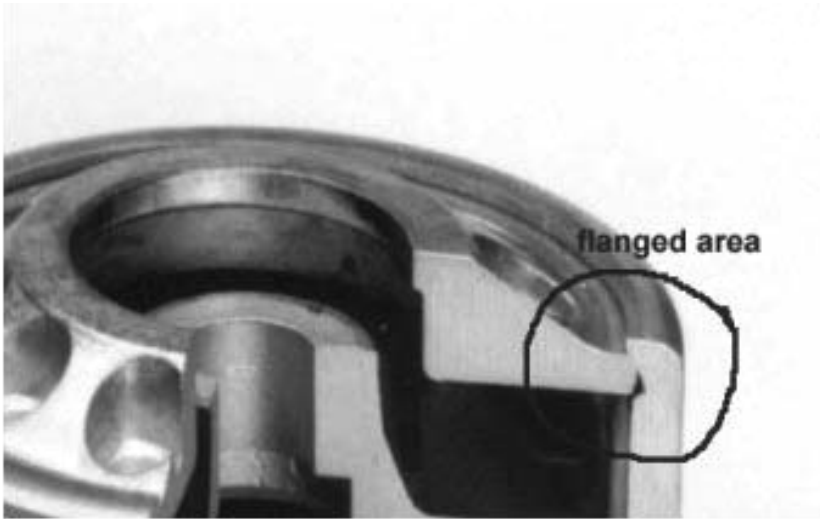

Figure 2.35 Damping part showing flanged area, magnesium content 0.15%. Temper F [50].

Figure 2.36 Rear swinging fork, YAMAHA YZF-R6 [51].

Another interesting application in T5 condition is the rear swing arm of the new YAMAHA YZF-R6 motorcycle shown in Figure 2.36. This is the first street motorcycle ever to use YAMAHA'S new Controlled Filling Die Casting Technique resulting in a lighter Aluminum chassis that is stiffer. What once took 16 welds now requires only two [51**].** It is produced with a Magnesium content of 0.2% and has a T5 heat treatment to

shift the yield strength above 200 MPa**.** The two halves were welded together using MIG welding technique. Therefore the melt has to be degassed properly and the gating system must avoid turbulence in the areas to be welded.

YAMAHA YZF-R6 motorbikes seat frame also using silafont-36 successfully which provides more stiffness and saves weight (Figure 2.37).

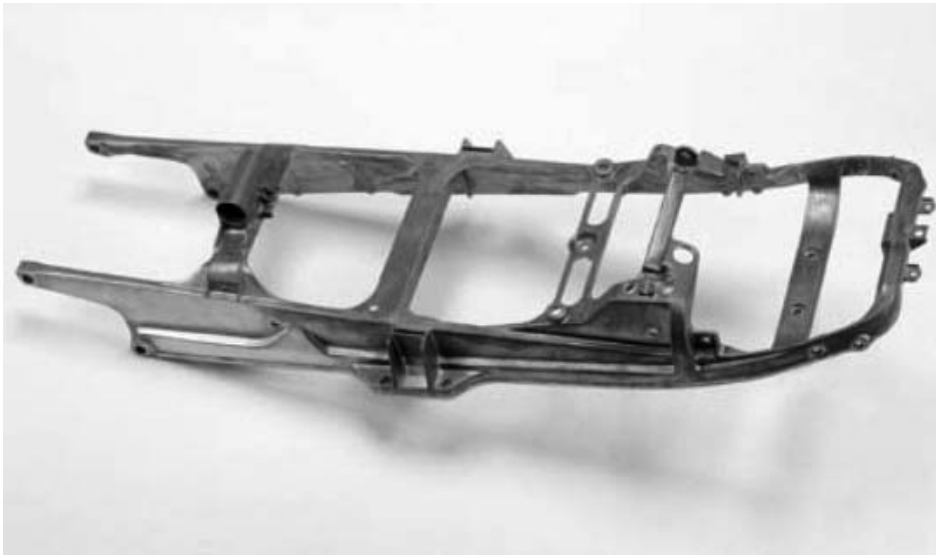

Figure 2.37 Seat frame, YAMAHA YZF-R6, gives more stiffness and saves weight [51].

2.8.1.4 Properties at a Glance of Silafont-36

Silafont-36 alloy provides the following outstanding quality which makes it very attractive in automotive sectors [48]:

- Excellent castability
- Suitable for minimum wall thicknesses
- No sticking to the die
- Magnesium content can be adjusted to different requirements
- Heat-treatable to maximum elongation and high energy absorption

- Very good corrosion resistance
- High fatigue strength
- Excellent weldability
- Excellent machinability
- Suitable for self-piercing riveting

2.9 Heat Treatment of Die Cast Aluminum Alloys

2.9.1 Purpose of Heat Treatment

The principal purpose of heat treatment is to develop the best combination of mechanical properties that will meet the critical needs required for the specific application. Heat treatment provides the following advantages in casting products:

Homogenization—because of alloying and presence of impurity elements, segregation of elements into the grain boundaries observes during cooling. Because of this segregation effect, microstructure of castings in the as-cast state usually not homogeneous. However, concentrations of elements vary depending on alloy type and solidification rate. Homogenization is thus desirable to distribute elements throughout the matrix so properties in the casting will be more uniform.

Stress relief--residual stresses are created during cooling from elevated casting and solution temperatures. Upon cooling, the hot liquid metal starts to freeze and becomes solid at the melting point if it is a pure substance or a eutectic or over a temperature range if it is an alloy. As the liquid is turning into a solid it starts to develop stresses as a result of the denser and more crystalline regularity present in the atomic arrangement, which is held by stronger interatomic binding forces than in the liquid state. In die casting residual

stress often arises due to high solidification rate and pressure induce during injection of molten metal in to die cavity. Heating the casting to an intermediate temperature can relieve internal stresses and make the casting dimensionally stable.

Improved stability and machinability--changes in the microstructure can leads castings to grow over time. To maintain tight dimensional tolerances during and after machining, castings should be heat treated to form stable phase.

Mechanical property improvement--mechanical properties are improved by spheroidizing constituent phase particles and by precipitation hardening. Corrosion resistance is improved by homogenizing. Age hardening principles can be used to tailor heat treatments to applications.

2.9.2 Types of Thermal Treatment

In foundry ten different thermal treatments (Table 2-6) generally practiced with many additional variations. Naturally aging method at room temperature is a classical approach to improve properties but usually this process takes several weeks. Therefore artificial aging becomes popular to save time as well as to attain maximum mechanical properties.

Table 2-6 Temper Designation [10]

T1	Cooled from an elevated temperature shaping process (such as extrusion or casting) and strengthened by naturally aging to a substantially stable condition. These products are not cold-worked.
T2	Annealed to improve ductility and dimensional stability of a product. These products are cold-worked.
T3	Solution heat-treated (quenched), cold-worked by a flattening or straightening operation to strengthen the product, and naturally aged to a substantially stable condition.

T4	Solution heat-treated (quenched) and strengthened by naturally aging to a substantially stable condition.
T5	Partially solution heat-treated (quenched), then artificially aged. These products are not cold-worked.
T6	Solution heat-treated (quenched) and artificially aged. These products are not cold-worked.
T7	Solution heat-treated (quenched), then overaged/stabilized. These products are artificially aged to carry them beyond a point of maximum strength to provide control of some significant characteristic other than mechanical properties.
T8	Solution heat-treated (quenched), cold-worked, then artificially aged.
T9	Solution heat-treated (quenched), artificially aged, then cold-worked to strengthen the product.
T10	Partially solution heat-treated (quenched), artificially aged, and then cold worked to strengthen the product.

2.9.3 Method of Heat Treatments

The most important heat treatment methods for aluminum alloys are soft annealing and precipitation hardening [52].

2.9.3.1 Soft Annealing

This is a world wide used process in casting industry as a means for improving ductility, toughness as well as to homogenize the castings products. Annealing is applied to both grades (wrought and cast) to promote softening. Complete and partial annealing heat treatments are the only ones used for the non-heat treatable alloys. The exception is the 5000 series alloys which are sometimes given low temperature stabilisation treatment and this is carried out by the producer. This is usually used where the casting products suffers chemical segregation during solidification which in turn have a detrimental effect on mechanical properties.

A common problem arise by chemical segregation is dendrite formation during solidification. By annealing, namely heating the sample to sufficiently higher temperature for specific time duration can resolve the negative effect of dendrite formation. The annealing time for homogenization is a function of temperature and dendrite arm spacing [53]. Usually the shorter the dendrite arm spacing (DAS), the higher the annealing temperature is needed.

Usually temperature between 350˚C to 520˚C is used to temper the alloy in order to achieve lowest possible strength and highest possible ductility. Heating times at temperature vary from 0.5 to 3 hours, conditional on the size of the load and the alloy type. Generally, the time need not be longer than that required to stabilise the load at temperature. Rate of cooling after annealing is not critical [54].

2.9.3.2 Precipitation Hardening

The most important heat treatment for aluminium alloys is precipitation hardening. The main propose of this process to create a dispersion of particles in matrix which in turn will prevent the dislocation movement.

The success of precipitation hardening depends on some special metallurgical process for which some prerequisites must be created or must already exist within the system [52]. A successful precipitation hardening mostly relies on the understanding of basic mechanism and their affects on mechanical properties.

The prerequisites for precipitation hardening is the presence of a α-solid solution exhibiting solubility for a certain alloy constituent that decreases with temperature and that has been cooled so rapidly from a temperature of high solubility that it is converted to a strongly supersaturated state. The alloy convert in this supersaturated solution tends

naturally to reach the thermodynamic equilibrium state corresponding to lower temperatures. This leads to the segregation and precipitation as mentioned above.

For precipitation hardening to occur, the second phase must be soluble at an elevated temperature but must exhibit decreasing solid solubility with decreasing temperature. Heat-treatable (precipitation-hardening) aluminum alloys contains elements that decrease its solubility with decreasing temperature, and in concentrations that exceed their equilibrium solid solubility at room temperature and moderately higher temperatures.

In general there are three main steps in the precipitation hardening heat treatment [55, 56]:

I. Solution Heat Treatment

The purpose of solution heat treatment is the dissolution of the maximum amount of soluble elements from the alloy into solid solution. The process consists of heating and holding the alloy at a temperature sufficiently high and for a long enough period of time to achieve a nearly homogenous solid solution in which all phases have dissolved [Figure 2.38].

In the as-cast condition due to limited solid solubility, a large proportion of the precipitate-forming elements are contained in constituent phases. Hence, the primary purpose of the solution treatment is to dissolve the constituent phases and enrich the α-aluminum solid solution in solute element.

The second aim of solution treatment is spheroidization of some constituents that are present in quantities that cannot be fully dissolved. In Al-Si-Mg or Al-Si-Cu-Mg alloys, excess silicon is always present. As-cast eutectic silicon forms either flakes, fibres or lamellae (the latter two result from eutectic modification treatments). During solution

treatment, silicon particles globularize and begin to coarsen. It should be mentioned that the modified alloys undergo rapid spheroidization while complete spheroidization is not achieved in unmodified alloys even after very long time.

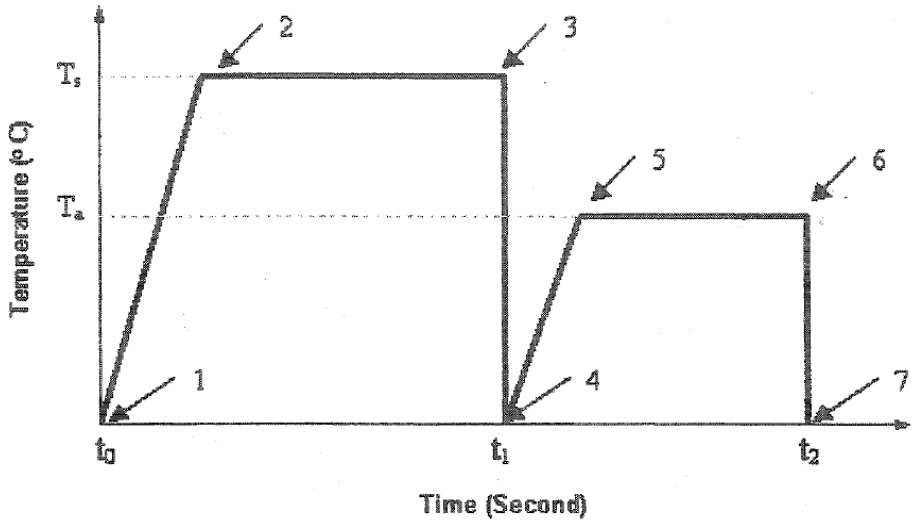

Figure 2.38 T6 (Solution treatment) Heat Treatment- Temperature Vs Time Plot.

The third effect of solution treatment is to homogenize the microstructure. In addition to eliminating the effects of coring & segregation (Compositional non-uniformity due to delayed reactions) the elements in the constituent are more evenly distributed when they dissolve. Prior to age hardening, it is desirable to have the greatest possible concentration of precipitate-forming elements in some solution. Hence, solution temperatures must be high to facilitate diffusion of alloying element atoms and to increase their solubility.

A potential for localized melting exists because of the presence of low melting point nonequilibrium eutectic colonies that form during solidification. These eutectic colonies melt if the liquidus temperature that corresponds to their local composition is

exceeded, a process called incipient melting. Expansion is followed by contraction as the region melts and (after approaching equilibrium with the surrounding metal) resolidifies. This creates voids that approximate the breadth of the melted zone [57].

II. Quenching

This step applied when the materials become completely homogenous. At this time casting is cooled from the solution temperature and the solubility of hardening elements starts to decrease. Solutes are lost from the enriched α-aluminum solid solution by precipitation and by diffusion to grain boundaries, processes that occur most rapidly between 260-400°C. Hence, rapid cooling or quenching is necessary to retain the high concentrations that were in equilibrium at the solution temperature, particularly near grain boundaries. Although rapid quenching increases response to age hardening, it also creates residual stresses and distortion, factors that must be considered for each casting design.

III. Age Hardening

The excess solutes that are supersaturated in α-aluminum will eventually precipitate, but this occurs slowly at room temperature. After days and weeks at room temperature, some alloys, such as those belonging to the Al-Zn-Mg system, harden appreciably - a process called natural aging. However, aging may be accelerated by heating castings in the as-quenched condition to intermediate temperatures, a process called artificial aging.

After the initial stages of aging, the structure is said to be underaged. Increased time at temperature or aging at a greater temperature further evolves the precipitate structure, and hardness increases to a maximum, known as the peak hardness condition. Further aging decreases hardness, and the structure becomes overaged. Progression of the

aging process also affects ductility. Ductility, while high in the as-quenched condition, reduces during hardening. In overaging conditions, loss of hardness permits more extensive deformation of the metal matrix to occur before fracture (i.e., ductility increases). Annealing, which can be described as an extreme overaging, maximizes ductility.

2.9.4 Heat Treatment Selection Criteria for Die Casting

High-pressure die-casting (HPDC) is a popular and cost-effective method for mass producing metal components where physical dimensions must be accurately replicated and surface finish is important. Approximately half of all castings worldwide that are made from aluminum alloys are manufactured this way, and these are used for a wide range of automotive parts and other consumer goods. However, two features of conventionally produced HPDCs are the extreme turbulence experienced by the molten metal as it is forced at high speed into a die, and the very rapid rate at which it then solidifies. Because of this, castings usually contain internal pores in which gases such as air, or vapours formed by the decomposition of organic die wall lubricants are entrapped. Porosity may also result because of metal shrinkage during solidification as mentioned in the preceding sections. Planar defects such as oxide skins and cold shuts may also be present. Whereas it is normal to accept some level of porosity in die-castings, the presence of internal gas-filled pores does have the major disadvantage that components made from aluminum alloys which have the capacity to respond to age hardening cannot be heat treated at high temperatures. Heat treatment cannot be used because, during solution treatment (e.g. 8 h at 540˚C), gas pressure in the pores causes them to expand,

resulting in unacceptable surface blistering. Moreover, the dimensions of die-cast parts may change due to swelling, and mechanical properties are adversely affected.

In Aluminum alloys, heat treatment is one of the superior tools to improve mechanical properties. This is successfully proved in several research works. Among all types of heat treatment, solution heat treatment is the most popular one which significantly improve the microstructure of the alloy and in turns improve the mechanical properties by creating some strengthening phase as well as by improving the morphology of silicon. However in die cast aluminum alloys, entrapment of gaseous substances creates the main obstacle for the improvement of die cast aluminum alloys by heat treatment. NADCA (North American Die Casting Association) experienced that die castings are not usually solution heat treated. Low temperature aging treatment may be used for stress relief or dimensional stability. A T2 or T5 temper may be given to improve properties. Because of the severe chill rate and ultra-fine grain size in die casting, their "as-cast" structure approaches that of the solution heat-treated condition. T4 and T5 temper results in properties quite similar to those which might be obtained if given full T6 temper. Moreover die castings are not generally gas or arc welded or brazed [1].

2.9.5 Heat Treatment of Vacuum Die Cast Aluminum Alloy

From the previous discussion it is already illustrated how vacuum assistance system facilitate in HPDC process. This unique method not only eliminates porosity from a casting component but it also enables the component heat treatable to improve mechanical properties without any blistering effect. Moreover as the porosity levels are significantly reduced with this process now the casting component can be used in structural purposes.

According to Niu et al. [24] vacuum assisted high pressure die casting shows significant improvements of mechanical properties by heat treatment (T6). However when the similar treatment was applied to conventional die casting due to the expansion of the air in the porosity beneath the part surface, the formation of surface blisters was evident. In contrast, the surface blister defect is reduced markedly in vacuum assisted die castings, particularly for the hypoeutectic (Al±8%Si) alloy (Figure 2.39 b and 2.40 d), indicating that heat treatment is possible.

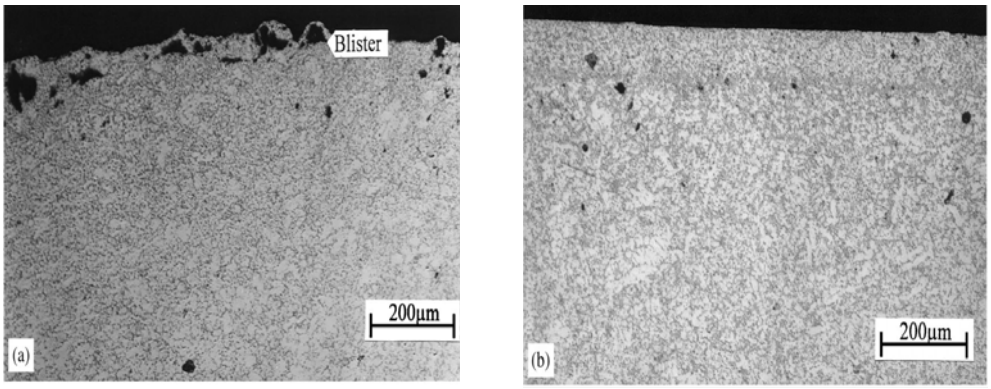

Figure 2.39 Light optical micrograph showing the casting surface after T6 heat treatment on hypoeutectic Al-Si: (a) conventional; (b) Vacuum assisted hypoeutectic alloy [24].

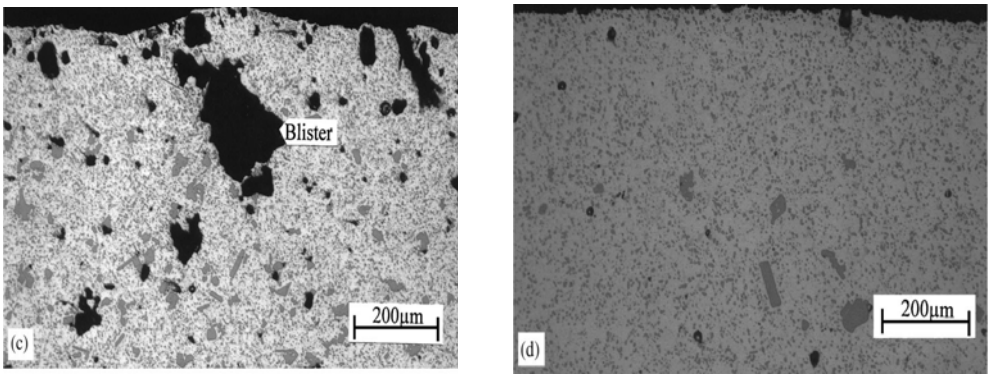

Figure 2.40 Light optical micrograph showing the casting surface after T6 heat treatment on hypereutectic Al-Si: (a) conventional; (b) Vacuum assisted hyper eutectic alloy [24].

The improvement of mechanical properties under heat treatment with vacuum assistance is shown by the data listed in Table 2-7.

Table 2-7 Comparison between as-cast and as-heat-treated alloys [24]

Alloy	**Process**	**UTS (MPa)**	**Elongation (%)**	**Hardness (HRF)**
Al-5% Si	T6 Tempering	266 ± 8.4	8.1±1.5	87±1.5
	As Cast	209±10.9	4.5±1.2	74±1.3
Al-8% Si	T6 Tempering	317±7.7	19.6±1.7	94±1.0
	As Cast	276±4.5	6.0±0.4	80±1.5
Al-18% Si	T6 Tempering	276±13.4	3.9±0.5	102±1.3
	As Cast	249±8.3	2.2±0.2	100±0.8

Therefore the improved soundness of die castings enables them to be heat treatable. Again it has been shown that an isothermal solution treatment followed by an artificial aging can improve the impact toughness of vacuum die cast A380 considerably [43]. Schneider and Feikus et al. [52] studied the effect of solution treatment parameters on tensile properties of vacuum die cast test bars of GD-AlSi9Cu3 (German standard) alloy which is equivalent to A380 in North America. They found that both solution treatment temperature and time affect the tensile properties of vacuum die cast alloy GD-AlSi9Cu3.

According to Hu et al. [58] high pressure vacuum die casting alloy A380 responds to solution treatments. It was shown that solution temperature has a strong affect on

tensile properties of solution treated A380. Moreover the treatment also changes the morphology of silicon phases which enhance the ductility and UTS as well.

Wang et al. [59] found interesting features on A380 alloy (vacuum die casted) by performing solution heat treatment at 480˚C for 12 hours, where the average elongation value has improved 3.91% from 1.11% in as cast condition. Moreover the UTS was found about 273 MPa from 182 MPa for the as-cast state. In his study he found that the silicon morphology was improved which has a sound effect on the tensile properties of the vacuum die cast A380 alloy. The spheroidization of silicon particles during solution treatment enhances not only the ductility but the strength as well. Again it was found that an increase in solution treatment temperatures enhances the growth of silicon particles, and the supersaturation of solid solution to a large extent, which in turn results in a significant improvement in the ultimate strength and microhardness. Average UTS and percent elongation at different solution treatment conditions in Wang study is listed in table 2-8.

Table 2-8 Average UTS and Percent Elongation at Different Solution Treatment condition on A380 Alloy [59]

Treatment Condition	**Average UTS value (MPa)**	**Average Elongation (%)**
As-cast	182.18± 47.74	1.11± 0.61
480˚C × 0.5 hr	249.86± 32.26	1.23± 0.46
460˚C × 12 hrs	250.35±23.97	3.22±0.90
480˚C × 12 hrs	260.69±22.20	3.91±1.07
500˚C ×12 hrs	273.27±6.77	3.68±0.72
480˚C × 0.5 hr	197±12.20	1.78±0.35

The work by Lumley et al. [60] indicated that blistering is substantially reduced and eventually completely eliminated as the temperature and time of solution treatment are decreased. They have studied on aluminum alloy 360 (Al-9Si-0.7Fe-0.6Mg-0.3Cu-0.2Zn-0.1Mn) and found at temperature below 525˚C for 15 minutes have no blistering or dimensional instability.

Timelli et al. [61] studied the effect of solution treatments on microstructure and mechanical properties of a die-cast AlSi7MgMn alloy. According to his study a solution heat treatment of 15 minutes at 475˚C, or a heat treatment involving even more time at 525˚C, causes spheroidization, coarsening, and an increase in the interparticle distance of the eutectic silicon particles, leading to substantial changes in the microstructure and mechanical properties (Figure 2.41). Moreover the distribution of the silicon particles (eutectic Si) is significantly affected by a short solution heat treatment time. The fraction of eutectic Si has been immediately reduced after a solution treatment of 15 minutes.

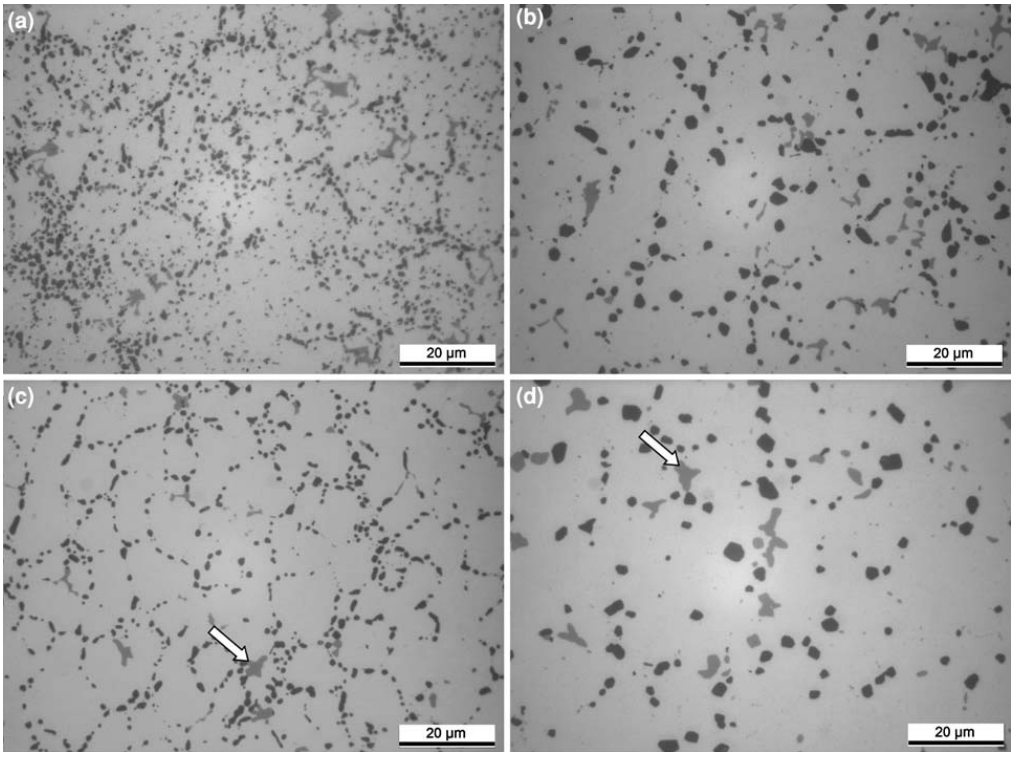

Figure 2.41 Microstructure of die-cast AlSi7MgMn alloy after solution heat treatment. The alloy have been solutionized at 475˚C for (a) 15 min and (b) 480 min, at 525˚C for (c) 15 min and (d) 480 min. Arrows indicate α-Al(FeMnSi) intermetallic particles [61].

2.9.6 Problems in High Temperature Treatment

From the preceding section it is learnt that in vacuum assisted system a vacuum valve is incorporate in to the die in order to evacuate the entrapped air from cavity. Niu et al. [24] reported a significant reduction of porosity in their sample casting compared to castings made by the same process without vacuum assistance, but admitted that it was impossible to avoid gas entrapment and gas porosity completely. One reason given for this was the false air pulled into the die via the die parting line and sliding core guides. In vacuum-assisted HPDC the dies are usually unsealed, and a flow of external air into the

die is very possible. Wang et al.[45] reported that the leakage rates of roughly 230 mbar/s in an unsealed die.

Moreover the movement of the plunger in the first stage of the shot is very critical for casting quality. Generally the fill ratio of liquid melt in the sleeve reaches only 50% and is sometimes lower, while the rest of the volume is filled with air. If this air is trapped in the melt during the shot, the casting will show compressed air porosity and will not be heat treatable or weldable without blistering [40].

Kim et al. [42] presented results from a study on the HPDC of an automotive component which required pressure tightness, and found that the best results were obtained by combining vacuum-assisted HPDC with one local squeeze pin in the die.

Ryobi Die Casting Co. (experimental samples provider) experienced that the gas content of 10cc/100 gm (in final filling area) is not even suitable for T6 heat treatment. However they are currently using a process called HV2 (high vacuum and high velocity) which can be introduced to those components where the fast shot velocity is required very high (3 m/sec) in order to fill thin sections (less than 2 mm) [62].

Besides this Niu et al. [24] also showed that using a pressure level of about 18×10^{-3}-28×10^{-3} MPa during casting was relatively higher than the suggested pressure level (5×10^{-4} MPa) and eventually this effects on the vacuum level due to the vacuum leakage via the parting line. This low vacuum causes porosity in casting and will suffer blistering problem at high temperature treatment like T6.

As mentioned before in the preceding section that NADCA also recommended that it is not always essential to apply solution heat treatment on die castings as because of severe chill rate and ultra fine grain size in die casting their as cast structure approaches almost similar microstructural condition of solution heat treatment. So, low

temperature aging treatment (T2 or T5) may be good enough for stress relief or dimensional stability [1].

2.9.7 Heat Treatment of Silafont-36

According to Koch H.[48] mechanical properties of Silafont-36 depends on magnesium content and heat treatment which is shown in Figure 2.42.

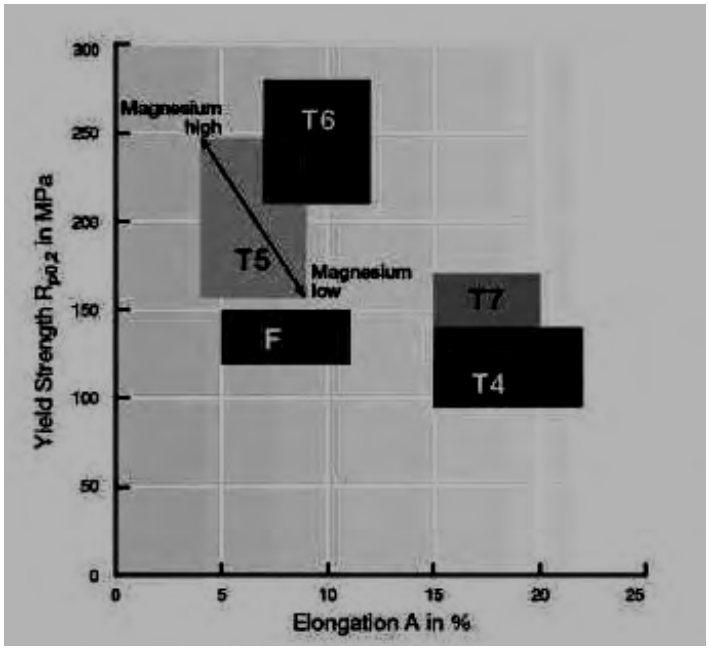

Figure 2.42 Mechanical properties of Silafont-36, depending on Mg content and heat treatment [48].

The chemical analysis used by Koch is shown in Table 2-9 Magnesium was added in the range of 0.003 up to 0.1%.The manganese content was kept at the optimum level of 0.6% and the strontium content of 120 ppm which provides a good modification of the eutectic silicon. A test sample with dimension of 220 mm x 60 mm x 3 mm was cast to determine mechanical properties. The test plate was cast in a single cavity die. Again, a 400 t die-casting machine was used with an adapted forced venting system. The melt was

degassed by using spinning nozzle techniques and the quality was checked with the low pressure test. Before degassing density index was observed to be between 3% and 5%. After treatment a density index was less than 2%.

Table 2-9 Chemical composition for trials with different Magnesium content, wt.% [48]

Heat	Si	Fe	Cu	Mn	Mg	Zn	Ti	Sr
1	10.2	0.09	0.001	0.60	0.003	0.005	0.081	126
2	10.0	0.09	0.001	0.60	0.020	0.005	0.080	121
3	10.5	0.10	0.002	0.60	0.040	0.006	0.084	150
4	10.3	0.09	0.002	0.59	0.082	0.005	0.088	120
5	10.3	0.09	0.002	0.61	0.102	0.005	0.084	120

It was also shown that there is a significant dependence of yield strength on Magnesium content at various heat treatments which is shown in Figure 2. 43.

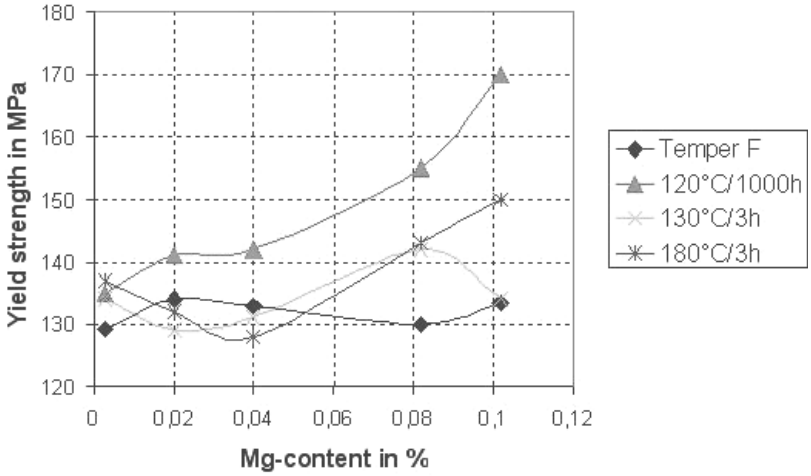

Figure 2.43 Yield strength as a function of magnesium content after several heat treatments. Test sample: 220 mm x 60 mm x 3 mm plate [48].

Figure 2.43 shows the results of the mechanical properties concerning the yield strength after various heat treatments. Except in the as-cast state, all heat treatments tend to influence the yield strength. The aging starts at a magnesium level between 0.04% and 0.08%. A limit could be estimated to be less than 0.06% magnesium. Concerning the ultimate tensile strength, there was no marked influence. The same could be observed with the elongation. With all conditions the elongation was in a range from 10% to 12%, which is quite high for an aluminum-silicon alloy in the as-cast state [48].

NADCA also experienced some significant mechanical properties on Silafont-36 with low magnesium content at low temperature treatment [47]. They are shown in the following cycle in Table 2-10.

Table 2-10 Mechanical properties resulted from aging trials with low magnesium content [47]

	Temper F			**Temper 120˚C/1000 hr**			**Temper 130˚C/3hr**			**Temper 180˚C/3hr**		
Mg Content (%)	**YS (MPa)**	**UTS (MPa)**	**El (%)**	**YS (MPa)**	**UTS (MPa)**	**El (%)**	**YS (MPa)**	**UTS (MPa)**	**El (%)**	**YS (MPa)**	**UTS (MPa)**	**El (%)**
0.003	129	273	12.9	135	273	11.5	134	278	12.2	137	276	11.4
0.02	134	279	11.3	141	269	11.3	129	277	13.3	132	277	11.8
0.04	133	282	12.2	142	274	11.4	131	274	12.4	128	279	11.9
0.082	130	280	11.8	155	280	10.0	142	287	10.0	143	280	10.3
0.102	133	279	10.7	170	292	10.0	134	281	11.3	150	284	10.2

It can be seen that the addition of magnesium effects on yield strength upon heat treatment specifically, the temper 120˚C/1000hr provides much better yield strength with successive increase of Magnesium. However they doesn't effect on UTS or elongation significantly.

Moreover SAG (Salzburger Aluminium Group, Austria) offers the following mechanical properties on Silafont-36 under different heat treatment condition, which are given in Table 2-11. Temper T5 and T6 provides much better strength and microhardness on Silafont-36 alloy. However temper T4 and T7 makes the alloy more ductile with compromising the strength of the associated alloy.

Table 2-11 Mechanical Properties Variation under Different Heat-Treatment on Silafont-36

Casting process condition	**0.2% YS $R_{P0.2}$ N/mm^2**	**Tensile strength R_m N/mm^2**	**Ductile Yield A5 (%)**	**Brinell Hardness HB 5/250**
GD- F	120-150	250-290	5-10%	75-100
GD- T4	95-140	210-260	15-22%	60-75
GD- T5	120-150	260-330	3-10	90-115
GD- T6	150-240	290-350	6-12	100-115
GD- T7	120-170	200-240	15-20	60-75

*GD represents as German Standard

2.10 Quality Index of Aluminum Alloys

Quality index, Q is an empirical parameter that is generally used to characterize the mechanical performance of 356/357 casting alloys [63]. The first quality index developed by Drouzy et al. [64] is given by

$$Q = UTS + d \log (s_f) \quad \text{.....(2.4)}$$

Where UTS is the tensile strength (MPa), s_f is the elongation to fracture (%). Lines generated with Eq.2.4 is called iso-Q lines.

Caceres analytical model

This model provides an overview of the strength-ductility relationship of the material. The model describes the material with the following Ramberg-Osgood relationship [64]:

$$\sigma = K\varepsilon^n \quad \text{.....(2.5)}$$

where σ is the true stress, K is the strength coefficient, n is the strain hardening exponent and ε is the true strain.

Ignoring the elastic component of the total strain, the nominal stress-strain curve can be approximated by

$$P = K[\ln (1+ s)]^n e^{-\ln(1+s)} \quad \text{.....(2.6)}$$

$$n = s/q$$

$$P = Ks^{s/q} e^{-s} \quad \text{.....(2.7)}$$

where, P and s are the engineering values of stress and strain, q is the relative ductility parameter.

The relative ductility parameter q, defined as the ration between the strain hardening exponent of the material, n and the elongation to fracture, s_f.

The quality index developed by Caceres is given by

$$Q = K[(qn)^n e^{-qn} + 0.4 \log (100qn)] \quad \text{.....(2.8)}$$

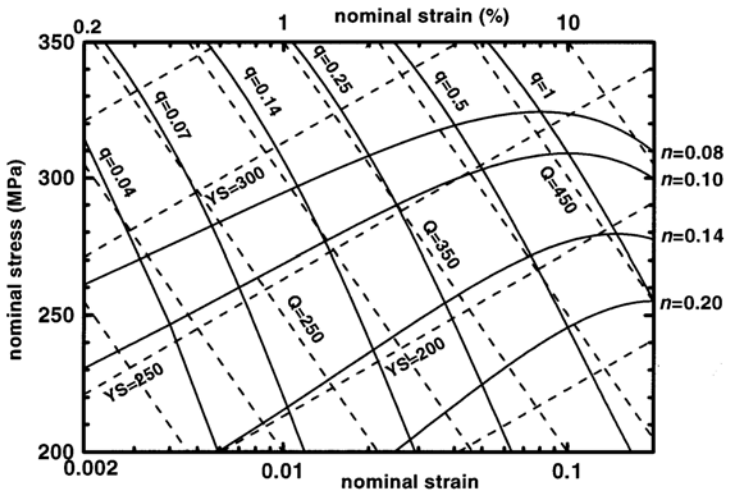

Figure 4.44 A quality index chart for alloy 356. The dashed lines represent the quality index chart as determined with Eq. (2.6) and Eq. (2.7) and Eq. (2.8) [63].

2.11 Summary of Literature Review

Al-Si alloys like 319,356, 380 respond to solution heat treatments which significantly change their microstructure, such as the morphological of silicon particles from acicular needle like shape to globular shape and formation of different strengthening phases like Al_2Cu, Fe-containing phase and Mg-containing phase and in turns, improve their mechanical properties.

It was also shown that vacuum assisted die cast aluminum alloys also respond to solution heat treatment by forming essential Al_2Cu strengthening phase in microstructure. However, proper die sealing and vacuum levels are usually needed to eliminate the inherent entrapment of gases which expands during solution heat treatments. This is because solution treatment performs at relatively high temperature (above 400˚C). These

high temperatures provide sufficient external forces into the casting to release dissolved gases which reduces mechanical properties considerably. Therefore high temperature heat treatments like T4 and T6 are only preferable to the die casting components when a sufficient level of protections from gaseous hazard is adopted during casting.

For emerging Silafont-36 type alloys, even the as-cast product provides good mechanical properties as mentioned in section 2.8.1. As the alloy further modified by strontium, silicon particles should have an enhanced morphology rather the detrimental effect of needle like silicon particles. In the as cast condition this type of alloy should provide 10-12% elongation which is relatively good for Al-Si alloys. The yield strength and ultimate tensile strength are about 150 and 290 MPa, respectively, which are sufficient for engineering requirements of certain structural components. Since the modified Silafont-36 alloy posse's high mechanical properties in the as-cast condition where a moderate level of vacuum system is applied during casting, it is not economically feasible to apply costly solution heat treatment on the as-cast alloy which can meet the required mechanical properties of certain applications. However, in high pressure die casting, residual stresses are usually trapped in large complex thin wall castings the due to high cooling rate during solidification. This residual stress has a negative impact on dimensional stability of the casting during machining and service. Hence, it is necessary to remove this residual stress by applying a low temperature thermal treatment.

As mentioned before, it can never be possible to produce a die cast component without any porosity. So, any kind of heat treatment (either low or high temperature) should have some effect on this inherent porosity of casting components. Therefore a detailed investigation is very essential for determining treatment temperature and time at

which residual stress would be removed from cast components for their dimensional stability while their mechanical properties are at least maintained.

Chapter-III

Experimental Procedure

3.1 Outline of General Procedure

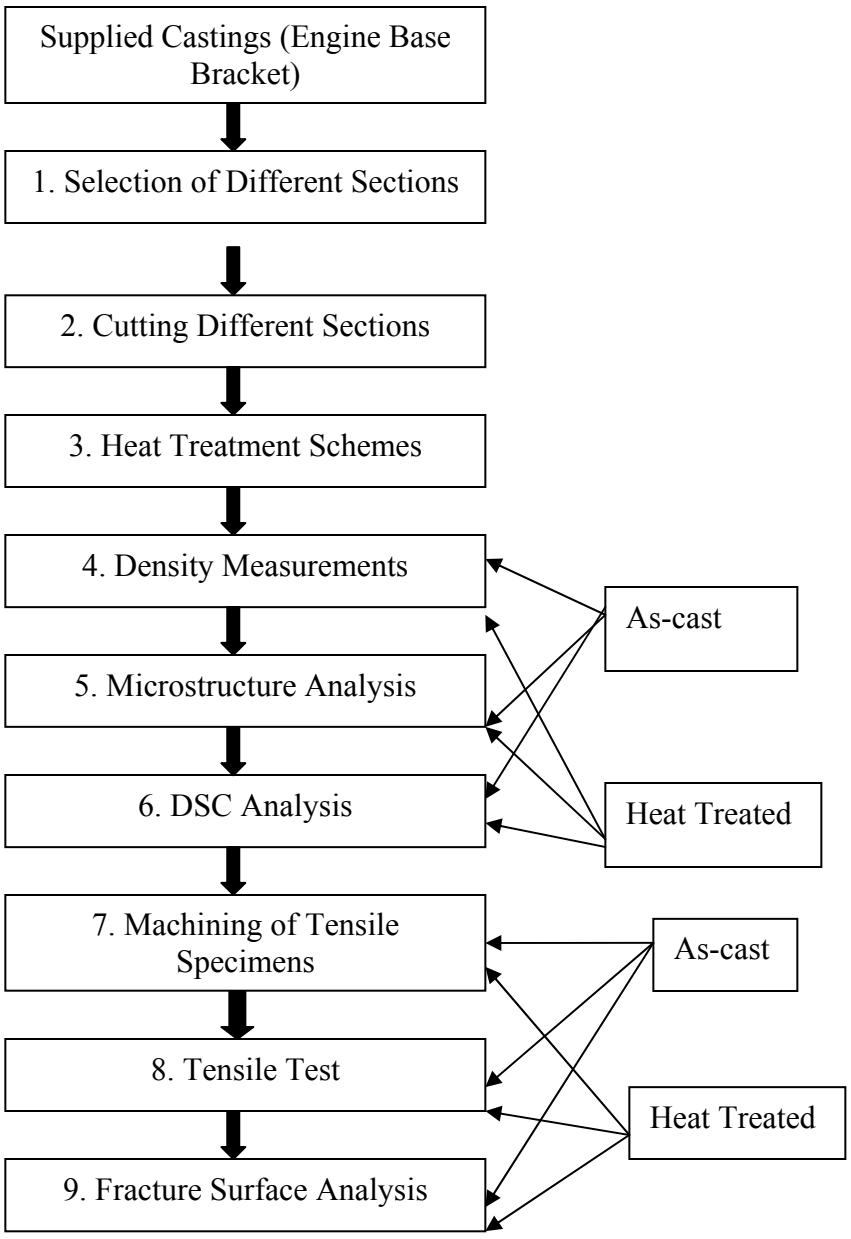

3.2 Supplied Casting

All the experimented samples were provided by Ryobi Die Casting (USA), Inc. The casting component is an engine base bracket which is an adapter between transmission, engine and cradle and is mounted on top of the vehicle's sub-frame, under the engine. In past the base bracket was made of stamped steel with welded nuts and punched holes. This made the bracket too heavy (11 lb) and it also consisted of 16 parts as well. Ryobi invented a new design for this particular component and cast the sample using a vacuum system in die casting. The casting weight was reduced to 6.2 pounds, with a weight savings of 43.66% compared with the steel stamping. Ryobi invented new base bracket is shown in Figure 3.1.

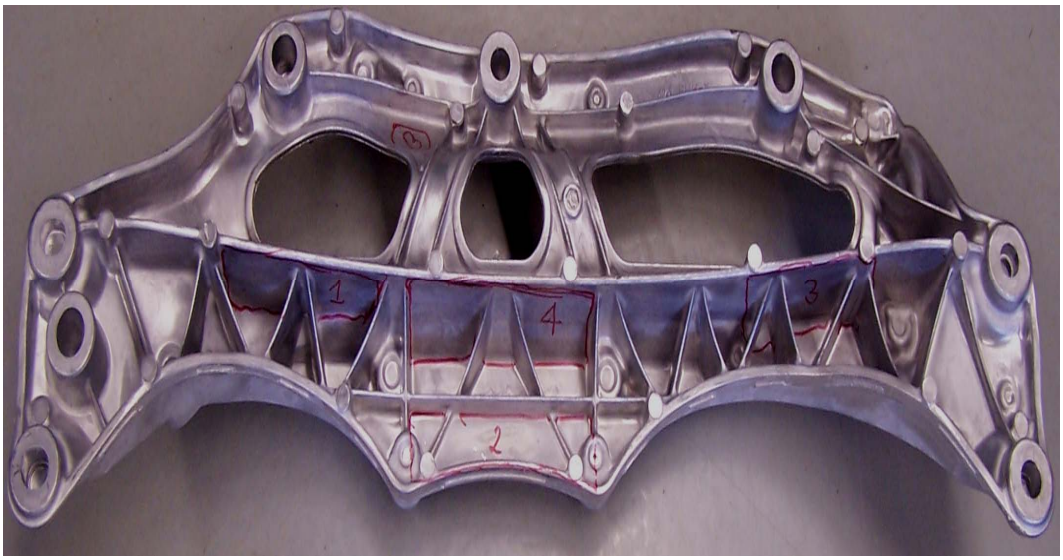

Figure 3.1 Engine base bracket provide by Ryobi Die Casting Inc. (1, 2, 3, 4 showing the sectioned locations).

3.3 Cutting and Selection of Different Sections

Ryobi-provided engine base brackets were marked in some specific locations for analysis. The marked locations in Figure 3.1 were sectioned to prepare specimens for

microstructure analyses as well as well as tensile testing. About 22 engine brackets were used for this study. Numerous numbers of specimens were cut from all these brackets and were analyzed to characterize the heat treatment schemes and to obtain optimum mechanical properties statistically.

The chemical composition of the experimented alloy is listed in Table 3-1. Ryobi Die Casting Inc. commercially named the alloy as RYOBI HD-3SF.The experimented alloy is actually a low silicon, strontium modified Silafont-36 or AA-365 alloy. The alloy composition for Silafont-36 is already shown in Chapter II in Table 2-5.

Table 3-1 Chemical composition of experimented alloy (Ryobi HD-3SF)

Alloy	**Element (in wt.%)**								
	Si	**Fe**	**Mn**	**Mg**	**Zn**	**Ni**	**Sn**	**Cr**	**Sr**
Ryobi HD3SF	7.75-8.25	0.05-0.15	0.325-0.375	0.225-0.275	<0.04	<0.02	<0.02	<0.02	<0.01-0.02

3.4 Heat Treatment Schemes

Several heat treatment schemes were performed on the samples at 120˚C, 150˚C, 180˚C, 200˚C, 250˚C, 300˚C and at 350˚C and hold for 120 minutes at the corresponding temperatures. Samples were then cooled at air after heat treatments. Moreover, to investigate the effect of time duration, at optimum temperature (to be discussed on chapter IV) heat treatments were carried out at 30, 60 and 90 minutes.

All the heat treatments were conducted in a electrical muffle furnace (shown in Figure 3.2) with a temperature control of ± 5˚C. To simulate real stress relief treatment in the industry evacuated capsule was not used for these thermal treatments. Also, oxide layers quickly develop on aluminum during treatments are capable of protecting the alloy from further internal oxidation at relatively low temperatures [65].

Figure 3.2 Electrical muffle furnace (Model LINDBERG BLUE M).

3.5 Density Measurements

The Archimedes' method was employed to find the density and porosity percentage at different conditions (both on as cast and heat treated samples) to compare the porosity levels of the samples treated at different conditions with that of the as-cast alloy. Figure 3.3 shows the experimental setup of using Archimedes' method to determine the density of the samples.

Archimedes Method for determining density is as follows:

1. Using a scale, obtain the mass of each sample in grams.
2. In a volumetric cylinder filled with distilled water record volume;
3. Place a single sample in the volumetric cylinder;
4. Record the mass of samples in water; and
5. Calculate density using the following formula:

Density = Mass in Air/Volume of sample

= Mass in Air/ (Mass in air-Mass in water)/Density of Water

Or, Density = $\mathbf{W_1 \times \rho_{water} / (W_1 - W_2)}$…….(3.1)

where,

W_1 = Mass in air; W_2 = Mass in water; ρ_{water} = Density of water.

Porosity level calculation

Percent porosity exists in different samples can be estimate by the following equation:

Porosity level = (Standard density-Measure density) × 100/ Standard density…….(3.2)

(Standard density here used is 2.635 g/cm) [1].

Figure 3.3 Experimental setup for density measurement.

3.6 Microstructural Analysis

Microstructural change caused by different heat treatments was examined using an optical microscope with a Buehler optical image analyzer (model 2002) and a SEM (JEOL Model JSM – 5800 LV) shown in Figures 3.4 and 3.5 respectively.

Figure 3.4 BUEHLER Optical Image Analyzer Model 2002.

Samples for metallographic observation were prepared following the conventional preparation procedure.

Following steps were carried out for sample preparation for microstructural analysis:

1. Samples were cut into rectangular shape;
2. Mounted with DIALLYL PHTHALATE (Mounting powder);
3. Polished with emery paper (to 600 grades);
4. Fine polishes using 1 μm gamma alumina powder; and

5. Etched with 0.5% HF acid solution. Performed by submerging the sample into the etchant for 20/25 seconds for optical microscope and about 40 seconds for SEM, rinsing with water and finally cleaned with ethanol specimen surface with running water and ethanol.

The microstructure of as-cast and heat treated samples were analyzed by an optical and image analysis technique to assess the significant microstructural changes that occurred during the heat treatment. The Buehler optical image analyzer 2002 system (Figure 3.4) was used to determine structural characteristics of silicon particles as well as to observe the porosity severity in the associated samples. The observation fields were selected randomly. At least 10 fields were analyzed from a single specimen in each location. The grain sizes, porosity size, silicon morphology as well as its distribution was observed. Grain size and porosity size were measured by using IMAGE TOOL for Windows software (Version 3.00).

A JSM-5800 scanning electron microscope (SEM) was employed (Figure 3.5) with a maximum resolution of 200nm in a backscattered mode/ 2μm in X-Ray diffraction mapping mode for elemental analysis in a particular phase. Both higher and lower magnification was used in order to analyze different phases as well as to characterize the microstructure of specimens. Eutectic particles were also analyzed by using higher magnification to observe their morphology at different heat treating condition.

Fracture surface of tensile specimens were also analysed by the SEM to ascertain the fracture surface, different significant scenario (gas porosity when they exist, shape of eutectic silicon and primary dendrites) as well as to observe the nature of fracture mechanism.

Figure 3.5 Scanning Electron Microscope (JEOL Model JSM – 5800 LV).

3.7 Differential Scanning Calorimetry (DSC)

Both DTA (Differential thermal analysis) and DSC are concerned with the measurement of heat evolved from a substance during heating or cooling. The main distinction between DTA and DSC is that the equipment can be calibrated such that the heat evolution from the sample can be measured quantitatively in DSC, while this is often not possible for DTA [68]. There are two types of DSC: the heat flux DSC and the power compensation DSC [69].For power compensation, the DSC signals is related to the differential heat provided to keep the sample and the reference to the same temperature. For heat flux DSC, the signal derives directly from the difference of temperature between

the sample and the reference and in that sense a heat flux DSC is similar to a DTA. For the heat flux DSC, the heat flux measurement has to be calibrated by performing calibration runs with standards that display a reaction for which the heat evolution is well known [70].DSC, which has the characteristics of speed, convenience, accuracy and versatility, is probably the most popular of all such techniques according to the number of publications on thermal analysis techniques.

In this study thermal analysis was carried out using a Differential scanning calorimetry thermogravimetric analyzer (DSC-TGA Q600) manufactured by TA instrument, as shown in Figure 3.6. DSC has done to estimate the phase exists in the microstruecture at different heat treating condition.

An argon flow rate of 100 ml/min was used to prevent sample from contamination of the measurement beams and from the oxidation during and after DSC runs. The DSC tests were run at heating/cooling rates of 10-20˚C/min over the temperature range of 50 to 700˚C. After heating, nitrogen-cooing was used for all runs. Before each DSC run, the SDT Q600 TA instrument was calibrated for TGA weight, DTA baseline, temperature and DSC heat flow. Samples to be analyzed were put in an alumina cup on the sample beam, while an empty alumina cup was put on the reference beam. Right before or after each DSC run, a baseline run was required by running a separate test with two clean, empty alumina cups on the sample and reference beams. The DSC was then corrected by subtracting the baseline.

Figure 3.6 Differential scanning calorimetry-thermo gravimetric analyzer (DSC-TGA Q600).

3.8 Machining Tensile Specimens

Subsize flat tensile specimens were machined out of samples from different locations of the supplied samples according to ASTM standard B557. All test specimens were polished to have a finish of 1.6 μm in order to prevent from premature failure. Figure 3.7 shows the geometry and dimensions of the tensile specimen used in this study.

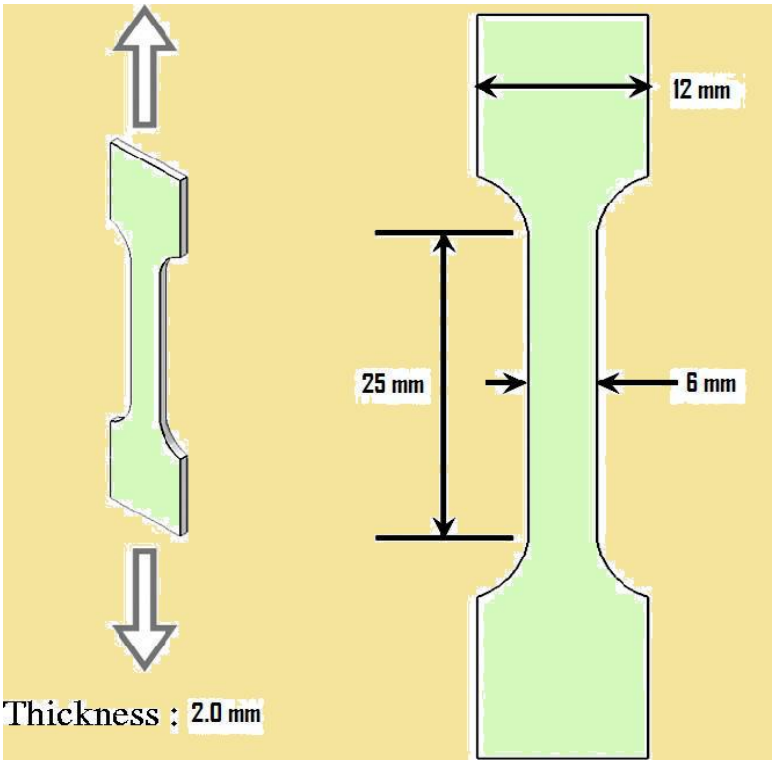

Fig 3.7 Schematic illustration of a tensile test specimen.

3.9 Tensile Testing

Using the Instron Tensile Test Machine, Model 8562 with a computer data acquisition system (Figure 3.8), the heat treated and as-cast tensile specimens were tensile tested to fracture at room temperature at a strain rate of 0.5 mm/min. A strain extensometer (Instron Model 2620-824 0.5 in ± 0.2 in. range) was attached to the test specimen for measuring elongation during testing.

Tensile properties, namely, yield strength (YS) at 0.2% offset strain, ultimate tensile strength (UTS), fracture elongation (E_f%), work hardening coefficient n and true strain at fracture point ε_f were derived from the data recorded by the data acquisition system.

Figure 3.8 Instron Tensile Test Machine (Model 8562).

3.10 Fracture Surface Analysis

Samples were cut at the tip of tensile specimens, where breaking occurs to analyze the fracture surface SEM was employed. first of all SEM has done on the fracture surface. After SEM these fracture, samples were mounted and polished to analyze the surface beneath the tensile surface [60]. Precaution was taken during polishing to keep the fracture pattern unchanged. Etched the samples with 0.5% HF for 20/25 seconds and observed in optical microscope.

CHAPTER-IV

RESULTS AND DISCUSSION

4.1 Microstructural Analysis

4.1.1 Primary and Secondary Phases

All the samples at different conditions contains two predominating phases which are the primary Al (α-Al) and the eutectic phase at the boundary of the primary Al grains (Figure 4.1 -4.3). EDS mapping on the corresponding phases, confirmed the primary phase as Aluminum (Figure 4.4-a) and secondary phase is as eutectic Si (Figure 4.4-b).

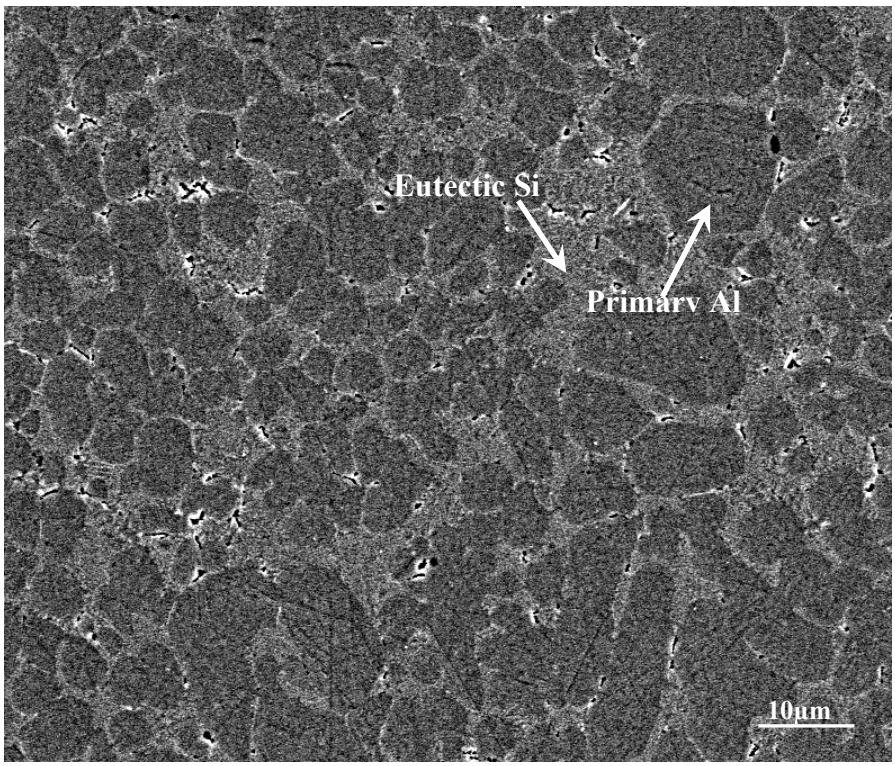

Figure 4.1 Primary and secondary phase in the as-cast alloy.

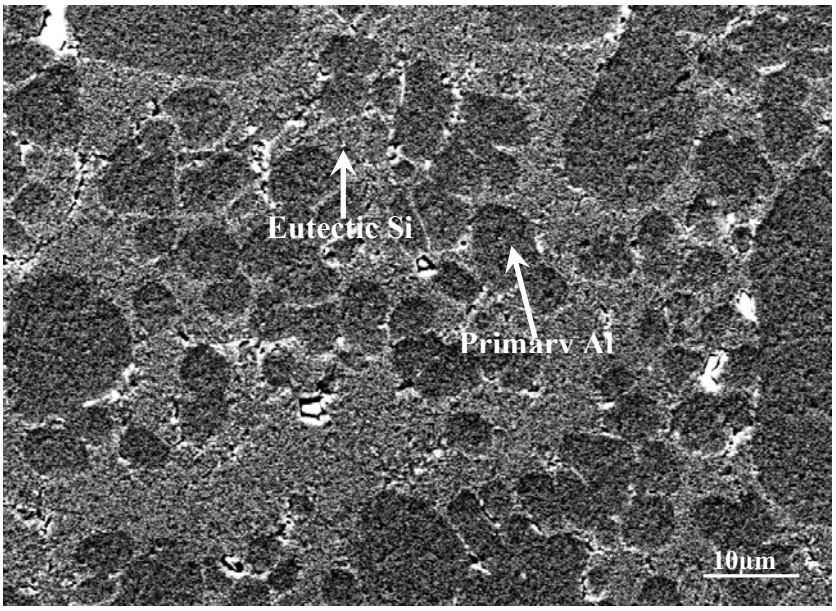

Figure 4.2 Primary and secondary phases in the alloy heat treated at 200˚C for 120 minutes.

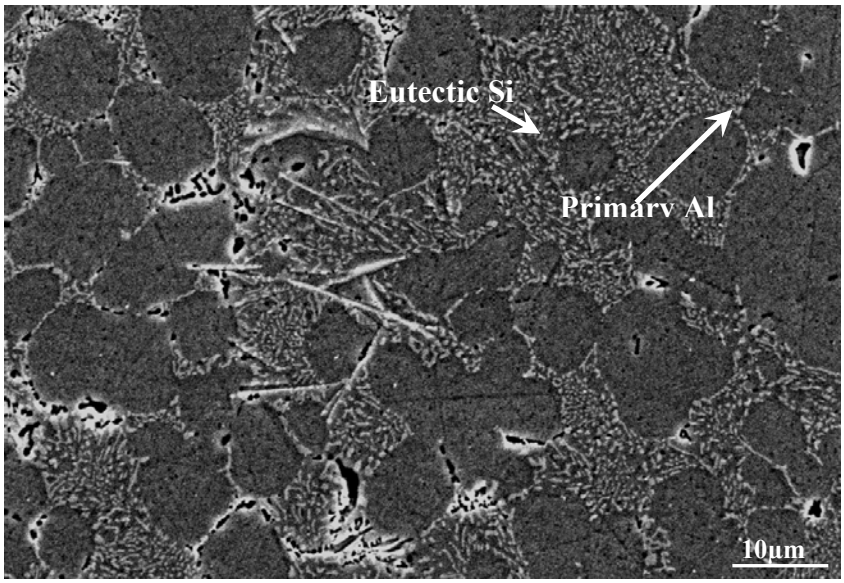

Figure 4.3 Primary and secondary phases in the alloy heat treated at 350˚C for 120 minutes.

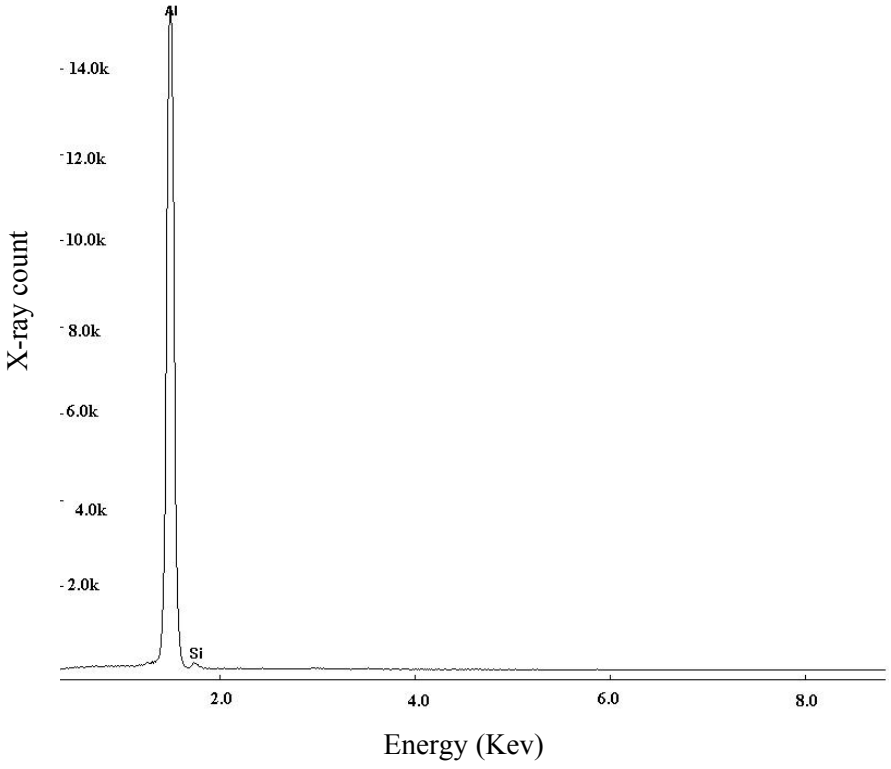

(a)

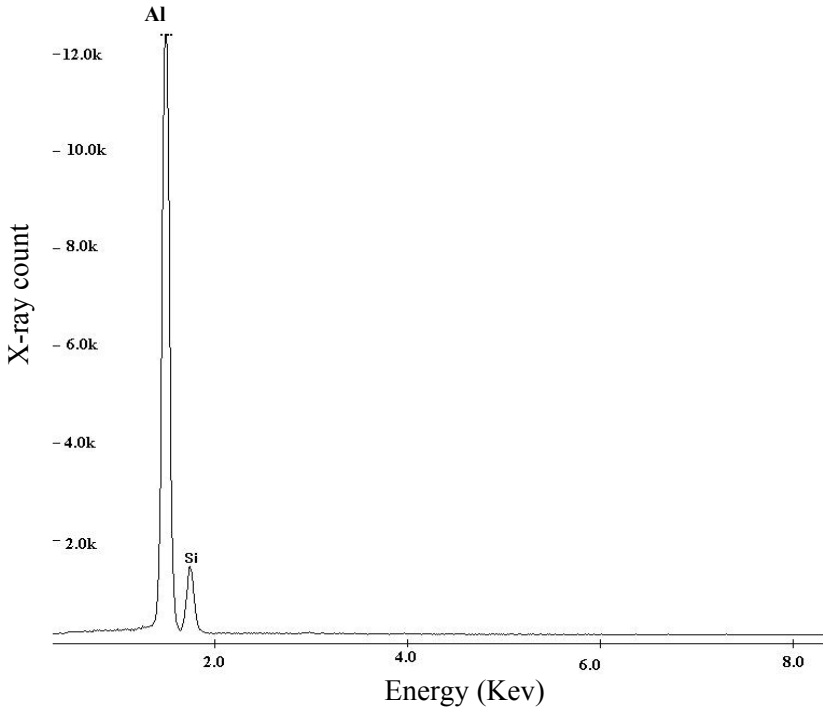

(b)

Figure 4.4 EDS analysis on (a) Primary Al, (b) Eutectic phase.

4.1.2 Intermetallic Phases

Besides the primary and secondary phases, there were three major intermetallic phases were also found in the microstructure. They are manganese-based intermetallic phase and magnesium-based intermetallic phase and Iron-based intermetallic phases (Figures 4.5- 4.15). The trace of Mn-based intermetallic phase ($Al_{12}Mn_3Si_2$) was found in all treatments. According to Zovi [50] manganese content in the low iron die casting aluminum alloy has very negligible effect on ultimate tensile strength and yield strength. However, samples with no manganese showed a different behaviour which might be caused by the very poor ejection. Therefore manganese has been employed in the experimented alloy to improve fluidity and minimize die soldering.

Rivlin et al. [70] and Richards et al. [71] have shown that in hypoeutectic Al-Si alloy if the local iron concentration reaches about 0.05 wt%, precipitation of the $Al_9Si_2Fe_2$ occurred. As the experimented alloy contains the iron content of about 0.05-0.15 wt%, this is obvious that the microstructure contains the (Figure 4.9) the iron rich intermetallic phase as well. Koch et al. [48] has suggested that it is desirable to keep iron content below 0.12 wt% to minimize the formation of AlFeSi-phases that appear as needle-like shapes in the cast microstructure. Their acicular morphology deteriorates overall strength, elongation and fatigue behaviour of the alloy.

It is interesting that, with successive heat treatments, Mg rich intermetallic phase (Mg_2Si) was decreasing and at about 350˚C it was hard to find in microstructure. At high treatment temperatures most of this phase might be dissolved in the matrix (Figure 4.13) which could be a possible reason to drop the strength. Koch et al. [48] studied on Silafont-36 alloy which is almost similar (low silicon and strontium modified) to the experimented alloy, and found that the magnesium content determined the mechanical

properties and aging behaviour of the alloy. Therefore the disappearance of magnesium intermetallic phase might be responsible for the reduction in strengths of the alloy treated at high temperature. The study of Edelson et al. [72] shows that not all second phases take part in strengthening in alloy. It is always necessary to have a strong bond among particles to matrix to contribute strengths in alloys by particles or intermetallic phases. Moreover, the shape, size and distribution of the intermetallic phases also have significant influence on the matrix in terms of strength of the alloy.

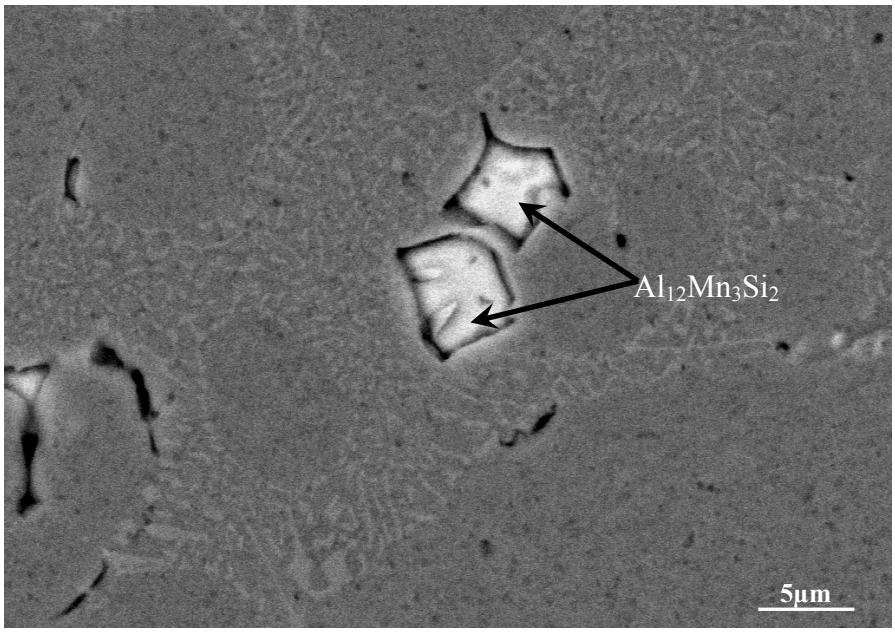

Figure 4.5 Backscattered electron image showing the manganese (Mn) containing phase in the as-cast alloy.

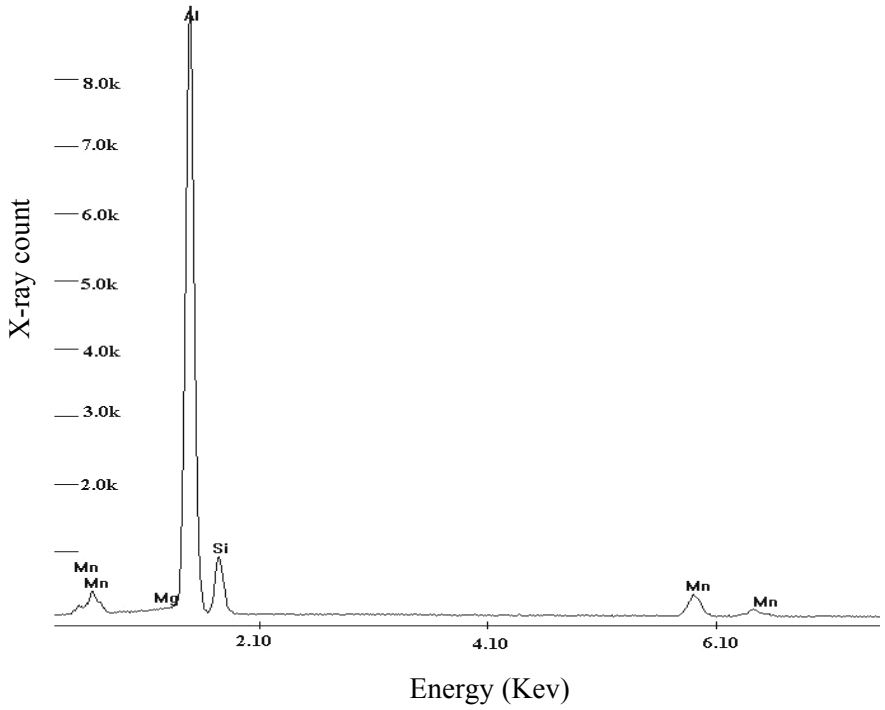

Figure 4.6 EDS analysis showing the elements contains in corresponding Mn-based phase.

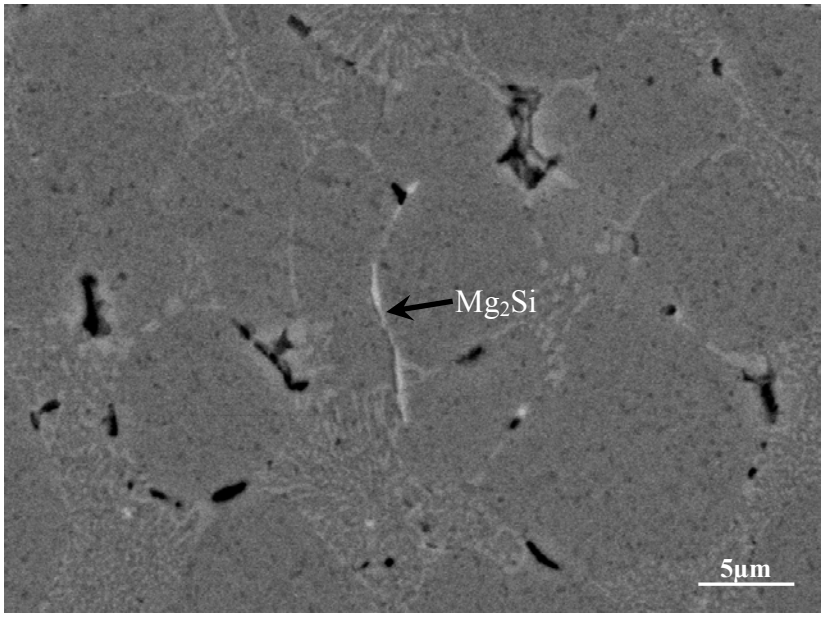

Figure 4.7 Backscattered electron image showing the magnesium (Mg) containing phase in the as-cast alloy.

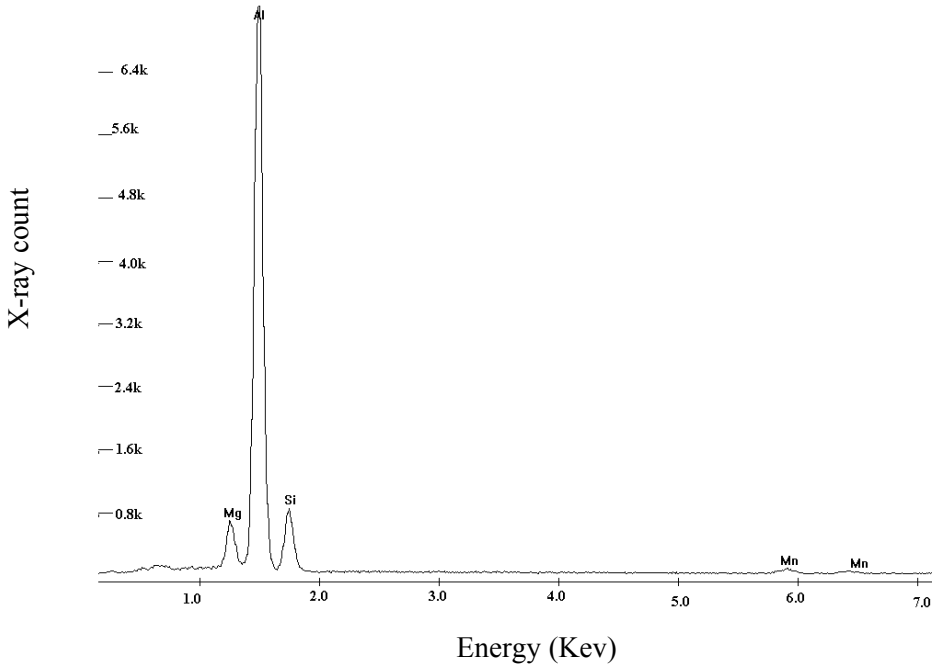

Figure 4.8 EDS analysis showing the elements contains in corresponding Mg-based Phase of Figure 4.7.

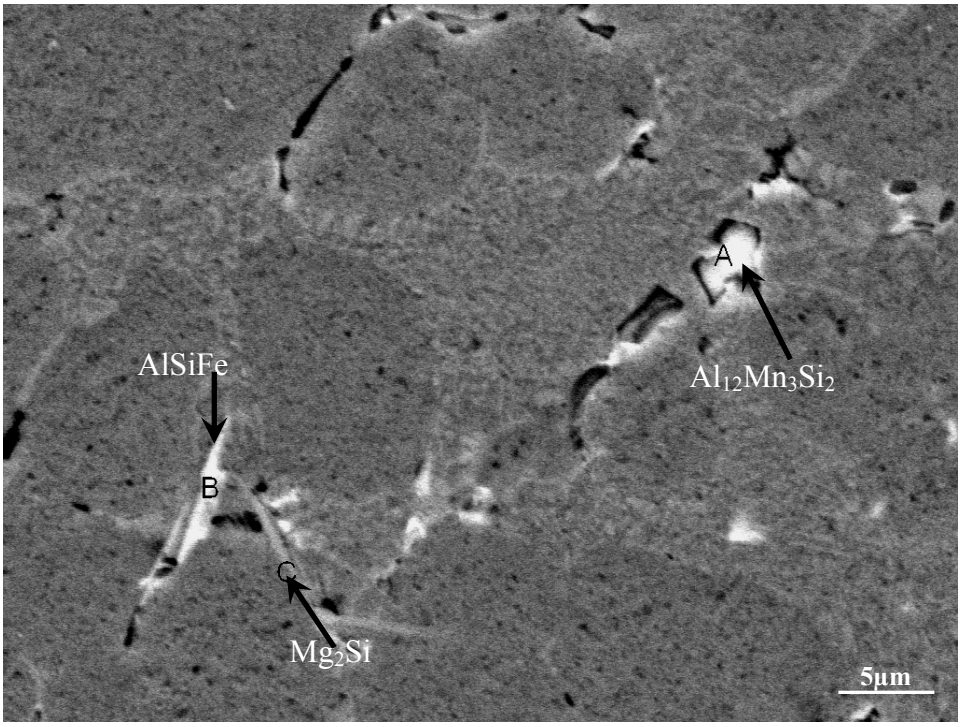

Figure 4.9 SEM micrograph showing different intermetallic phases in the alloy treated at 200˚C for 120 minutes.

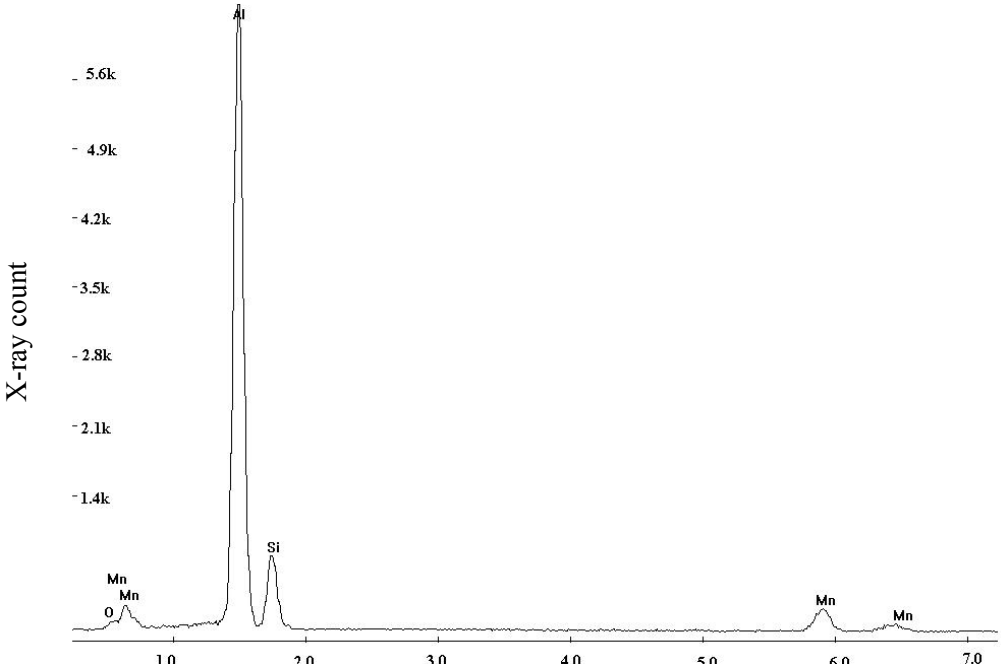

Figure 4.10 EDS analysis (particle A on Figure 4.9) showing the elements in Mn-based phase.

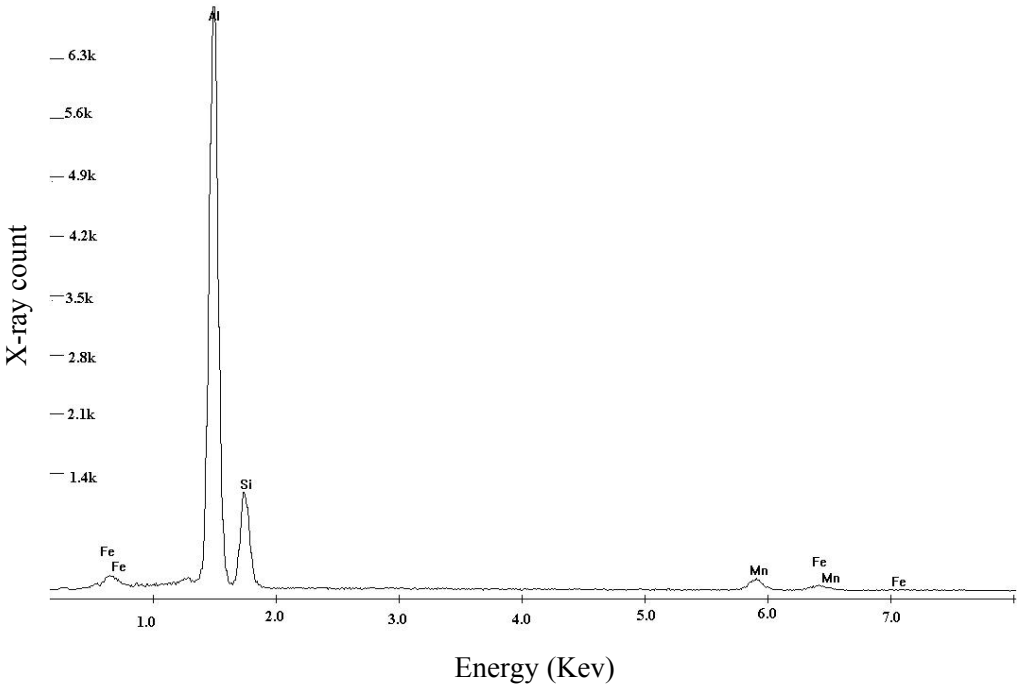

Figure 4.11 EDS analysis (particle B on Figure 4.9) showing the elements in Iron (Fe)-based phase.

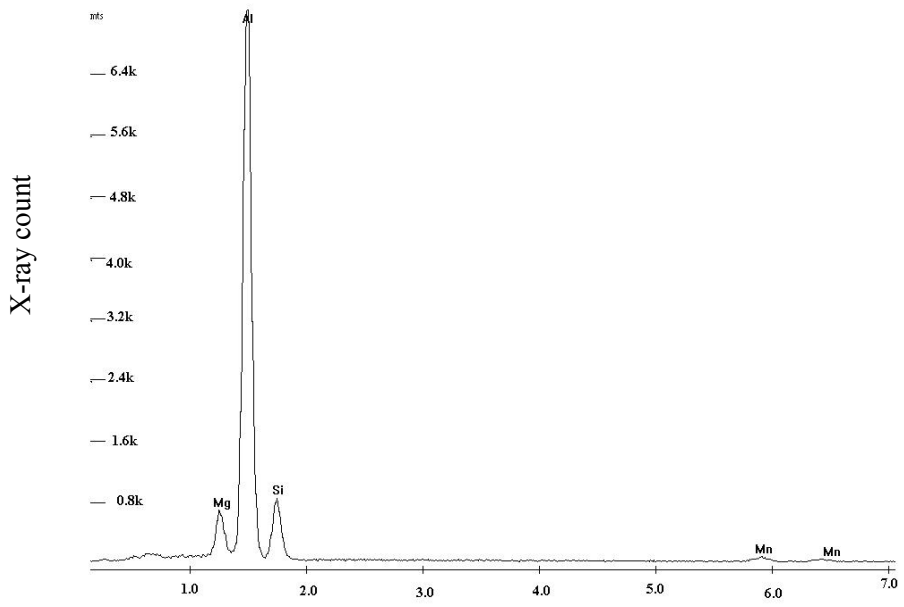

Figure 4.12 EDS analysis (particle C on Figure 4.9) showing the elements in Mg-based phase.

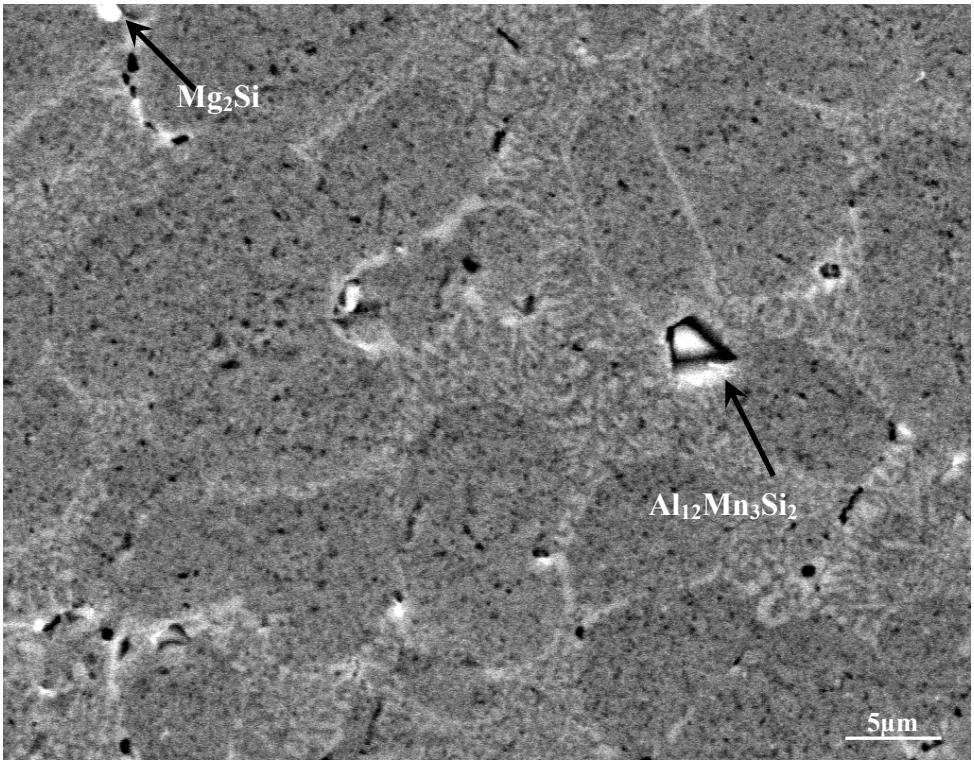

Figure 4.13 Different intermetalic phases in the alloy heat treated at 350˚C for 120 minutes.

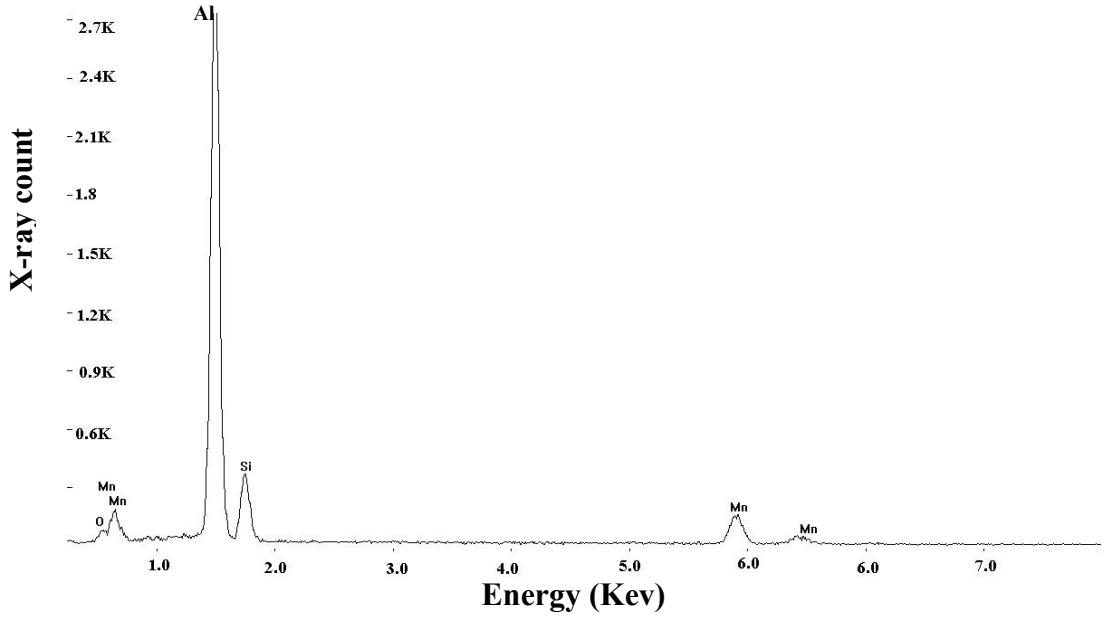

Figure 4.14 EDS analysis showing the elements in Mn-based phase of Figure 4.13.

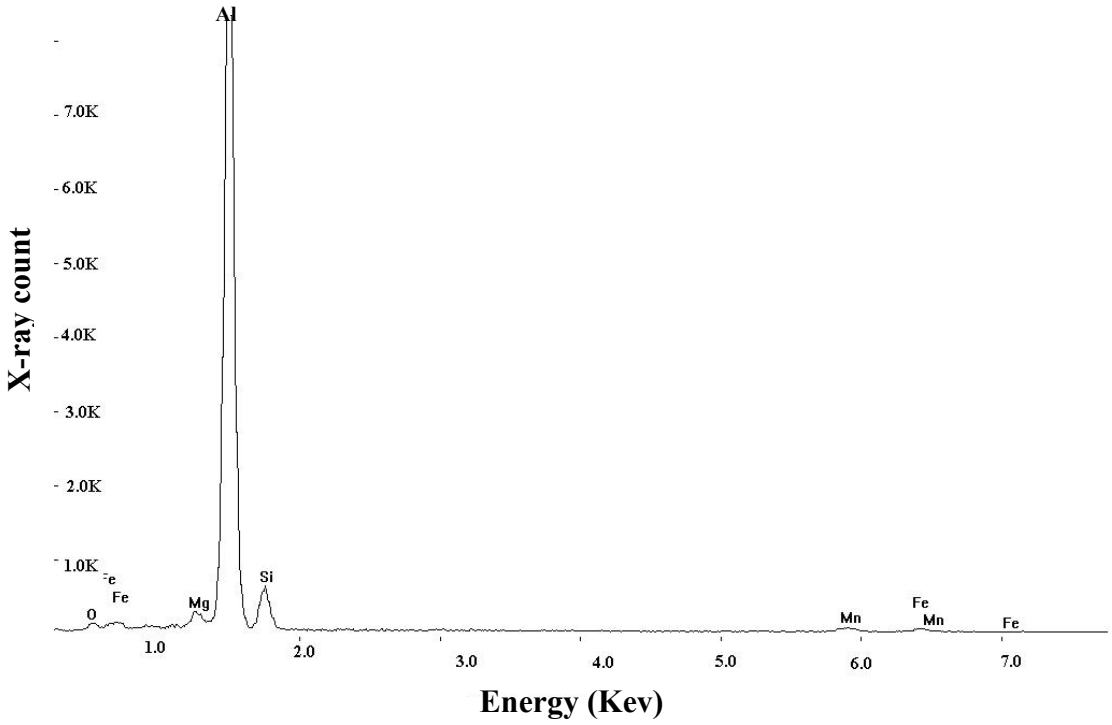

Figure 4.15 EDS analysis showing the elements in Mg-based phase of Figure 4.13.

4.1.3 Eutectic Silicon Morphology

It has been experimentally proved that silicon crystals in the eutectic mixture grow in faceted manner in Al-Si alloy which is already shown in chapter two (Figure 2.2). Silicon crystals usually develop ahead of the aluminum phase and the morphology of the silicon crystals looks fan-shaped in metallographic sections (Figure 2.2-b) and they consist of silicon flakes, which seem to grow out from a few nucleation sites. Therefore, this kind of eutectic structure gives rather poor mechanical properties to the casting and makes the material brittle [73].

Hanna et al. [74] have reported that fine eutectic silicon along with fine primary aluminum grains improves mechanical properties. Therefore modification of eutectic silicon is of general interest in Al-Si system. There are three well-known eutectic modification methods have been developed so far, namely (1) chemical modification which produces fine fibrous silicon structure through the addition with trace-levels of several alloying elements, such as sodium, antimony, potassium, calcium, strontium, and barium; (2) quench modification which results in silicon forming an exceedingly fine form when compared to the unquenched silicon, through high cooling rates and rapid solidification in the growth rate ranging from 400 μm/s to 1000 μm/s; and (3) superheating modification, which requires the presence of magnesium in the alloy to obtain fibrous silicon by heating up the melt from the usual pouring temperature (for example, 680˚C) to a temperature of 850–900˚C and then holding for about 15–30 min, then quickly cooling to the pouring temperature before casting [75]. Among all these modification processes chemical modification by addition of trace amount of elements is very popular as it provides very fine and fibrous eutectic silicon phase which in turn improved mechanical properties.

Sodium was practiced for silicon modification but due to it's over modification tendency by forming AlNaSi, high vapour pressure and also for high affinity with oxygen, commercially they are obsolete as a silicon modifier.

Strontium becomes very popular as an additive in foundry now a days. It was also briefly explained in Chapter II that strontium not only helps to modify the silicon particles but also lower the nucleation and growth temperature which in turn decrease the growth rate and thus create fine silicon Si particles. A very low amount (about 0.005%) of strontium has a greater influence in Al-Si system which has shown in Figures 2.5 and 2.6.

In this study, the experimented alloy has been modified with using trace amount of strontium of about 0.01 wt%. The associated alloy has die casted with using vacuum system incorporated during the processing which provides both rapid die cavity filling and very high cooling rate. Therefore, it is expected that the microstructure even in the as-cast condition should have refined eutectic silicon particles with fine primary aluminum grains as the solidification rate in the die casting process is relatively high enough to prevent dendritic or columnar structure in microstructure. Figure 4.16 displayed a microstructure of continuous very fine Al–Si eutectic interspersed with fine globular primary aluminum grains. The shape and size of individual eutectic silicon grains were not distinguishable at such a magnification which will be shown in the succeeding section.

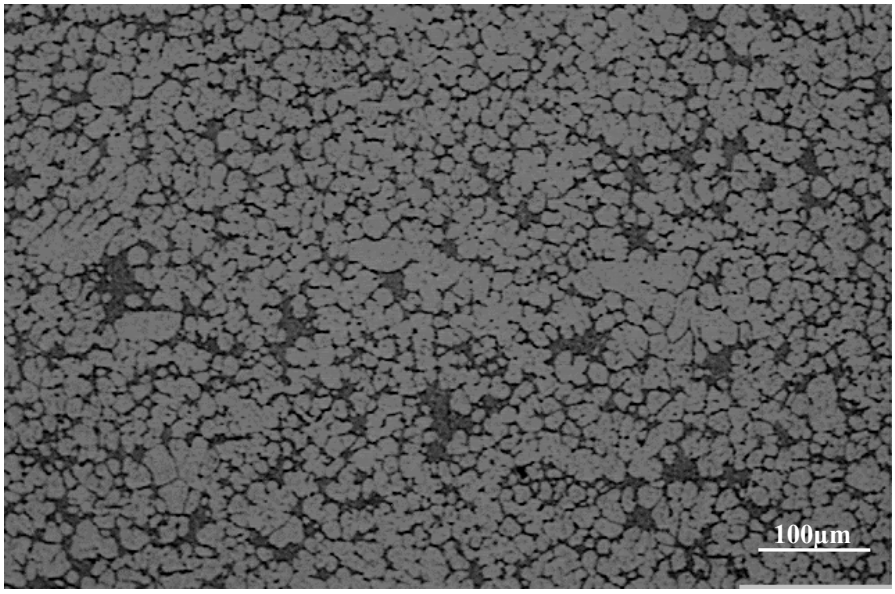

Figure 4.16 Light optical micrograph of RYOBI HD-3SF (modified silafont-36 or AA365) in as-cast condition.

The microstructures at different heat treated conditions were analysed at high magnification to observe the change in eutectic silicon morphology. It was shown in Figures 2.5 and 2.6 in Chapter II that, after the eutectic silicon modification achieved at an optimum level, they tend to coarse again after with excessive thermal treatment. The coarsening of eutectic silicons are not expected in microstructure, since they reduce overall mechanical properties.

Figures 4.17- 4.19 show the SEM micrographs at three conditions, namely as-cast condition, at 200˚C and at 350˚C for 120 minutes. All these micrographs illustrate that with successive increase of temperatures the interspacing between eutectic silicon particles increases.

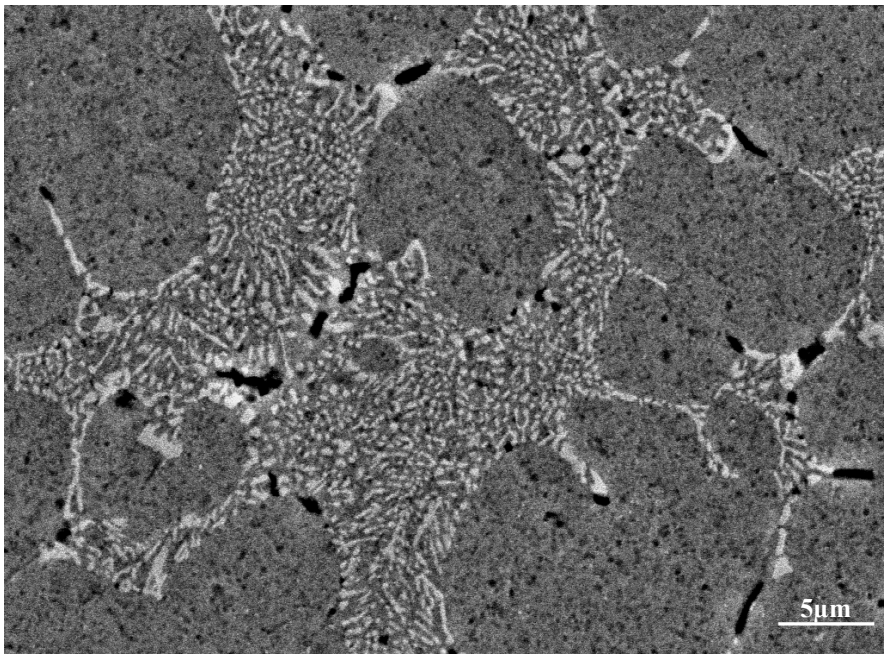

(a)

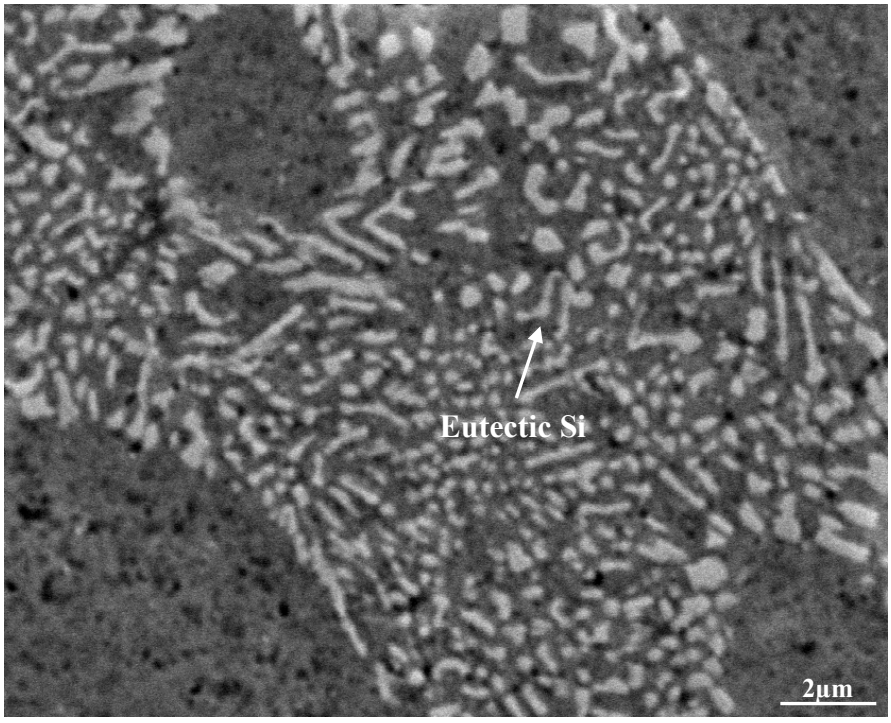

(b)

Figure 4.17 SEM micrograph showing eutectic silicon particles distribution in the as-cast condition: (a) at 3000X; (b) at 5000X.

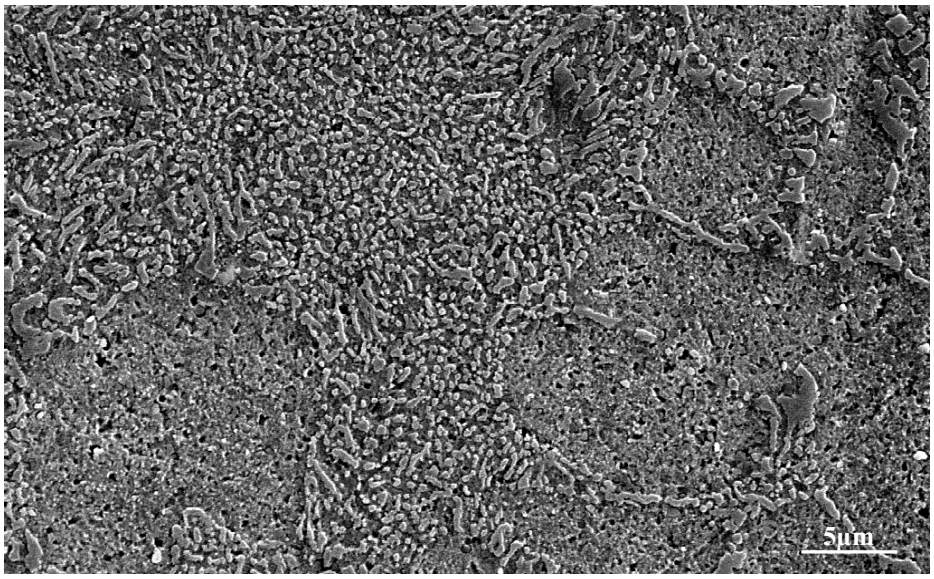

(a)

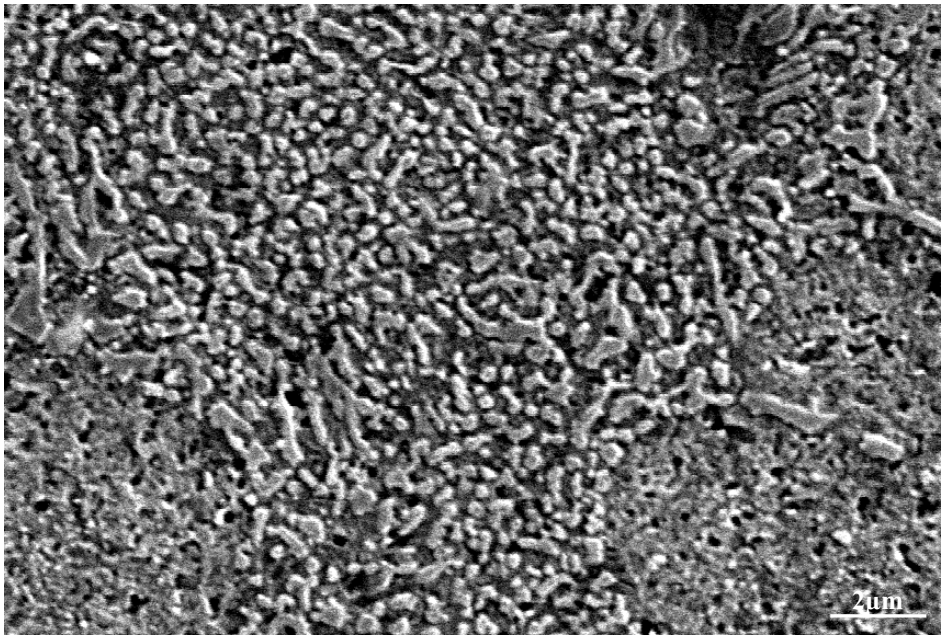

(b)

Figure 4.18 SEM micrograph showing eutectic silicon particles distribution at 200˚C for 120 minutes: (a) at 3000X ; (b) at 5000X magnification.

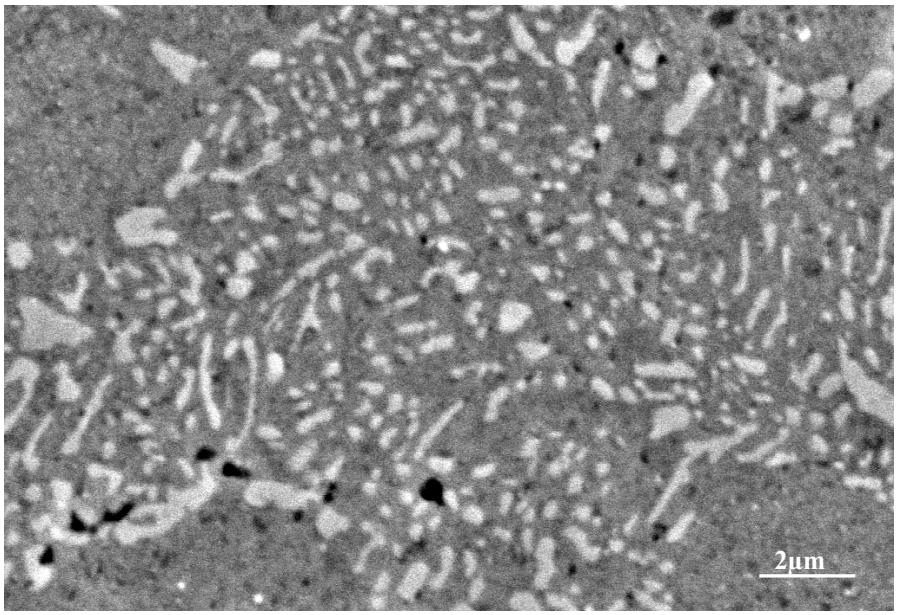

Figure 4.19 SEM micrograph showing eutectic silicon particles distribution at 350˚C for 120 minutes.

Eutectic silicon morphology was analyzed at different heat treated condition at higher magnification. Figure 4.17(a), 4.18 (b) and 4.19 shows that with successive increase of temperature, eutectic particles become coarse at higher temperature. It is also observed in Figure 4.18 that eutectic particles become more spherical which improves mechanical strength at 200˚C temperature. Although the particles at higher temperature (350˚C) become more spherical but the interspacing between these particles significantly increased which also might be responsible to lower the strength at higher temperature. Figure 4.20 shows the change of length and width of eutectic silicon particles at different temperature. Figure 4.20(a) shows that in as-cast temperature the eutectic particles length were comparatively greater but the widths are lower than the width of the particles at higher thermal treatment. Therefore the overall aspect ratio (Length/width) is greater in as

cast condition (aspect ratio=3.29 in as-cast). Although, the aspect ratio at 350˚C is much lower (1.64) at 350˚C thermal treatment.

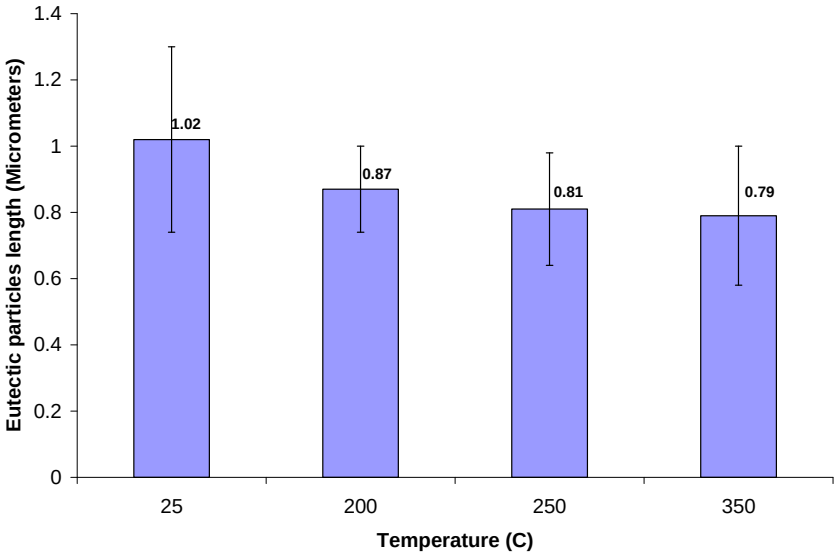

(a)

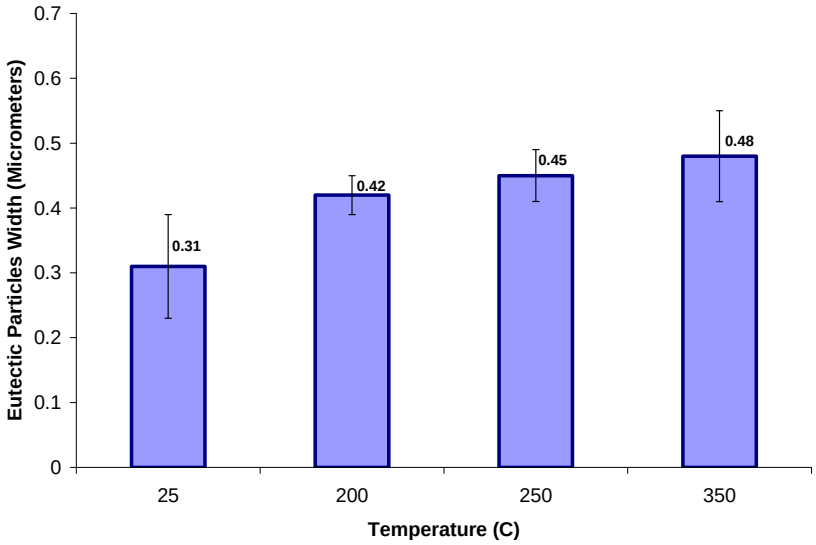

(b)

Figure 4.20 Eutectic particles average (a) length and (b) width variation at different treatment conditions of as-cast (25˚C), 200, 250 and 350˚C for 120 minutes.

But the interspacing between the eutectic particles at this temperature is very significant (0.41 microns) than the lower thermal treatment. Therefore this may deteriorates the strength of the overall alloy at this temperature. However at 200˚C an optimum aspect ratio (about 2.07) is achieved with lower interspacing (0.26 microns) of eutectic particles. Therefore all these circumstances have optimized the strength of the alloy at this temperature (200˚C).

4.2. DSC Analysis for Phase Detection

DSC analysis of samples treated at different conditions (as-cast, 200 and 350˚C for 120 minutes) were performed to confirm the phases exist in associated microstructures. Figures 4.21-4.23 show the DSC analysis in the as-cast, 200˚C and at 350˚C heat treated samples, respectively. The two predominant phases namely the eutectic phases were formed around 570˚C, and primary aluminum or α-phase is formed around at 600˚C.

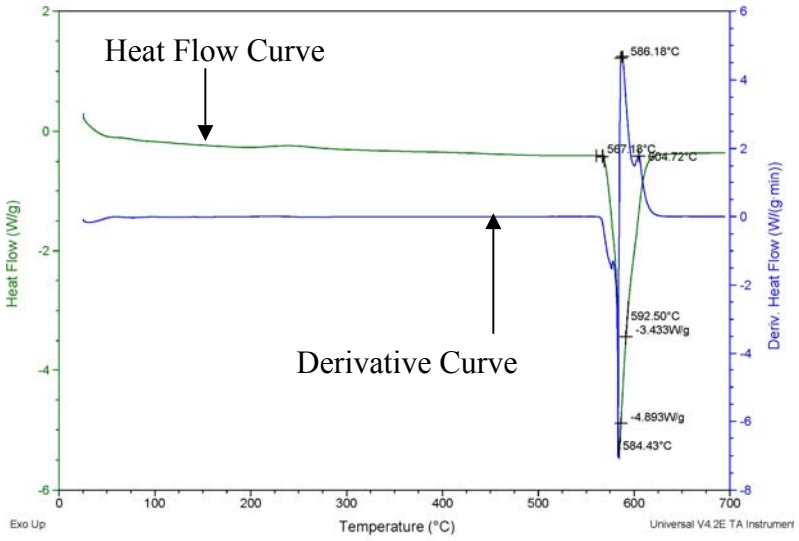

Figure 4.21 DSC analysis of the as-cast alloy showing phase formation.

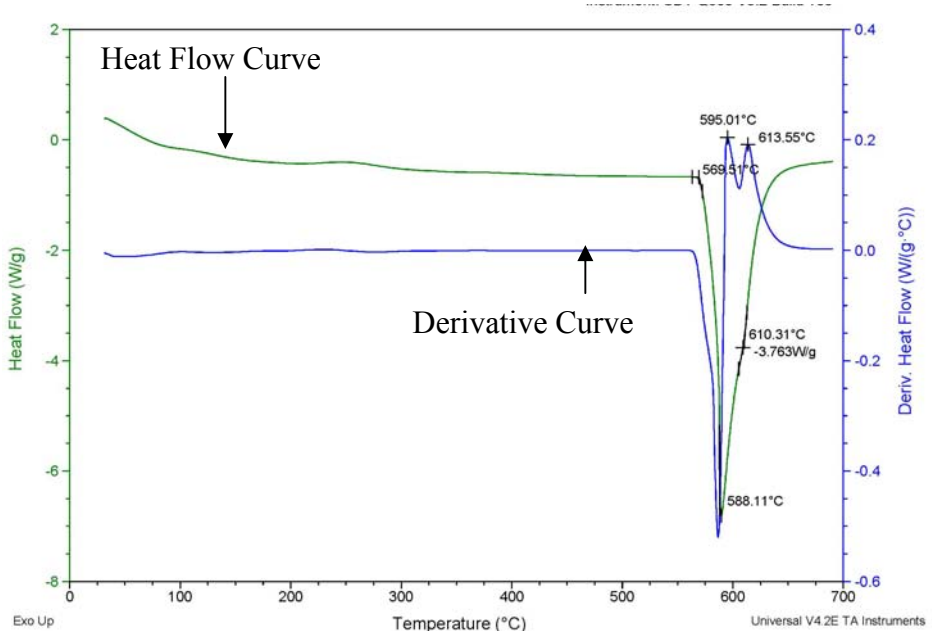

Figure 4.22 DSC analysis of the alloy treated at 200˚C for 120 minutes showing phase formation.

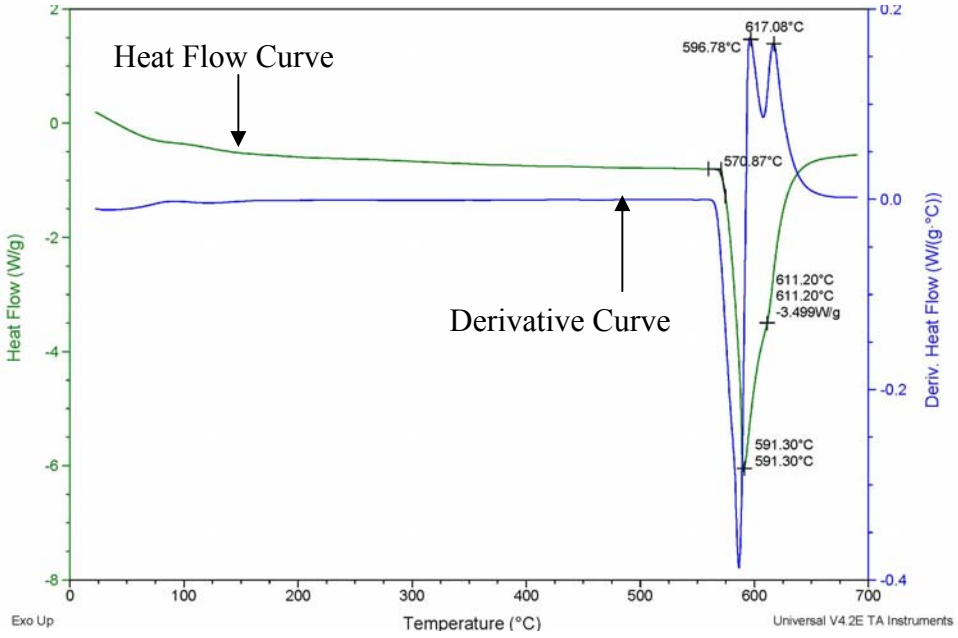

Figure 4.23 DSC analysis of the alloy treated at 350˚C for 120 minutes showing phase formation.

The DSC analysis has performed to determine the dissolution and melting mechanisms of these phases in the tested alloy under the thermal treatment schemes of this study. In Figures 4.21-4.23, the green lines show the change of heat flow with temperature and the blue lines shows the derivatives of heat flow curves which represents the instantaneous heat flow with change of temperature. All these three figures shows mostly two significant peaks at around 570˚C and at around 610˚C. It has shown that [12] in Al-Si system eutectic phase started to form usually around 570˚C. Therefore, the first peak in the heat flow curve represents the formation of the eutectic phase disappearance. Further increase in temperature dissolves the manganese containing intermetallic phase which usually forms between the eutectic and solidus temperature of primary aluminum. The derivative curve depicts the peak for the dissolution of this trace amount of intermetallic phase at around 587˚C and finally the primary aluminum or α-phase starts to melt at around 610˚C. Above this temperature, the alloy goes to liquidus state. Although there should have a magnesium phase formation peak, due to its non-homogenous distribution and very low quantity as well as limitation of the DSC it is almost impossible to detect the magnesium-containing phase.

From the DSC analysis, it is clear that the heat treatment schemes does not affect on the dissolution and melting of the most predominating phases, i.e, Mn-containing phase, eutectic Si and primary α-Al of the experimented alloy. Unfortunately this analysis could not explain the effect of other intermetallic phases which also exists in the experimented alloy. However, numerous EDS analysis has done on the microstructures at different temperatures to observe the effect of heat treatment on those associated intermetallic particles which has already explained in the previous section.

4.3 Tensile Properties

Tensile specimens were prepared from different sections (marked as 1, 2, 3 and 4) of the Engine base bracket following ASTM standard B557. Samples were then heat treated for 120 minutes at 120, 150, 180, 200, 250, 300 and at 350˚C. Moreover for analysis the time effect, three different time duration has selected at 200˚c for 30 minutes, 60 minutes and 90 minutes. The reason why all the time variation set at 200˚C is because it was evaluated that, at 200˚C most of the optimum mechanical properties were achieved.

Tensile properties of the specimens treated at different temperatures and at different times are summarised in Table 4-1 and Table 4-2. The properties at different temperature are also graphically depicted in Figures 4.24 and 4.25. Variations in properties at different times are similarly represented by Figures 4.26 and 4.27.

Table 4-1 Average mechanical properties at different temperature for 120 minutes

Treatment Temperature (˚C)	0.2% Offset Yield Strength (MPa)	Ultimate Tensile Strength (MPa)	Elongation (%)
25	133.66±8.8	251.45 ±11.8	10.7±1.27
120	134.8 ±2.08	252.6 ±8.04	10.3±0.98
150	165.9±16.1	275.1 ±28.3	9.8±1.06
180	185.27 ±12.27	286.3 ±22.1	7.4±0.47
200	192.6 ±7.4	286.3 ±6.9	7.2±0.87
250	157.3 ±9.64	224.3 ±16.1	7.9±1.18
300	150.2 ±5.8	230.4 ±22.2	8.7±0.7
350	114.3 ±13.28	214.6 ±8.3	9.67±2.46

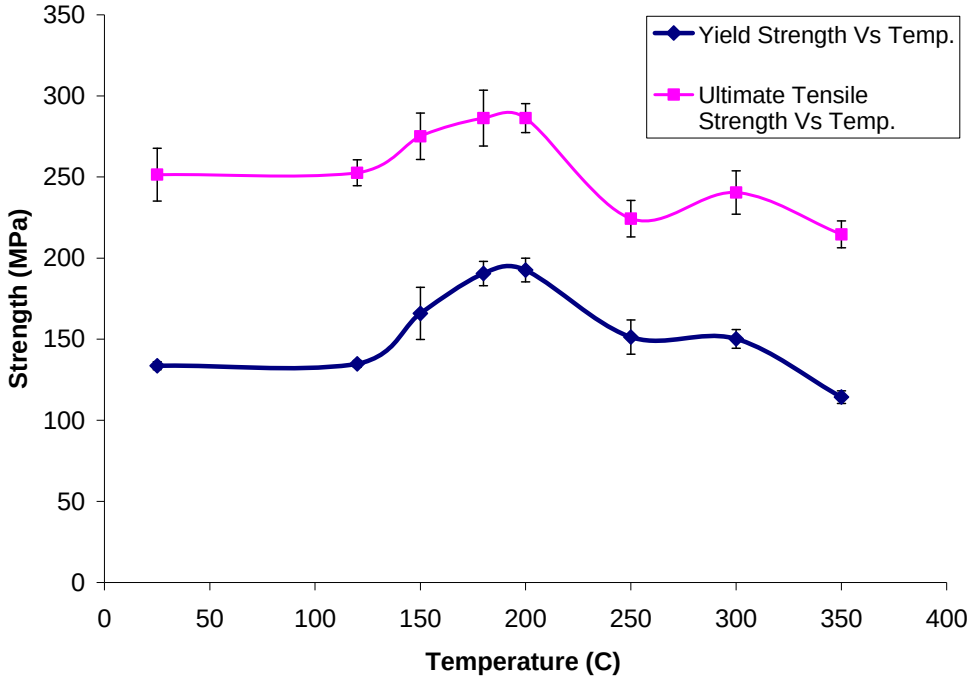

Figure 4.24 Average mechanical (YS and UTS) strength at different thermal treatment temperatures.

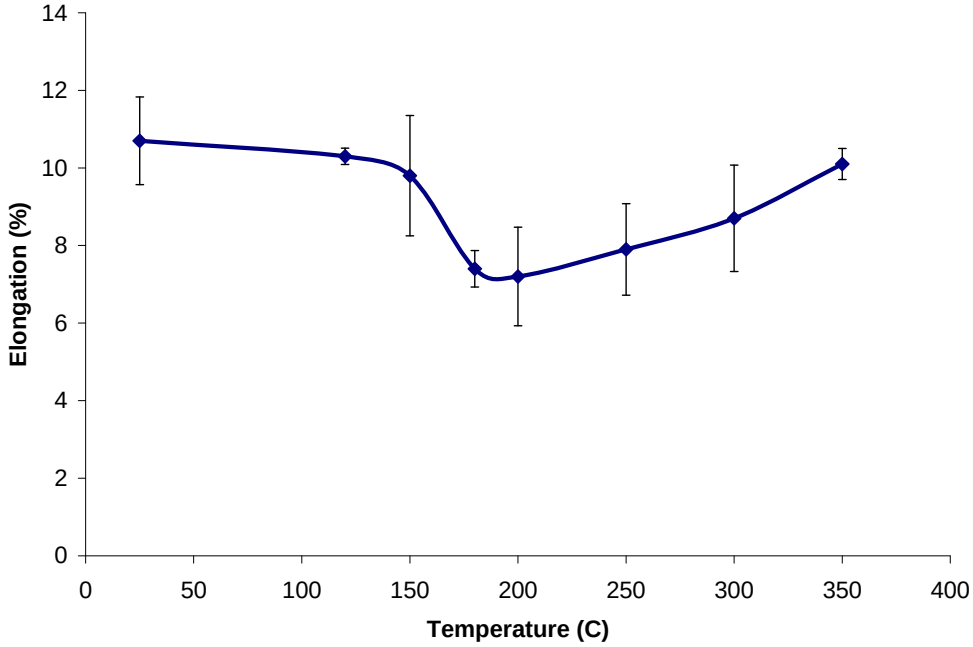

Figure 4.25 Average elongation percent at different thermal treatment temperature.

Table 4-2 Average mechanical properties for different thermal treatment time at 200˚C

Treatment Time (Minutes)	**0.2% Offset Yield Strength (MPa)**	**Ultimate Tensile Strength (MPa)**	**Elongation (%)**
30	160.25±2.5	261.92±15.7	9.43±0.49
60	169±8.4	267.87±5.78	7.67±0.59
90	193.8±5.8	286.02±9.3	7.83±0.4
120	192.6 ±7.3	286.3 ±6.9	7.2±0.36

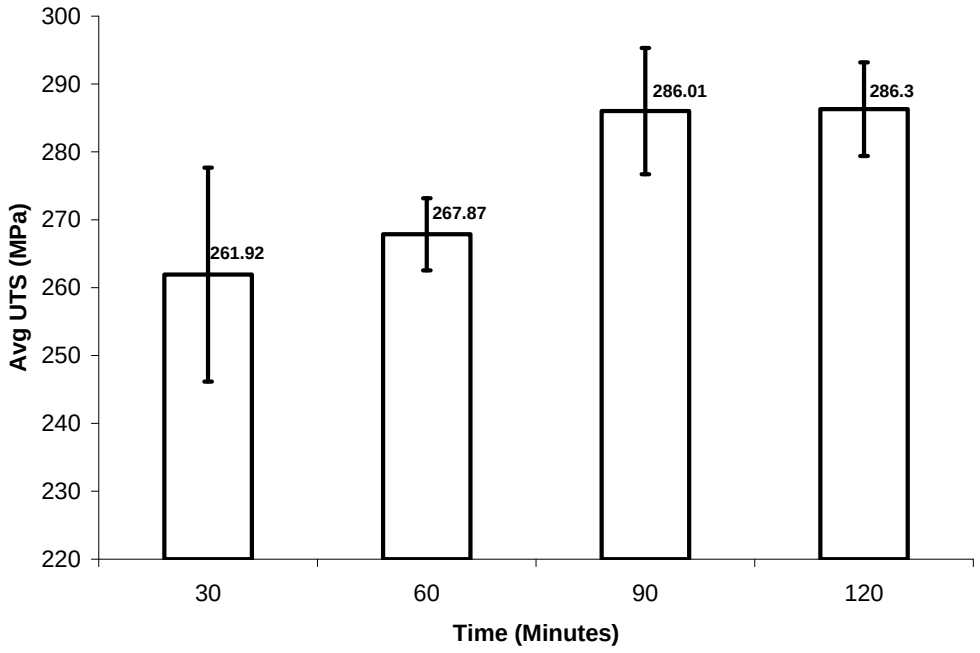

Figure 4.26 Average tensile strength for different thermal treatment time at 200˚C.

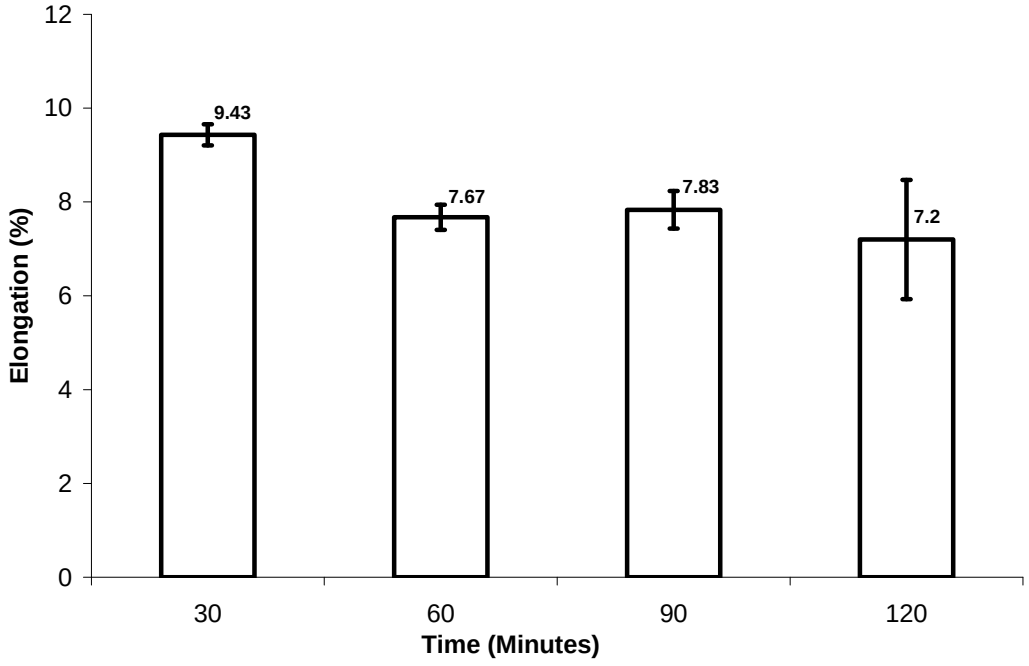

Figure 4.27 Average elongation for different thermal treatment time at 200˚C.

It can be seen from Table 4-1 as well as from the illustration of Figure 4.24, both yield strength (YS) and ultimate tensile strength (UTS) has increased until the heat treatment at 200˚C. YS has increased to 193 MPa (at 200˚C) from 134 MPa (in as-cast state). UTS has also raised to 286 (200˚C) MPa from 251 (in as-cast state). However, with increasing the temperature from this point YS and UTS has decreased to 114 MPa and 215 MPa respectively.

Figure 4.25 shows that the elongation or ductility started to decrease after about 150˚C and at around 200˚C it became the lowest. However, with an increase in temperatures the elongation value rose to about 10%.

It is worthwhile noting that tensile properties of the alloy also vary with thermal treatment times as shown in Figures 4.26 and 4.27. Due to most of the optimum mechanical properties

found at around 200˚C heat treating temperature, all the time-varying thermal treatments were performed at this temperature. The results show that the yield strength has improved significantly from 160 to 190 MPa as the treatment time increased from 30 to 90 minutes at 200˚C. Thus, the yield strength has increased about 17% over that of half an hour treatment, and 44% compare to that of the as-cast condition, i.e. the optimum yield strength has achieved at 200˚C for 90 minutes treatment instead of 120 minutes. Moreover the ultimate tensile strength has increased for 90 minutes treatment to 286 MPa from 261 Mpa (30 minutes), which is almost the ultimate tensile strength achieved at 120 minutes. Elongation has decreased to 7.83% from 9.43% at 90 minutes and 30 minutes treatment respectively.

Discussion

1. The work of Crepeau et al. [76] on T5 treatment of 339 alloy shows that the cooperative precipitations of Al2Cu and Mg2Si phases are responsible for alloy hardening. During aging, these elements precipitate in the form of a large proportion of fine particles which in turn render the alloy its strength. Moreover, in the study of Koach et al. [48] has also indicated that an increase in magnesium content of Silafont-36 alloy enhances the yield strength even with low temperature heat treatment. Despite that Mg base intermetallics provide better ultimate tensile strength, they lower the elongation considerably. Therefore in the experimented alloy due to heat treatment Mg_2Si plays such a role in the strength at around 200˚C. EDS and SEM analyses have confirmed that, at this temperature, sufficient amount of Mg_2Si exists in the matrix, which provides relatively higher yield strength by reducing the elongation or ductility of the casting component.

2. Eutectic silicon morphology has certain effect on the enhancement of tensile strengths at 200˚C. Figures 4.17 to 4.19 it has shown that the distribution of eutectic silicon particles as well as their morphology has changed. At 200˚C eutectic silicon particles appear much more rounded than those in the as-cast samples (Figure 4.17). Although it is shown in Figure 4.20 that the width of the eutectic particles does not change considerably (31 microns in the as-cast state and 42 microns at 200˚C) the fine and rounded shape of eutectic particles reduces stress concentrate and consequently improves strengths at this treatment temperature.
3. It can be seen from Figure 4.24 that the yield and ultimate tensile strengths start to decrease. This may be due to at least partly the dissolution of the Mg_2Si intermetallics into the matrix. This type of intermetallic particles prevents the dislocation movement which in turn increases the strength of the alloy. Their absence (mostly) in specimens treated at high temperatures makes deformation process much more easily [76].
4. Moreover, at higher temperature, it can be seen from Figure 4.19 that the eutectic particles has coarsened significantly. Their width has increase to about 0.48 microns (0.31 microns in as-cast condition). Also, the interspacing within the intermetallic particles has also increased significantly (0.41 microns). Therefore these coarsening and change of distribution of eutectic particles should be responsible for lowering the strength as well.
5. Aniyi et al. [77] has shown that when residual stresses relieve from die casting components, their strength and hardness reduce. At high temperature, specifically above 200˚C, the residual stress has relieved from the experimented die cast

components, which implies the strength decreases should take place at high temperatures.

6. However it was found that the elongation or ductility has increased again at 350˚C which might be due to the absence (mostly) of Mg_2Si intermetallic phase and also the relief of residual stress.
7. The effect of time variation on mechanical properties has taken into consideration by the discussion in points 1 and 2.

4.4 Quality Index Analysis

Drouzy et al. [63] proposed quality index, Q as a new terms to describe the relationship among UTS, YS and %El. the Q is defined as,

$$Q = UTS + K \log E_f \quad \text{.....(4.1)}$$

where, K= strength co-efficient and E_f = elongation at fracture.

The quality index, together with yield strength, YS, can be represented by two sets of iso-lines (iso-YS and iso-Q) in a UTS-%E1 diagram. Some parameters *(e.g.* Mg content and aging condition) have an influence on YS but not on Q. On the other hand, the soundness of castings, modification process, cooling rate, and solution heat treatment can affect the quality index, Q. In general a process which produces sound, well-modified, and solution heat-treated castings possesses a high quality index, Q.

The quality index of the modified Silafont-36 alloy has calculated based on Caceres analytical model [64] which has already discussed in literature review of Chapter II. Eqs.(2.6), (2.7) and (2.8) were employed to plot the quality index.

4.4.1 True stress-strain curves

True stress-strain curves have been generated for different heat treatments from the engineering stress-strain curves by using the following equations:

True stress, $\sigma = s(e + 1)$……...(4.2)

and True strain, $\varepsilon = \ln(e + 1)$……..(4.3)

where, s= Engineering stress and e = Engineering strain

The representative curves for the treatments of as-cast, 200 and 350˚C for 120 minutes shown in Figures 4.28-4.30, respectively. From these figures it can be seen that 200˚C heat treated samples have high true stress in compare with those of the as-cast one. However, the alloy treated at 200˚C for 120 minutes has a relatively low true fracture strain which is about 7%. On the other hand in the as-cast alloy and the sample treated at 350˚C show a much high true fracture strain around 10%. Moreover, due to the complete residual stress relief and absence of magnesium intermetallic phase, the alloy treated at 350˚C posses lowest tensile strength among all the treatment conditions.

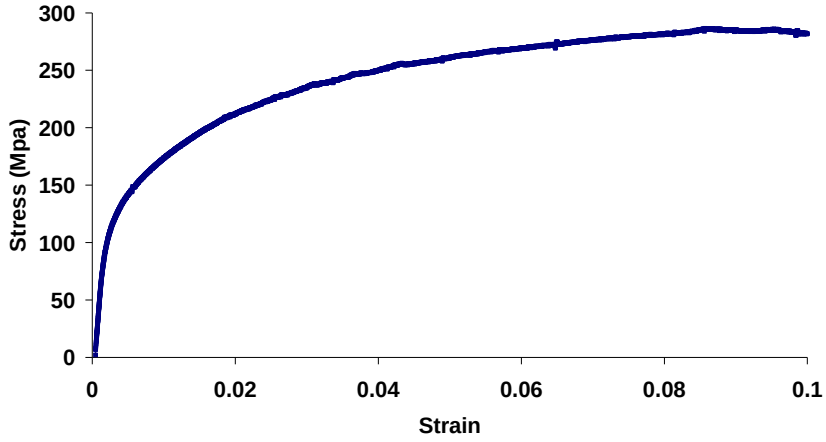

Figure 4.28 True stress-strain curves for the as-cast condition.

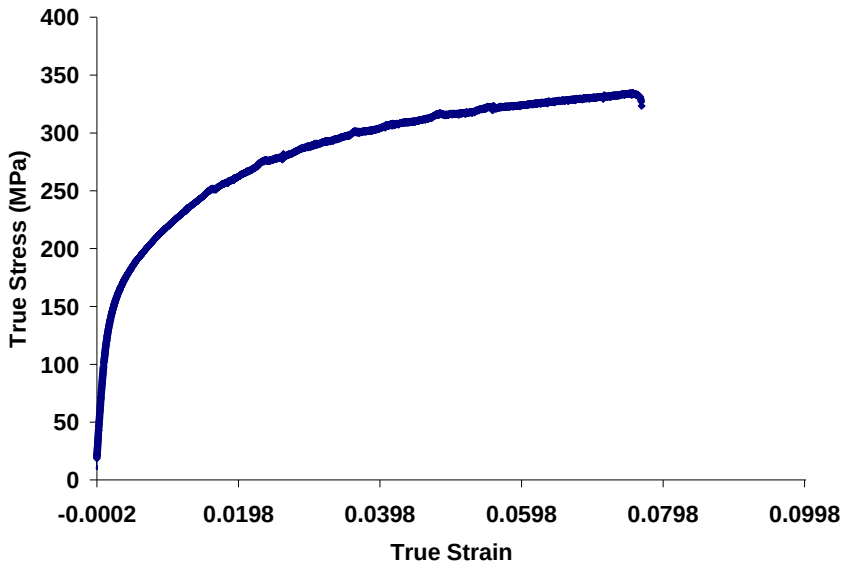

Figure 4.29 True stress-strain curves for the sample treated at 200˚C for 120 minutes.

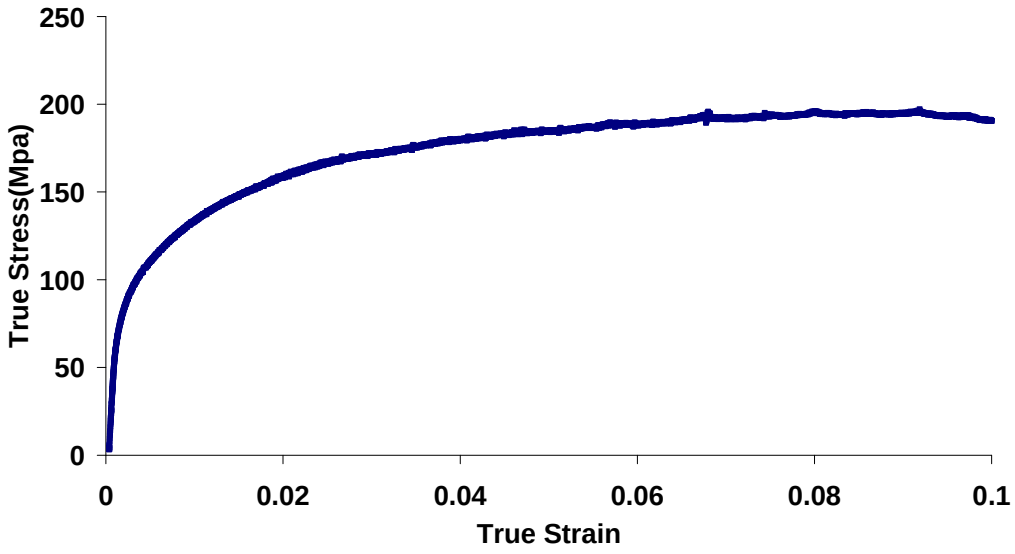

Figure 4.30 True stress-strain curves for the sample treated at 350˚C for 120 minutes.

4.4.2 K and n Values

The flow curve of metals in the region of uniform plastic deformation can be expressed by the Ramberg-Osgood relationship as [66],

$$\sigma = K\varepsilon^{n} \quad \text{.....(4.4)}$$

Here in Eq. (4.4), n is the strain hardening exponent and K is the strength co-efficient. A log-log plot of true stress and true strain up to maximum load will result in a straight line if Eq. (4.4) is satisfied by the data. The linear slope of this line is n and K is the true stress at $\varepsilon = 1.0$ [78] .The strain hardening exponent may have value from n=0 (perfectly plastic solid) to n =1 (perfectly elastic solid). Eq. (4.4) can be write in the following expression to define strain hardening rate,

$$d\sigma/d\varepsilon = n(\sigma/\varepsilon) \quad \text{.....(4.5)}$$

In this study materials strength co-efficient and strain hardening exponent has derived from the power curve on the plastic deformed regions of each heat treated samples and summarized in Table 4-3. The representative power curves have also drawn for three main treatment conditions of the as-cast, 200 and 350˚C for 120 minutes as shown in Figures 4.31-4.33.

Table 4-3 K and n values for different treatment

Treatment	K	n
As Cast	470± 16.32	0.2231±0.0091
120˚C	480±23.43	0.2183±0.0034
180˚C	490±17.45	0.1637±0.0056
200˚C	487±13.67	0.1571±0.00951
250˚C	389±9.78	0.1636±0.00514
300˚C	385±11.34	0.1625±0.00321
350˚C	349±14.23	0.2041±0.00365
	Average =440	

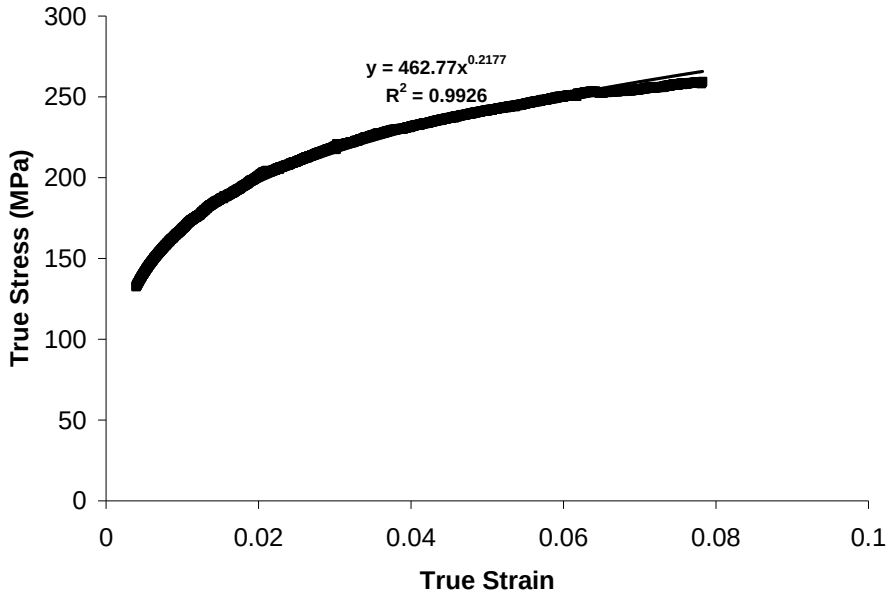

Figure 4.31 Power curve on plastic region of the as-cast sample.

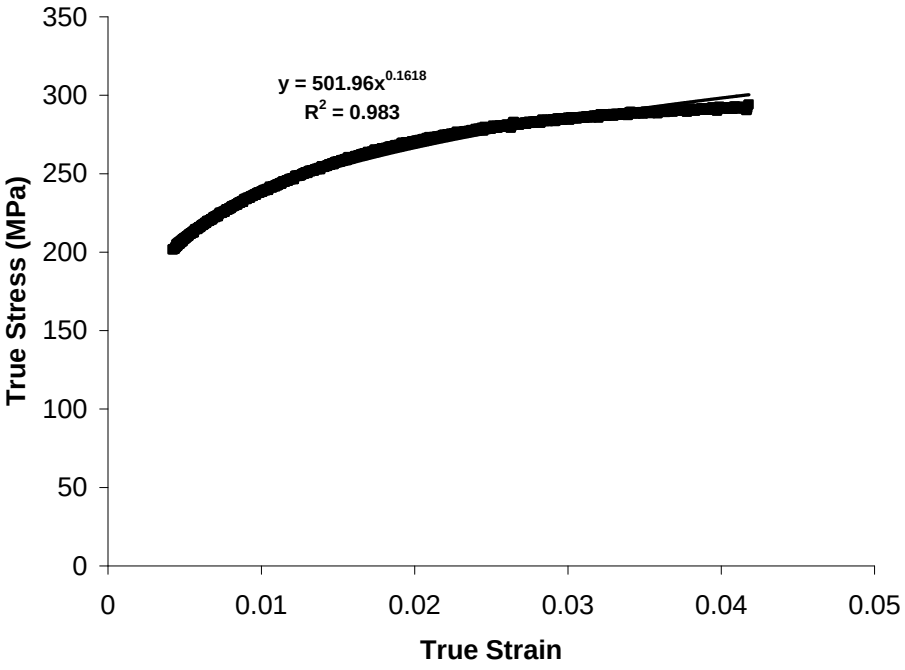

Figure 4.32 Power curve on plastic region at 200˚C for 120 minutes.

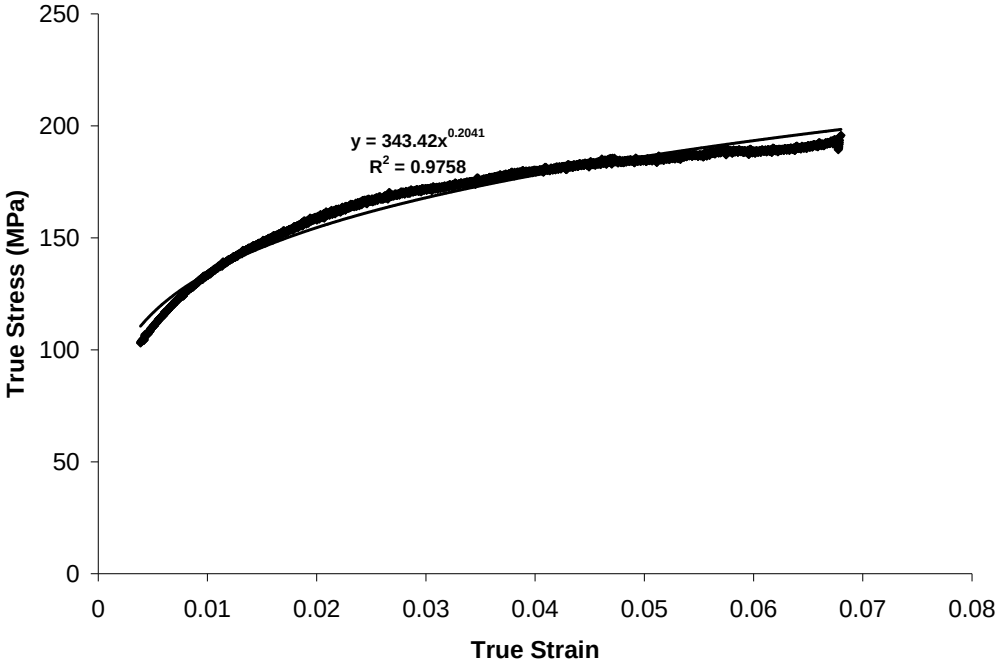

Figure 4.33 Power curve on plastic region at 350˚C for 120 minutes.

From the data of Table 4-3 it can be seen that the strength co-efficient (K value) appears to increase up to 200˚C, where high strengths exhibit within these range of temperature compare to the as-cast condition. Above 200˚C, the K value starts to decrease, which shows low strengths at high treatment temperatures. However, the strain hardening exponent (n values) has decreased from the as-cast condition to 200˚C treatment temperature, where the relatively low elongation is present. In addition, the n value has increased again at high treatment temperature, at which the alloy becomes relatively ductile again.

4.4.3 Quality Index Plot

The data in Table 4-3 were used to plot the quality index chart for the experimented alloy as given in Figure 4.34. For simplicity and in order to be able to compare both alloys on a common base, a single 'average' *K*-value (strength co-efficient) of 440 MPa (from Table 4-3) was assumed valid for all treatments. This value was used to generate the charts in Figure 4.34 using Eqs. (2.6), (2.7) and (2.8) from the Caceres model for a range of *n* values.

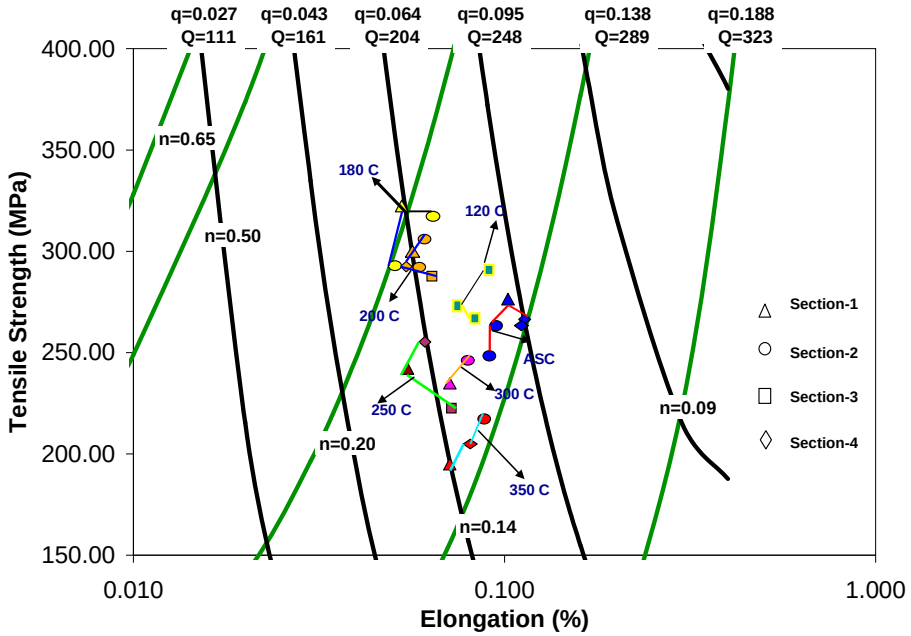

Figure 4.34 Quality index chart with tensile data at different thermal treatment conditions.

Figure 4.33 has two main axes i.e., tensile strength and ductility. Here q is referred as ductility parameter which is defined as,

$$q = S_f/n \quad \text{.....(4.6)}$$

where S_f is the nominal strain at fracture and n is strain hardening exponent.

The iso-q lines (black lines) are generated using Eq.2.7 from the Caceres model. The physical meaning of q is that when $q = 1$ the sample reaches necking, while $q < 1$ values identify progressively less ductile samples. Therefore, the high q values ductile materials.

From this analysis it can be seen that the alloy treated at 200˚C for 120 minutes possesses relatively high strengths than those of the as-cast one and treated at temperature above 200˚C samples. However, the 200˚C samples show comparatively less ductility than those of high temperature treated samples. On the other hand, high temperature thermal treatments improve the ductility but lower as q values become high at the temperatures above 200˚C. However, it can be seen from Figure 4.34 that although the thermal treatment at 200˚C for 120 minutes reduces the elongation or ductility with a low of value 0.064 the increase in strengths is evident. Figure 4.34 also shows that, 200˚C temperature, the quality index of Q value is about 204. Therefore, it can be concluded that the overall quality of the alloy treated at 200˚C for 120 minutes exhibits advantages over those of the other treatment conditions, and the thermal treatment at 200˚C optimizes the overall properties of the tested alloy.

4.5 Effect of Porosity on Mechanical Properties

As discussed in the preceding section, porosity always provides crack initiation sites which promote the early break at even low deformation. The porosity levels at different thermal treatment conditions are summarized in Table 4-4. The distribution of porosity and their effect with different thermal treatment has also shown in Figures 4.35 to 4.40. Due to vacuum assistance during the die casting process, the porosity level of the as-cast alloy was low in the cast component. However, this is almost impossible to

completely remove porosity from the casting part in die casting process because of the high pressure involvement, leakage at parting line, as well as turbulence effect resulting from high velocity injection to fill relatively thin sections of casting component. The fast shot velocity for the tested component was higher (about 4 m/sec) than that taking place in conventional die casting processes. This is because; the casting component (Engine base bracket) has several thin ribs around 2 mm in the thickness. To fill those thin sections it is necessary to apply a very high fast shot velocity. This may be one of the reasons for minor gas entrapment due to the possible turbulence of liquid metal caused by high cavity filling velocities. Moreover the applied vacuum level of 150 mbar may not be sufficient to completely prevent gas entrapment from the casting, which usually should be below 50mbar for high temperature thermal treatment such as solution heat treatment.

Table 4-4 Porosity and Density Variation at Different thermal treatment conditions

Treatment (˚C)	Avg. Density (gm/cc)	Porosity Percentage	Avg.Porosity size (Micrometer)
As Cast	2.627 ± 0.07	0.8	13.59 ± 3.1
120	2.623± 0.12	1.2	13.38 ± 2.52
180	2.621± 0.09	1.4	13.87 ± 2.67
200	2.618 ± 0.03	1.6	14.43 ± 1.04
250	2.614 ± 0.03	2.1	16.78 ± 1.46
300˚c	2.610 ± 0.02	2.4	17.46 ± 0.96
350	2.609± 0.02	2.7	19.23 ± 1.43

According to Niu et al. [26], the presence of gas porosity in castings is harmful as the mechanical properties and pressure tightness are adversely affected. In addition, the formed pores, particularly those located adjacent to the casting surface, tend to expand in size, leading to the formation of blisters at the casting surface when heat treated. Therefore, the applications of aluminum die castings are normally limited to certain structural components for which no heat treatment is required.

This is well approved in several research works [26, 44, 45, 58, 59] that the size and number of porosity increases with progressive heat treatment which is supported by the progressive decrease of density value of the particular alloy shown in Table 4-4 i.e., increase of thermal treatment temperature influence the size and amount of gas porosity which in turns reduce the overall density of the alloy.

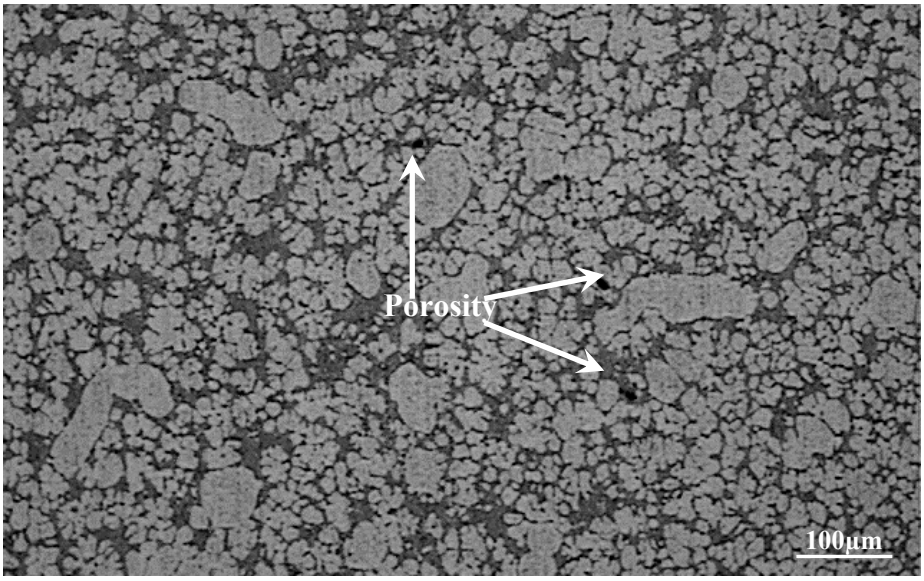

Figure 4.35 Porosity in an as-cast specimen.

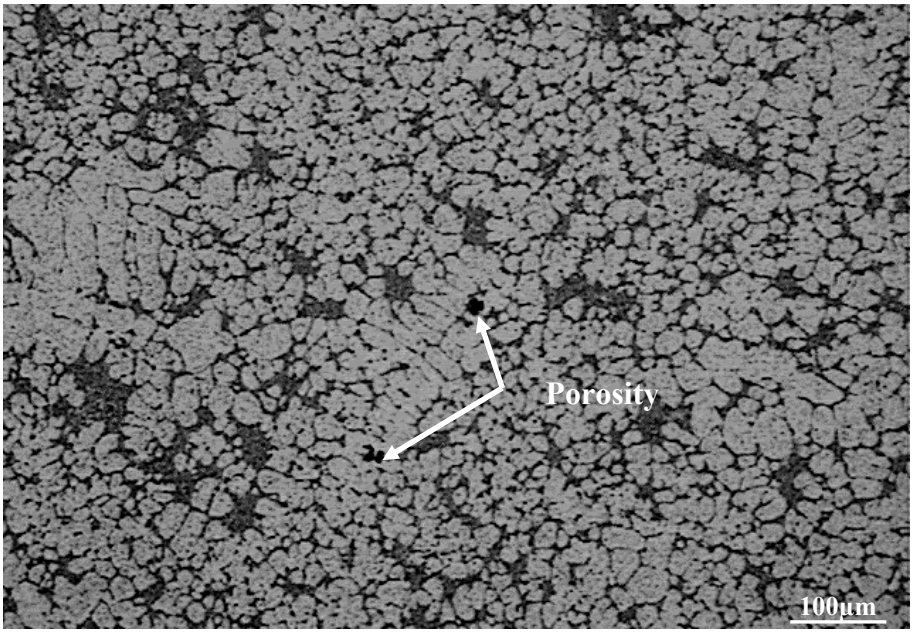

Figure 4.36 Porosity in a sample treated at 150˚C for 120 minutes.

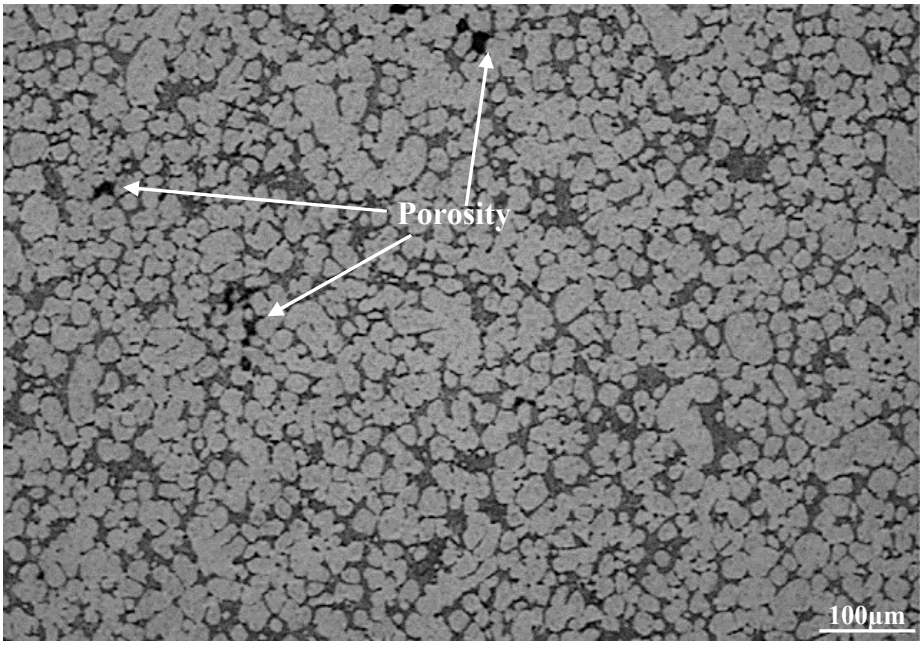

Figure 4.37 Porosity in a sample treated at 200˚C for 120 minutes.

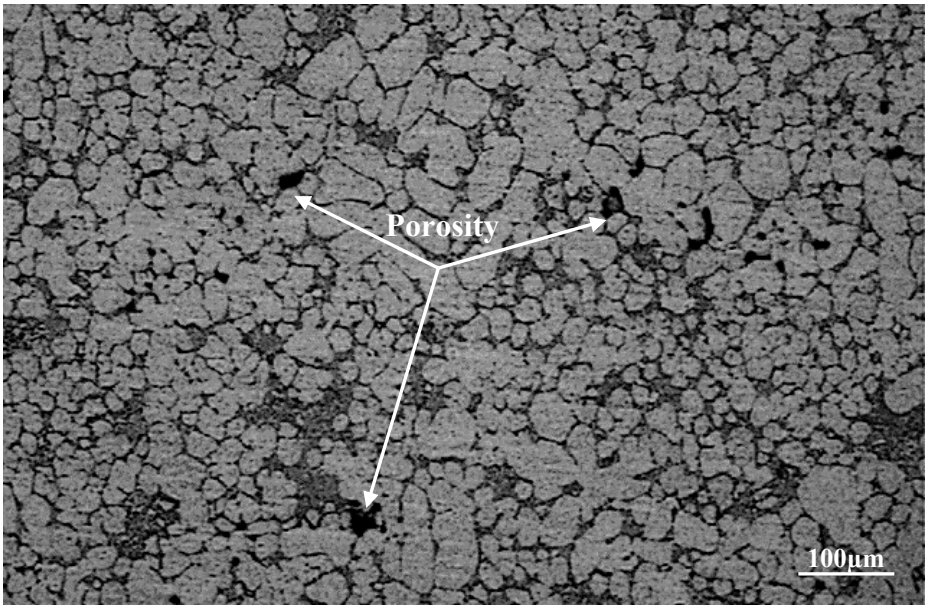

Figure 4.38 Porosity in a sample treated at 250˚C for 120 minutes.

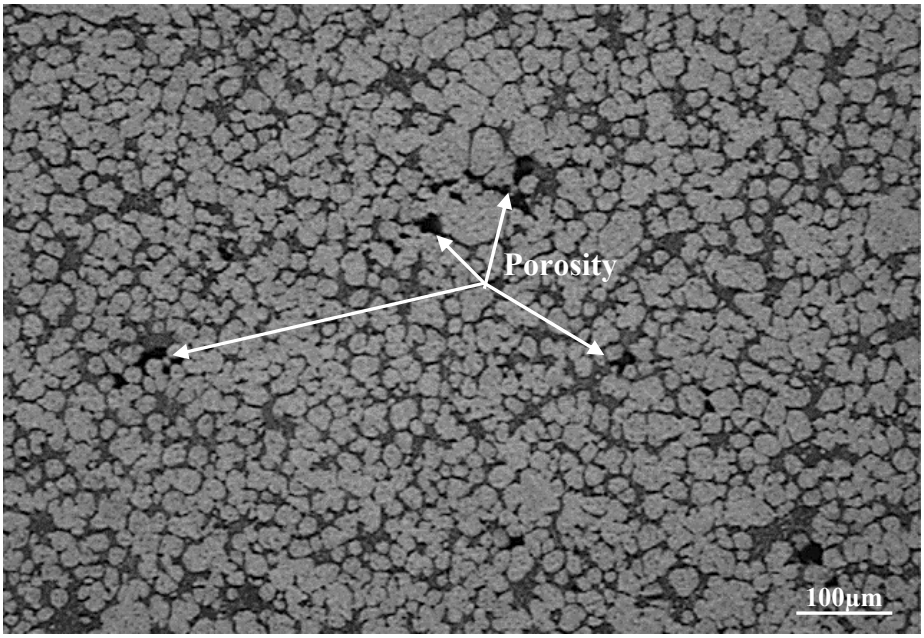

Figure 4.39 Porosity in a sample treated at 300˚C for 120 minutes.

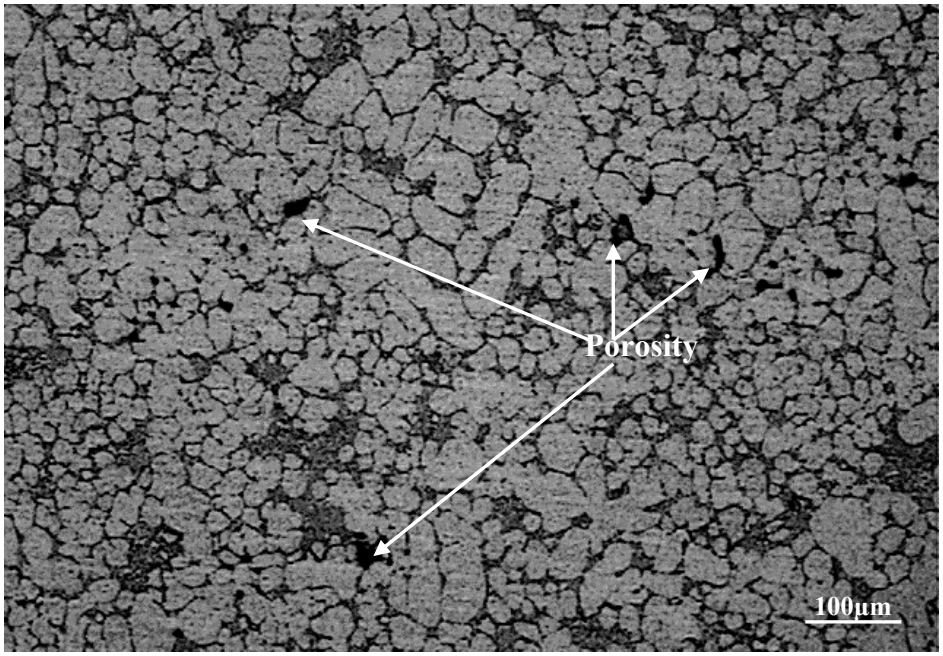

Figure 4.340 Porosity in a sample treated at 350˚C for 120 minutes.

From the experimental value of porosity level and density value, it can be seen that as the thermal treatment temperature increases, the porosity level raises from 0.8% to 2.7%. This observation indicates that the releasing rate of gas dissolved in the alloy increased with increasing temperature. The increasing trend of porosity level implies that high temperature exerts high driving forces for pore growth. Moreover, the size of the pores also increased. From Table 4.4, it can be seen that initially (as cast condition) the average size of the porosity was about 13µm but at the highest heat treated temperature (350˚C) the average porosity size became about 19 µm. Although the thermal treatment temperature was not very high, the results show that it has certain impact on the content of porosity. These enlargement and increase of the number of porosity provides relatively more crack initiation sites in the casting during tensile load.

Discussion

1. Ductility of any material is an important function of the material integrity and this property can be affected by any void and/or defect that de-coherent easily from the matrix, which significantly decreases the load-carrying cross-sectional area. Local inhomogenities (such as porosity, shrinkage or casting defects) increase the local concentration of strain and leads to lower elongation at failure. i.e. the materials fails without showing its actual deformation. According to Boileau [79] "the trend that for ductile failure, the elongation is a function of the number and the area fraction of defects, in general, as the number and area of the defects increased, the elongation decreased." This trend is also found in the elongation data obtained from this study.
2. The ultimate tensile strength (UTS) is a function of the factors affecting yield strength as well as with those factors affecting the degree of plastic elongation prior to failure. Since the level of porosity significantly affects the elongation, it is also expected to affect on the UTS as well.
3. Porosity can have the effect of: a) altering the field of stress to initiate fracture, b) affecting crack propagation, and c) reducing the effective load-bearing area of the component as mentioned in the preceding literature review.

As a result of these porosity creation and enlargement when a tensile load is applied to a component containing porosity, the stress is concentrated about the pores. In a very brittle alloy, the stress is concentrated immediately adjacent to the pore and fracture begins at this point. However in ductile alloy the scenario will be different as this stress can be distributed effectively that failure still occurs at other stress concentrating

features, such as silicon/eutectic silicon particles. Once a crack has formed these pores can act as pre-existing elements of the crack and hence lead to rapid crack propagation [60].

In this study the thermal treatment has given to observe its effect on tensile properties. In general, the thermal treatment temperatures were not very high (maximum temperature was 350˚C) which is far less than solutionization aging temperatures (about 540˚C). Therefore it is expected that the applied temperatures may not provide severe external forces to expand the porosity to make it much worse. In Wang's et al. [60] work, it was found that when the sample (A380 alloy) was solution heat treated at 525˚C for 6 hours the porosity level had increased to about 7.32% found (even with using vacuum assistance in the process). In this study the thermal treatment duration was also not very long (only for 120 minutes or 2 hours), therefore the thermal treatment effects on porosity level was not severe, although a minor effect of porosity expansion observed which may have certain effect on strength of the properties.

4.6 Facture Behaviour

To evaluate the fracture behaviour, fractured samples (after tensile test) at different treatment were analyzed with SEM. The representative micrographs of these fracture surfaces are shown in Figures 4.41 to 4.45. The optical micrographs beneath the tensile surface were also depicted in Figures 4.47-4.50 for the corresponding samples.

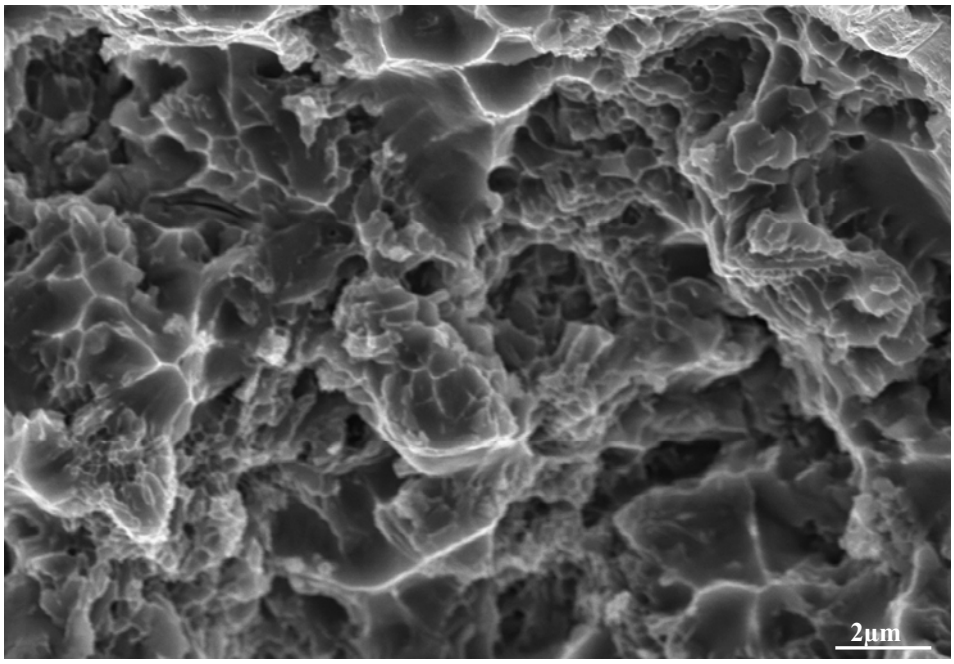

Figure 4.41 SEM micrograph showing the fracture surface of an as-cast sample.

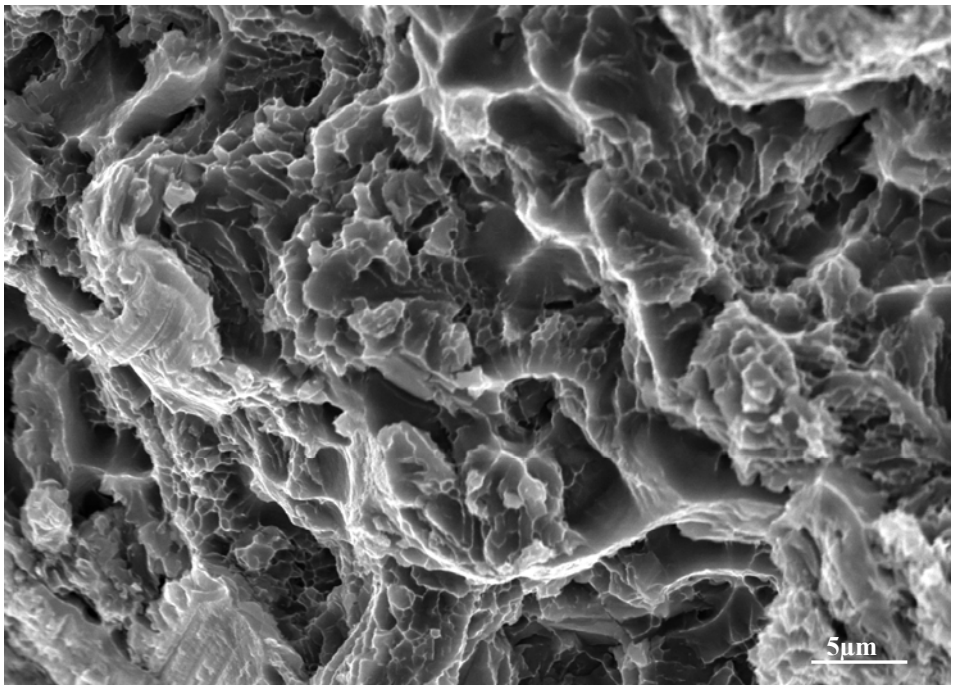

Figure 4.42 SEM micrograph showing the fracture surface of a sample heat treated at 200˚C for 120 minutes.

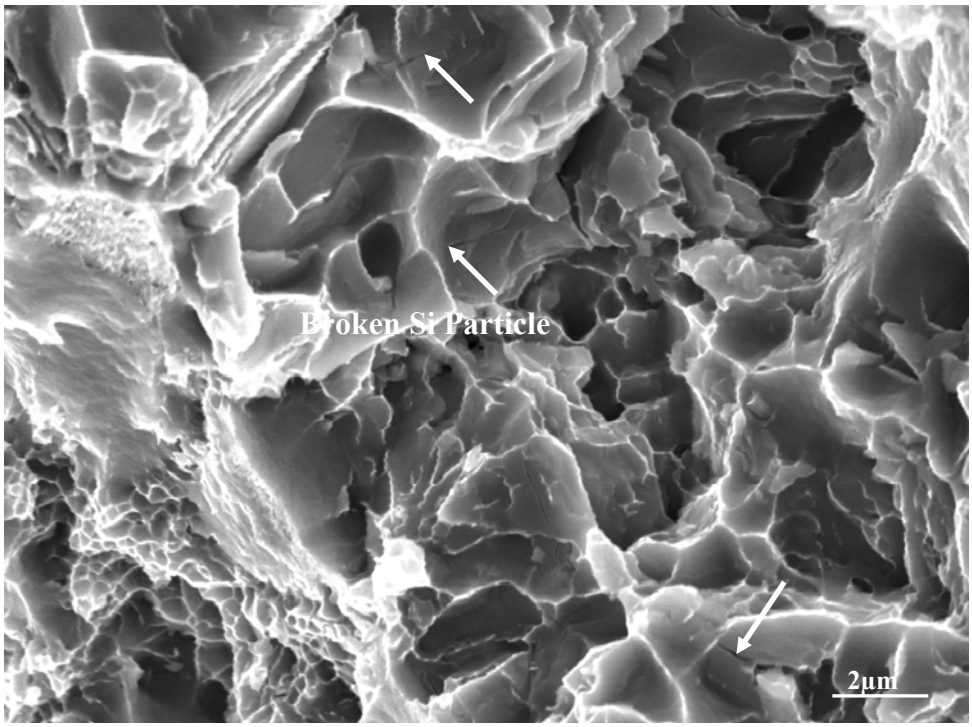

Figure 4.43 SEM micrograph showing the fracture surface of a sample heat treated at 200˚C for 120 minutes.

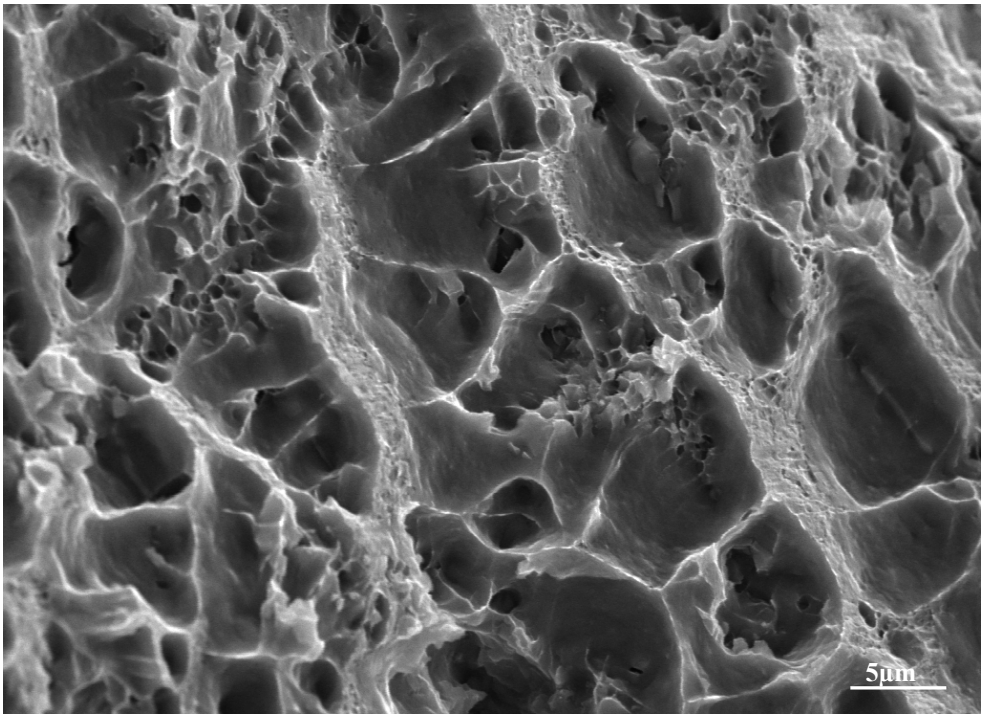

Figure 4.44 SEM micrograph showing the fracture surface of a sample heat treated at 350˚C for 120 minutes.

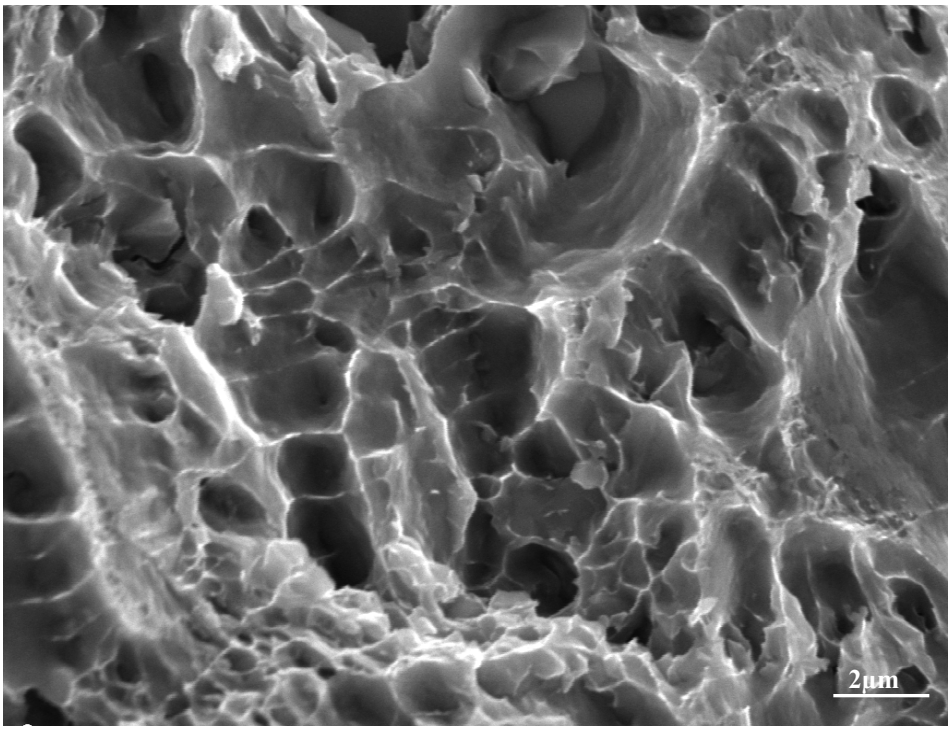

Figure 4.45 SEM micrograph showing the fracture surface of a sample heat treated at 350˚C for 120 minutes.

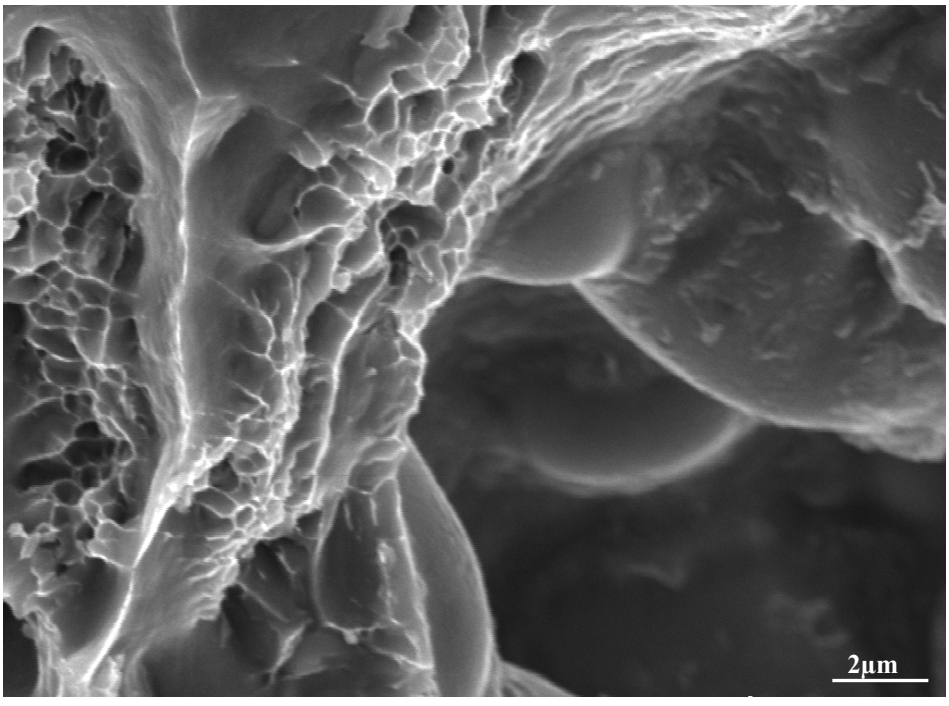

Figure 4.46 SEM micrograph showing the effect of porosity on fracture of a sample treated at 350˚C for 120 minutes.

It can be seen from Figure 4.41 to Figure 4.45 that extensive deformation has occurred in almost all thermal treatment which is characterized by deep dimples in almost all cases. As mentioned before that the experimented alloy is a low silicon and strontium modified Silafont-36 (AA365) alloy, sufficient modification of silicon was already done by strontium within the alloy and therefore the brittle nature of needle like silicon was not observed on the fracture surface. However, Figure 4.42 and Figure 4.43 show a remarkable feature as well. Although the samples at 200˚C, contains deep dimples in the microstructures, however some damage silicon particles has also observed at this particular thermal treatment which is shown in Figure 4.43. This implies that the samples at this thermal treatment may be suffered more tensile load which causes the damage of the silicon particles. Therefore at this thermal treatment the corresponding samples shows higher UTS (about 300MPa) and YS (about 200MPa) value with lower ductility (around 7%) in comparison to as-cast or 350˚C thermal treatment. However, as the tested alloy was high pressure die casted certain porosity features has also observed. For analysing the fracture behaviour along those porosity site Figure 4.46 is depicted as an example. Although this is shown only at 350˚C however, this feature has also rarely found at other thermal treatments as well. It can be seen from this analysis; smooth α-Al grains are presents around the porosity which indicates relatively low deformation in this region near a pore. Therefore the specimen fractured at this region under low stress and strain. This may scattered the properties, i.e., the regions which are free from these defects shows much better mechanical properties (specifically ductility). Fortunately, vacuum assistance mostly prevents the cast component from this unexpected defect. Thus, overall ductility of the alloy shows moderate level of ductility.

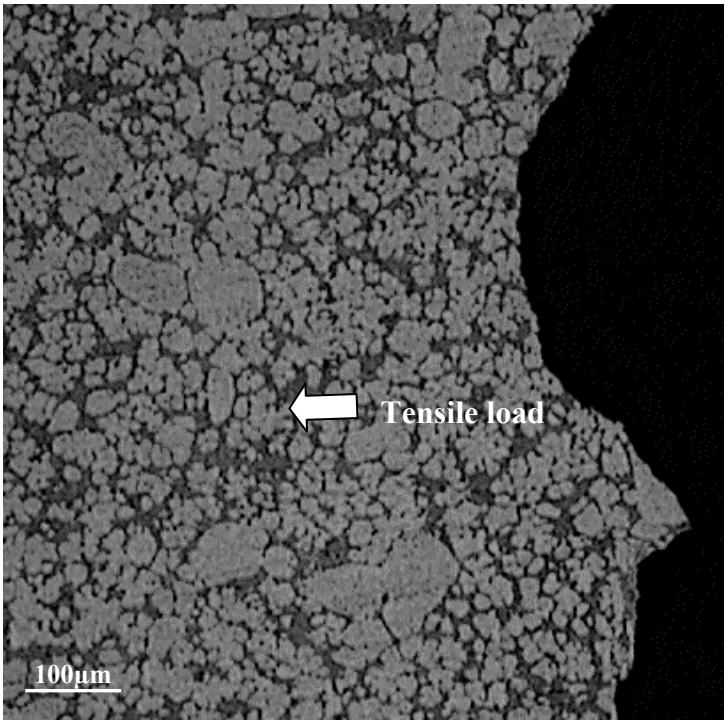

Figure 4.47 Optical Micrograph showing the longitudinal section of a fractured casting in as-cast Condition.

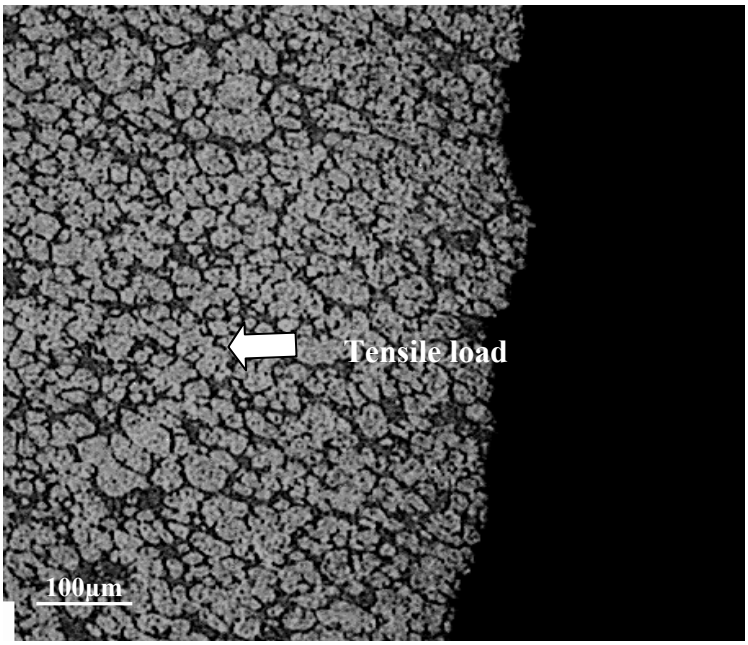

Figure 4.48 Optical Micrograph shows the longitudinal section of the fractured casting treated at 200˚C for 120 minutes.

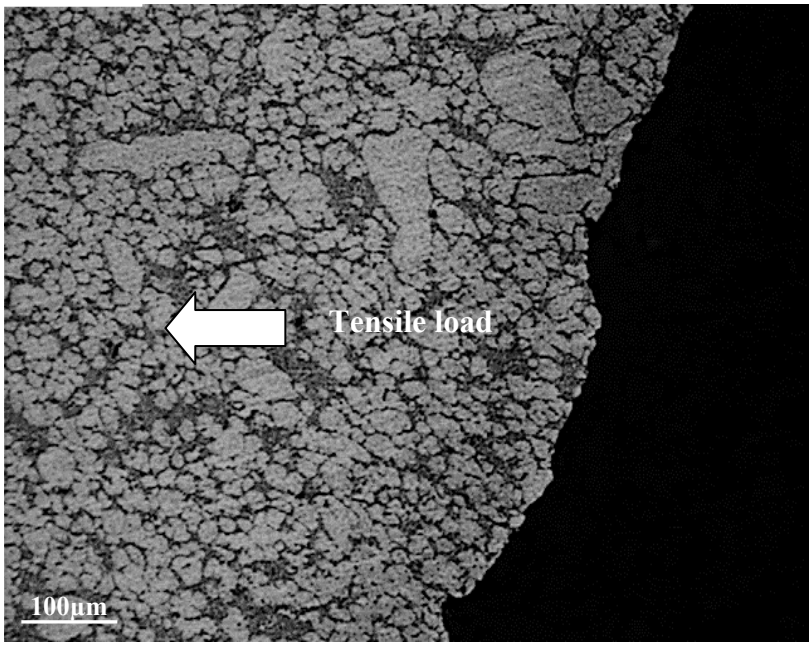

Figure 4.49 Optical Micrograph shows the longitudinal section of the fractured casting treated at 350˚C for 120 minutes.

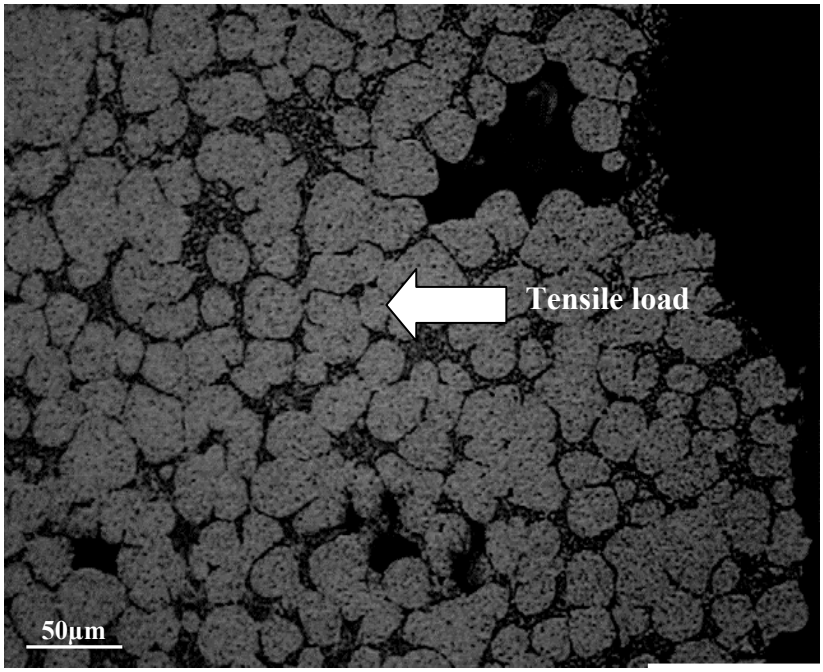

Figure 4.50 Optical micrograph shows fracture at porosity region at 350˚C for 120 minutes.

From Figures 4.47 to 4.49 it can be seen that almost in all thermal treatment fracture was found to originate from the eutectic silicon plates instead of transgranular fracture of α-Al grain. The fracture path is thus mainly along the boundary between the α-Al grains and the eutectic mixture which are clearly observed in these Figures. Therefore the experimented vacuum die cast component provides a moderate level of tensile strength (about 250MPa) and ductility (7-8%).

However from Table 4-4 it was shown that with successive increase of thermal treatment the porosity level has increased to 2.7%. Although the porosity level at this treatment is not that much severe which generally presents in conventional die casting process however, this level of porosity (2.7%) has may have some role in the microstructures which are depicted in Figure 4.50. The fracture mechanism around a pore is shown here (Figure 4.50). It can be seen from this figure that the cracks are easily formed in the porosity region because of high stress concentration due to the reduced effective area. The fracture path in these states (where porosity presents) is therefore along the interconnection of the porosity which in turns reduces the strength and ductility.

A throughout analysis at different position of microstructures at different thermal treatment confirmed that the minor level of porosity of the experimented casting component are not uniformly distributed. In addition due to their lower content they rarely affect on the mechanical properties.

In addition it has shown in Table 4-4 that the casting component does not suffers the porosity problem that much at 200˚C thermal treatment as well as it provides relatively higher strength and moderate level of ductility therefore this is considered as optimum condition for this study.

CHAPTER-V

CONCLUSIONS

1. High pressure vacuum die cast modified AA365 alloy needs to be thermally treated for the purpose of relief of residual stress for dimensional stability of casting. To understand the effect of thermal treatment on tensile properties, different thermal treatment schemes were investigated in this study. It is found that, under a thermal treatment scheme of 200˚C for 90 minutes, the relatively high YS and UTS of 193.8 and 286.0 MPa, respectively, are obtained compared to 133.6 MPa for the YS and 251.45 MPa for the UTS of the as-cast alloy. However, this thermal treatment scheme results in a decrease in elongation to 7.83% from 10.7% in the as-cast condition.
2. It is evident that the morphology of eutectic silicon has a sound effect on the tensile properties of the tested alloy. Fine eutectic particles and their proper distribution in the matrix enhance the mechanical strengths of the alloy.
3. The content of magnesium-containing intermetallic phase, their morphology and distribution throughout the matrix affects the mechanical properties. The reduction in the strengths of the alloy treated at 350˚C for 120 minutes should be attributed at least partly to the absence of the magnesium-containing intermetallic phase. However, the presence of sufficient amount of magnesium intermetallic phase had played an important role in strengthening the alloy thermally treated at 200˚C for 120 minutes.

4. The tensile properties of the alloy are sensitive to the presence of porosity, their size and contents. A high level of porosity and their expansion could lead to a deleterious effect on the tensile properties. The porosity-sensitivity at 200˚C thermal treatment for 90 minutes was not very significant. However, the relatively high temperature thermal treatment led to an increase in the porosity level of the alloy. The porosity level increase should result from the release of some dissolved gas, which may not respond at a relatively low thermal treatment temperature.
5. The application of vacuum assistance systems in die casting process minimizes and reduces gas entrapment in castings. A porosity level of only 0.8% was found in the as-cast condition which is relatively very low in compare with conventional die casting process (usually about 3%). The thermal treatment at low temperature below 200˚C does not affect the porosity level significantly, rather enhances the mechanical strengths with a moderate level of ductility.

CHAPTER-VI

SUGGESTIONS FOR FUTURE RESEARCH

1. Modified vacuum die cast AA365 alloy responds to thermal treatments. Tensile properties were influenced by both thermal treatment temperatures and times. Eutectic silicon morphology and their distribution around the matrix were affected by higher thermal treatment temperature. Intermetallic phases were dissolved at certain thermal treatment schemes. However, the dissolution kinetics, i.e., the exact amount of dissolved intermetallic phases (Mg_2Si) and their morphology change with successive thermal treatment needs to be further studied.
2. TEM technique could be employed to reveal and acquire more detailed microstructural information of the alloy, such as the propagation behaviour of dislocation in front of obstacle particles and voids if exists.
3. Solution treatments should be studied to further improve the mechanical properties by properly controlling the dissolution of strengthening phases in the matrix. Moreover, the effect of solution treatment on the change of eutectic silicon morphology also needs to be studied, which plays an important role in determining the tensile properties.
4. The maximum design stress is always an important issue for design purpose. By applying the Weibull analysis, it becomes possible to predict the probability of fracture, the maximum applicable stress for a certain casting component. Hence, to determine the design stress for vacuum die

cast AA365, a detail weibull analysis on tensile properties needs to be carried out.

5. Vacuum assistance provides substantial benefit on die casting process in terms of gas porosity. A throughout study on different levels of vacuum should be conducted to determine the optimum level of vacuum which minimizes the blistering effect and the porosity level increase during thermal treatment on modified AA365 alloy.

REFERENCES

1. NADCA Products Specifications for Die Castings, NADCA, USA, 2009**.**
2. C.E. Mobley, Quality of die casting, Presented at defining the state of Die casting technology workshop, Worecester. MA, USA, US department of Energy/North American Die casting association/University of Northern Iowa, March 1993.
3. H.K. Kirgin, 1994 super boom will softer somewhat in 95, Modern Casting, 85/1, 23-26, 1995.
4. Aluminum Die Casting, www.answers.com/topic/aluminum-die-castings, September 2009.
5. Modern casting, www.findarticles.com/p/articles/ontent;col1, September 2009.
6. Internet article: Modern Casting, 2006. Http://findarticles.com/p/articles/mi_hb6616/is_3_96/ai_n29253890/pg_2/?tag=content;col1, September 2009.
7. R. Elliot, Eutectic solidification processing, Butlerworth, London, 1983.
8. L.F. Mondolfo, Manganese in aluminum alloys, The Manganese Centre, Paris, 1977.
9. D. Beaulieu, Characteristics of structural aluminum, Presses de l'aluminum, Chicoutimi, Quebec, 2005.
10. R.D. Howard, Aluminum heat treatment processes- applications and equipment, www.industrialheating.com, September 2009.
11. L. Backerud, G. Chai, J. Tamminen, Solidification characteristics of aluminum alloys, AFS Transactions, 2, 24-37, 71-81, 1990.

12. S. Shankar, Y.W. Riddle, M.M. Makhlouf, Nucleation mechanism of the eutectic phases in aluminum-silicon hypoeutectic alloys, Acta Mat, 52/15, 4447-4460, 2004.
13. D.L. Zhang, B. Cantor, Heterogeneous nucleation of solidification of Si by solid AI in hypoeutectic Al-Si alloy, Metallurgical and Materials Transaction, A 24/5, 1195-1204, 1993.
14. C.R. Ho, B. Cantor, Heterogeneous nucleation of solidification of silicon in AlSi, Materials Science and Engineering A, 173/1-2, 37-40, 1993.
15. B. Cantor, Impurity effects on heterogeneous nucleation, Materials Science and Engineering A, 226-228, 151-156, 1997.
16. J.L. Murray, A.J. Mcallister, Bull alloy phase diagrams, 1984.
17. J. Gobrecht, C. Manan, S.V. Eisen, In Aluminum –Silicium-Gublegierurngen Teil 1, Geiberei 62 (10), 262-66, 1975 and JL. Jorstad, Understanding Sludge, Die Casting Engineer, 1986.
18. S. Nafisi, R. Ghomashchi, H.Vali, Eutectic nucleation in hypoeutectic Al-Si alloys, Materials Characterization, 59, 1466-1473, 2008.
19. S.Shankar, YW.Riddle, M.Makhlouf, Phases in Aluminum-Silicon Hypoeutectic Alloys", Acta Mat, 52, 4447–60, 2004.
20. A.K. Dahle, K. Nogita, J.W. Zindel, S.D. Mcdonald, L.M. Hogan, Eutectic nucleation and growth in hypoeutectic Al-Si alloys at different strontium levels, Metallurgical and Materials Transaction A, 32, 949-960, 2001.
21. K. Nogita, S.D. Mcdonald, K. Tsujimoto, K. Yasuda, A.K. Dahle, Aluminum phosphide as a eutectic nucleus in hypoeutectic Al-Si alloys, Journal of Electron Microscopy, 53, 361–369, 2004.

22. H. Doehler, Art of and apparatus for casting fluid metal, United States Patent 973, 483, United States Patent and Trademark Office, Washington, 25, October 1910.
23. H. Doehler, Die Casting, McGraw Hill Book Company, New York, 1951.
24. X.P. Niu, B.H. Hu, I. Pinwill, H. Li, Vacuum assisted high pressure die casting of aluminum alloys, Journal of Materials Processing Technology, 105, 119-127, 2000.
25. E. J. Vinarcik, High integrity die casting process, John Wiley & Sons Inc., USA, 2003.
26. D. Lindsey, J. Wallace, Effect of vent size and design, lubrication practice, metal degassing, die texturing and filling of shot sleeve on die casting soundness, Proceedings 7th International Die Casting Congress, 1–15, 1972.
27. D. Hayes, Plunger lubricants are important too!, Die Casting Engineer, 1, 32, 1983.
28. A. Gordon, G. Meszaros, J. Naizer, P. Gangasani, C. Mobley, Comparison of methods for characterizing porosity in die castings, Report No. ERC/NSM-91-51-C, The Ohio State University Engineering Research Center for Net Shape Manufacturing, August 1991.
29. G. Meszaros, Lubricant gasification as a contributing factor to porosity in die casting, Master's Thesis, The Ohio State University, Columbus, 1992.
30. A. Gordon, The effects of porosity on the tensile properties of die cast aluminum alloys B390 and B380, Master's Thesis, The Ohio State University, Columbus, 1992.
31. E. Vinarcik, C. Mobley, Decomposition and gasification characteristics of die casting plunger lubricants, Report No. ERC/NSM-UIRS-92-17, The Ohio State

University Engineering Research Center for Net Shape Manufacturing, October 1992.

32. A. Gordon, G. Meszaros, J. Naizer, C. Mobley, A method for predicting porosity in die castings. Technical Brief No. ERC/NSM-TB-91-04-C, The Ohio State University Engineering Research Center for Net Shape Manufacturing, September 1991.
33. R.Cornell, H.K.D.H. Bhadeshia, Aluminium-Silicon casting alloys, University of Cambridge, Lecture notes, www.msm.cam.ac.uk/phasetrans/abstracts/M7-8.html, September 2009.
34. L.Sulley, Die Casting, D. Stefanescu, Metals Handbook-Casting, 9th ed., ASM International, Materials Park, OH, 15, 286, 1988.
35. A. Kaye, A. Street, Die Casting Metallurgy, Butterworths, London, 1982.
36. A.Street, The Die Casting, Portcullis Press Ltd, 3-16, 625-641, 1977.
37. K. Baumgartner, Vacuum high technology for top quality pressure die castings, Proceedings of the 15th International Pressure Die Casting Conference, Montreaux, Switzerland, May 22, 1996.
38. P.Robbins, Vacuum assisted die casting today's most significant technology, NADCA Conference Paper Collection, 44, 279-284, 2003.
39. F.O.Stermann, Aluminum materials technology for automobile construction, Edited by W.J. Barts, United Kingdom, 1993.
40. H. Kaufmann, P. J. Uggowitzer, Metallurgy and processing of high-integrity light metal pressure casting, Schiele and Schon, Berlin, 2007.

41. H. Hu, Y. wang, A. T.Alpas, Y. Chu, P. Cheng, Solution heat treatment of vacuum high pressure die cast aluminum alloy A380, NADCA Conference Paper Collection, 2005.
42. E.S. Kim, K.H. Lee, Y.H. Moon, A feasibility study of the partial squeeze and vacuum die casting process, Journal of Materials Processing Technology, 105/1-2, 42-48, 2000.
43. S.Wiesner, Wirtschaftliche herstellung von gasarmem, schweiβbarem Aluminium-Druckguss, Dissertation, TU Braunschweig, Shaker Verlag, Aachen ISBN 3-8322-1388-0, 2003.
44. E.L. Rooy, Aluminum and Aluminum Alloys, ASM Handbook, 9th edition, 15, 747, 1993.
45. L.Wang, V. Alguine, M. Gershenzon, G. Savage, K. Rogers, Die leistungsfahigkeit einer vakuumanlage in einer industriellen druckgieβmaschine, Druckguss-Praxis, 1, 33-38, 2004.
46. Suppliers Directory, Official publication of the North American die casting association, ISSN 0012-253X, NADCA-2008.
47. Optimizing the Manganese and Magnesium Content for Structural Application, Code No-637, NADCA-2003.
48. H. Koch, U. Hielscher, H. Sternau, A.J. Franke, Silafont 36, the new low-iron high-pressure die-casting alloy, The Minerals, Metals & Materials Society, 1011-1018, 1995.
49. W.Schneider, W. Vogel, H. Baldering, Wärmebehandlung von Aluminium-Gußlegierungen für Druck-und Kokillenguß, 77, 693-699, 1990.

50. Z. Anna, C. Federico, The low iron ductile die casting alloy development and applications, Aluminium Rheinfelden, 33-38, 2007.
51. YAMAHA, Home page 2003, www.bikepics.com/yamaha/r1/03/, September 2009.
52. W. Schneider, F.J. Feikus, Heat treatment of aluminum alloys casting for vacuum die casting, Light Metal Age, 22-38, 1998.
53. B.Closset, R. Drew, J. Gruezleski, Eutectic silicon shape control by in situ measurement of resistivity, AFS Transactions, 94, 9-16, 1986.
54. Materials World, 12/ 3, 37-38, 2004.
55. Aluminum and Aluminum Alloys, ASM Handbook, 1st Edition, Materials Park, OH, 1993.
56. D.R.Askeland, The Science and Engineering of Materials, 3rd Edition, Chapman and Hall, United Kingdom, 1998.
57. D.O. Northwood, X. Sun, G. Byczynski, J.H. Sokolowski, J. Oswald, R. Thomas, D.E. Penrod, W.A. Esseltine, The Development of a two-stage solution treatment for cast Al-Si-Cu alloys, International Conference on Casting and Solidification of Light Alloys, Gold Coast, published in proceedings (ISBN 0958812829), Australia, 15-19, 1995.
58. H. Hu, A.S. Spadafora, R.F. Turchi, A.T. Alpas, Solution treatment and artificial aging of vacuum die cast alloy A380, Light Metals, Montreal, Canada, CIM, 475-486, 2002.
59. Y. Wang, Solution treatment of vacuum high pressure die cast aluminum alloy A380, Masters Thesis, University of Windsor, 2004.

60. R.N. Lumley, R.G.O. Donnell, D.R. Gunasegaram, M. Givord, New treatment for aluminum high pressure die castings, CSIRO Manufacturing and Infrastructure Technology, Australia, Heat Treating Progress Sep/Oct, 2006.
61. G. Timelli, O. Lohne, L. Arnberg, H. I. Laukli, Effect of solution heat treatments on the microstructure and mechanical properties of a die-cast AlSi7Mg Alloy, Metallurgical and Materials Transactions. A, Physical Metallurgy and Materials Science (ISSN: 1073-5623), 39A, 1747-1758, 2008.
62. Y. Chu, Private communication, Ryobi Die Casting, Shelville, IN, 2009.
63. C.H.Caceres, J. Sokolowski , P. Gallo, Effect of ageing and Mg content on the quality index of two model Al-Cu-Si-Mg alloys, Mat. Sci. & Eng. A, A127 (1-2), 53-61, 1999.
64. C.H. Caceres, Microstructure design and heat treatment selection for casting alloys using the quality index, J. of Mat. Eng. & Performance, 9(2), 215-221, 2000.
65. X.Tian, Berillium enhanced precipitation in Al-Mg-Si alloy of nucleation, entropy and interfacial energy, Masters thesis, Thesis collection of Leddy library, University of Windsor, Windsor, Canada, 1988.
66. J.H. Holloman, Tensile deformation, Trans AIME, 162, 268-275, 1945.
67. J.H. Rechardson and R.V.Peterson, Systematic materials analysis, academic press, New York, 1978.
68. C.Michaelsen, K.Barmak and T.P. Weihs, Investing the thermodynamics and kinetics of thin film reactions by differential scanning calorimetry", Journal of Physics D, 30(23), 3167-3186, 1997.

69. E.Aghion and B.Bronfin, Influence of process parameters on fluidity of investement casting, Procedings of 3rd International Magnesium Conference, Institute of Materials, London, 313-325, 1997.
70. Rivlin GV. Int Met Rev, 3, 133, 1981.
71. Richards RW. Int Met Rev, 39, 191, 1994.
72. B.I. Edeson and W.M. Baldwin, The effect of second phase on the mechanical properties of alloys, Jr. Trans. A, Soc, Met, 55, 230, 1962.
73. H.Chen, Effect of cooling rate, strontium modification, melt thermal treatment and solution heat treatment on the eutectic silicon particle characterestics and tensile properties of 356 alloy, Masters thesis, Universite Du Quebec A Chicoutimi, 150, 2005.
74. Hanna MD, Lu SZ, Hellawell A., The effect of SiC particles on the size and morphology of eutectic silicon in cast A356/SiC_p composites Metall Trans A, 15A, 459, 1984.
75. X. Jian, T.T. Meek, Q. Han, Refinement of eutectic silicon phase of aluminum A356 alloy using high-intensity ultrasonic vibration, Scripta Mat., 54, 893-896, 2005.
76. P.N. Crepeau, S.D. Antolovich and J.A. Worden, "Structure-Property Relationships in Aluminium Alloy 339-T5: Tensile Behavior at Room and Elevated Temperature", AFS Transactions, 98, 813-822, 1990.
77. J.A.Aniyi, F.L.Bello-Ochende and M.B. Adeyemi, Effect of pressure, die and stress-relief temperature on the residual stress and mechanical properties of squeeze-cast Aluminum rods, J. of Mat. Eng & Processing, 5, 399-404, 1996.

78. G. E.Dieter, Mechanical Metallurgy, SI Metric Edition, McGraw-Hill Book Company,Inc., 287, 1961.

79. J.M.Boileau, S.J.Weber, R.H.Salzman and J.E.Allison, The Porosity Size on the Tensile Properties of a Cast 319-T7 Aluminum Alloy, AFS Trans. 01-045, 419-32, 2001

APPENDICES

APPENDIX I

OPTICAL AND SEM IMAGES OF AS-CAST AND DIFFERENT THERMAL TREATMENTS

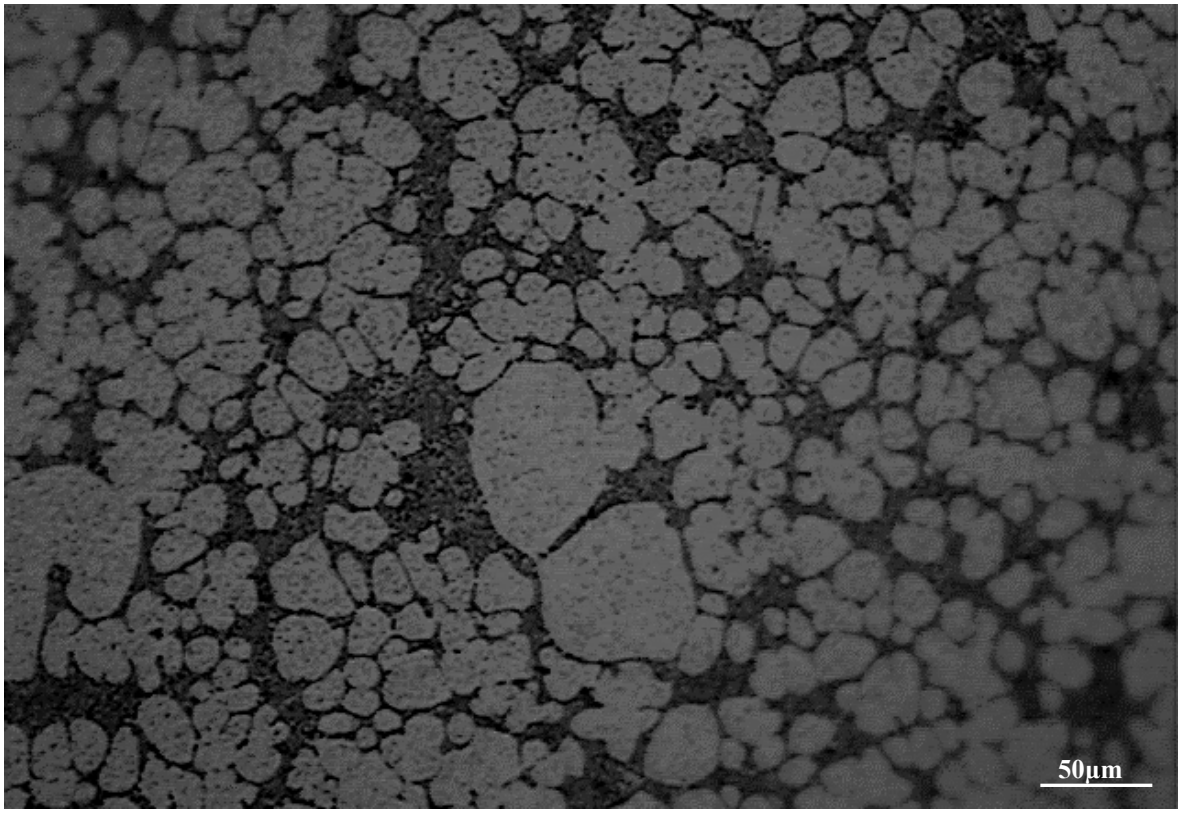

Figure Ap1.1 Optical image of as-cast sample

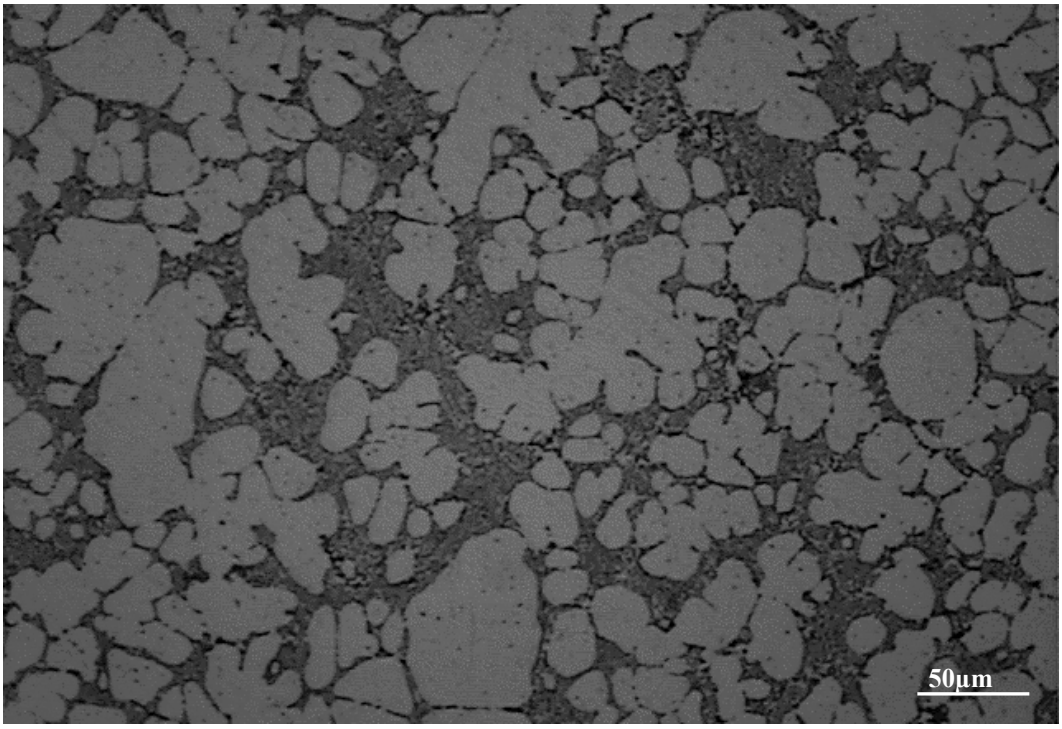

Figure Ap1.2 Optical image of 120˚C heat treated sample for 120 minutes.

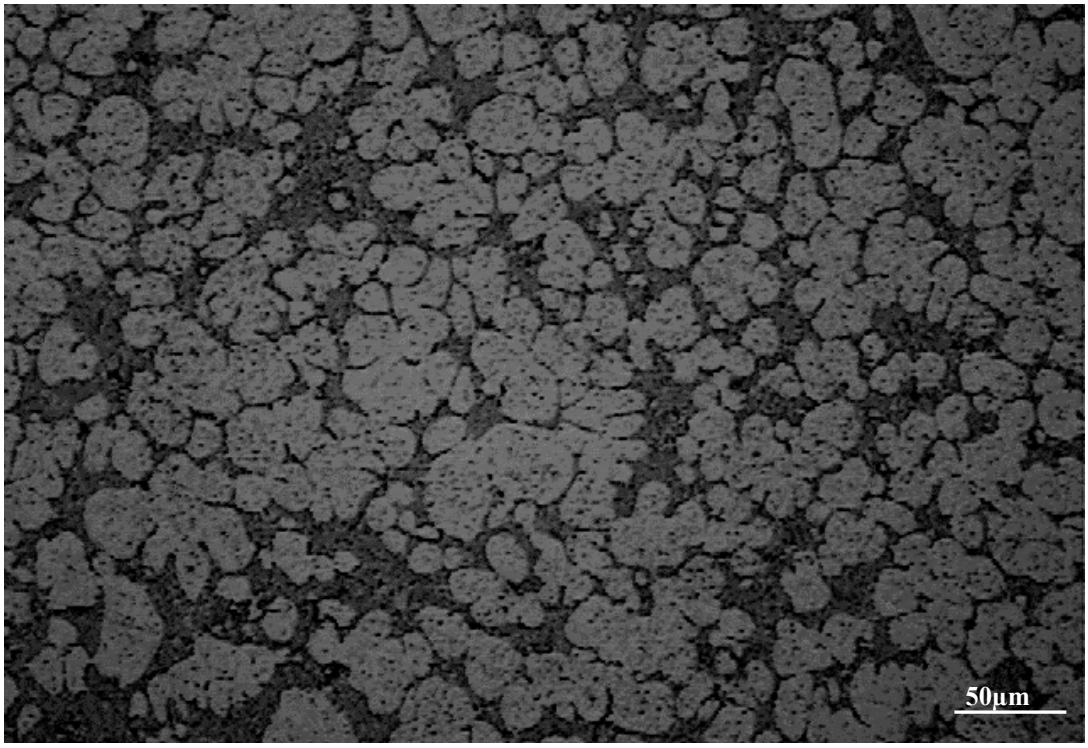

Figure Ap1.3 Optical image of 150˚C heat treated sample for 120 minutes.

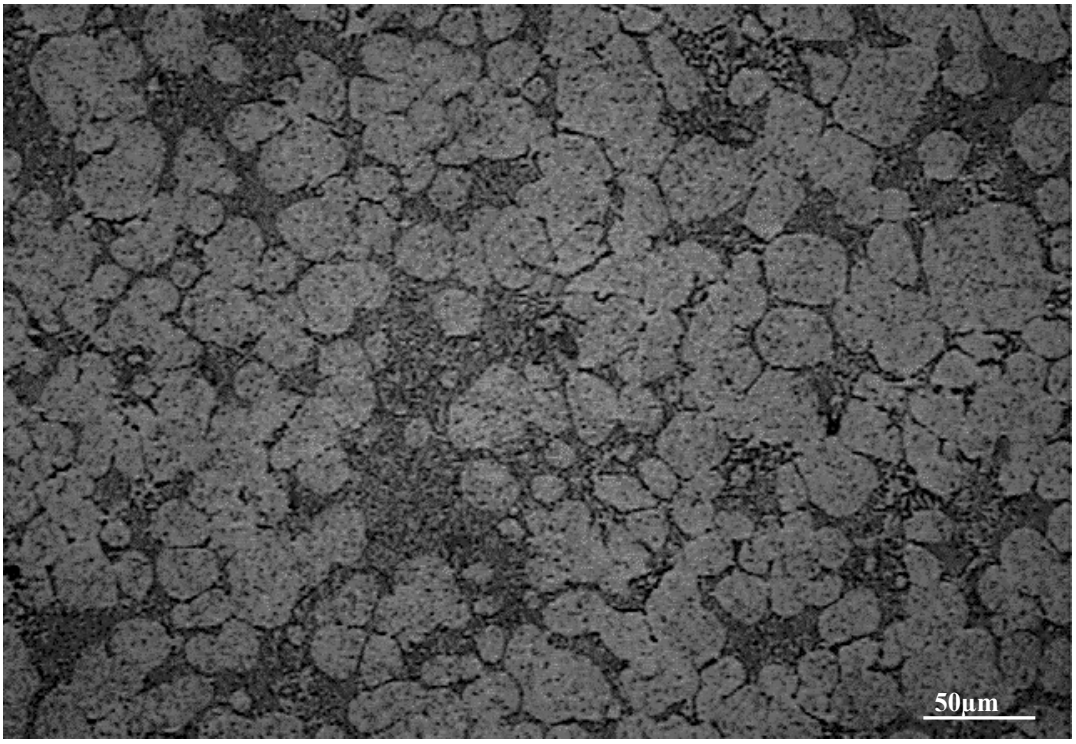

Figure Ap1.4 Optical image of 180˚C heat treated sample for 120 minutes.

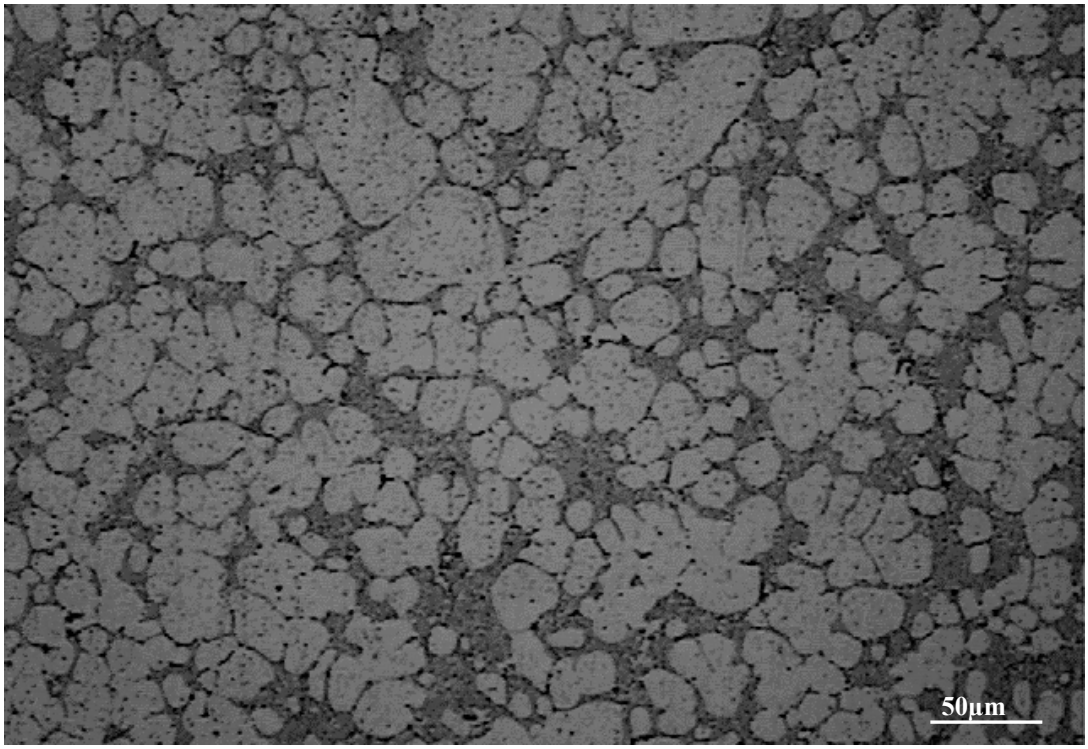

Figure Ap1.5 Optical image of 200˚C heat treated sample for 120 minutes.

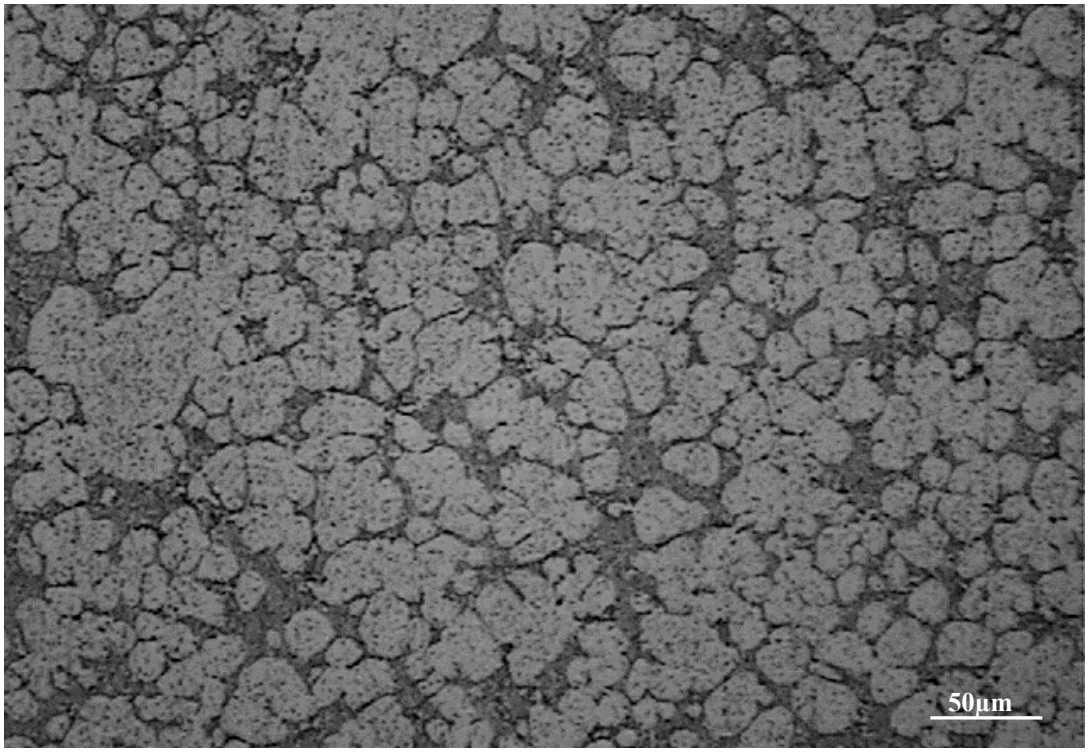

Figure Ap1.6 Optical image of 250˚C heat treated sample for 120 minutes.

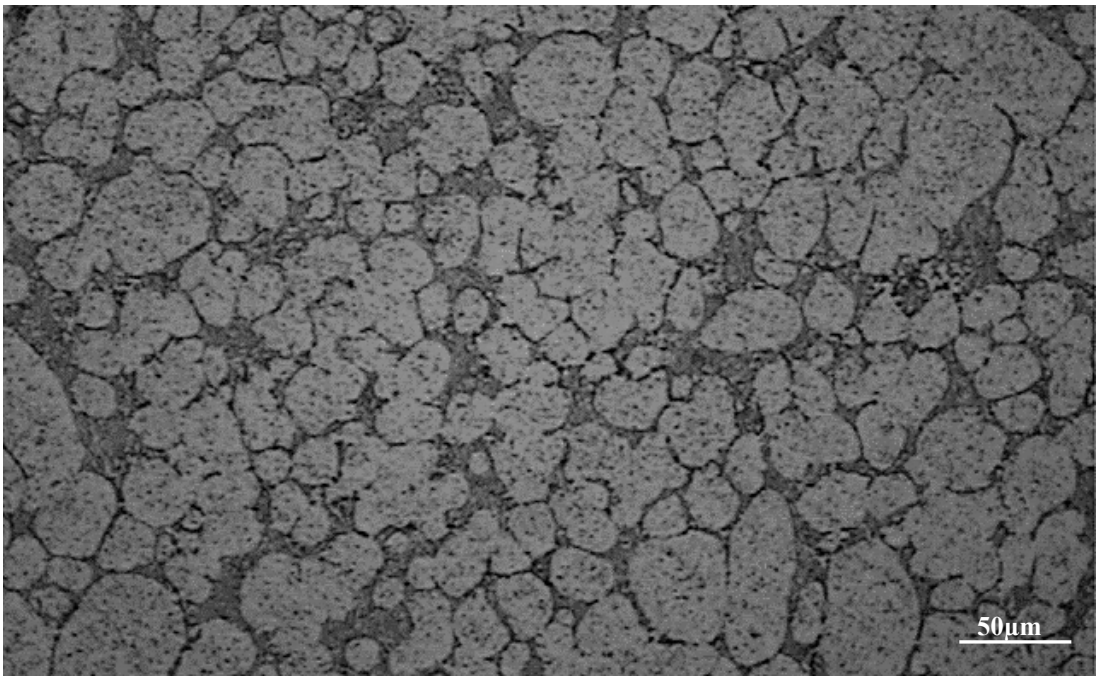

Figure Ap1.7 Optical image of 300˚C heat treated sample for 120 minutes.

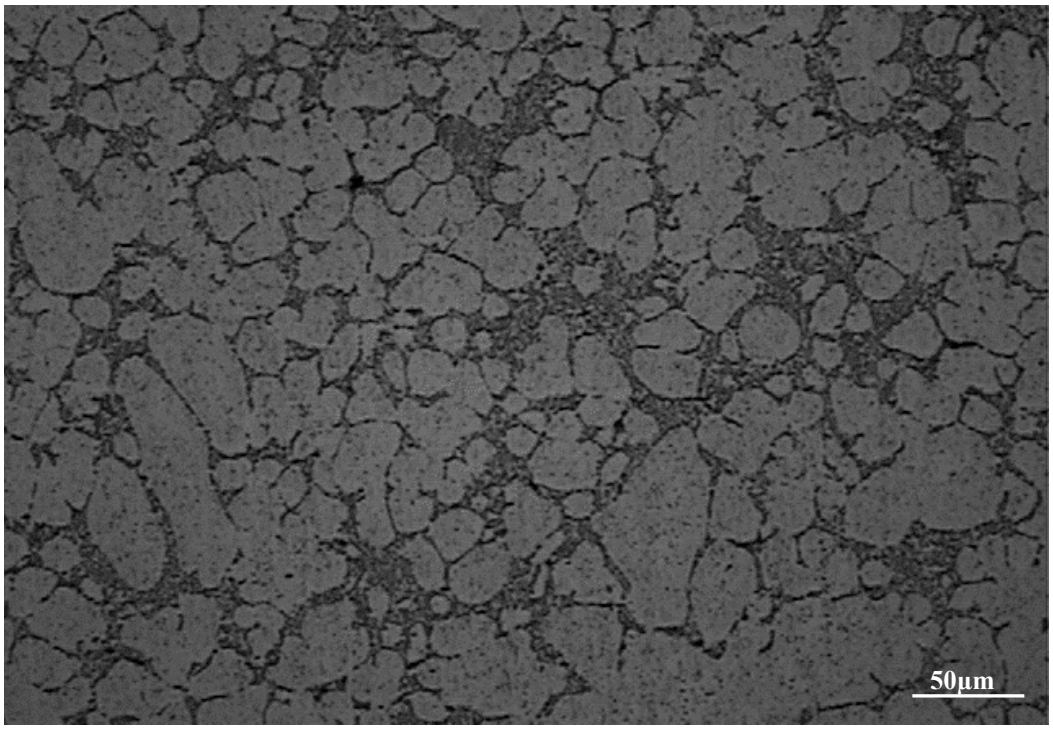

Figure Ap1.8 Optical image of 350˚C heat treated sample for 120 minutes.

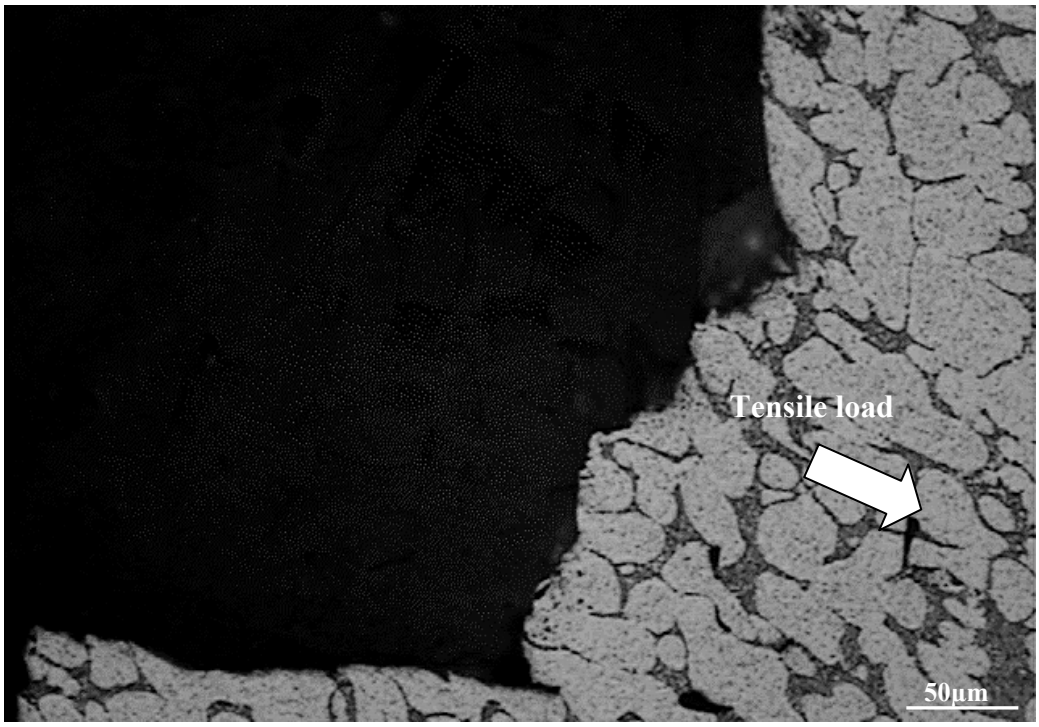

Figure Ap1.9 Optical Micrograph shows the longitudinal section of the fractured casting treated at 120˚C for 120 minutes.

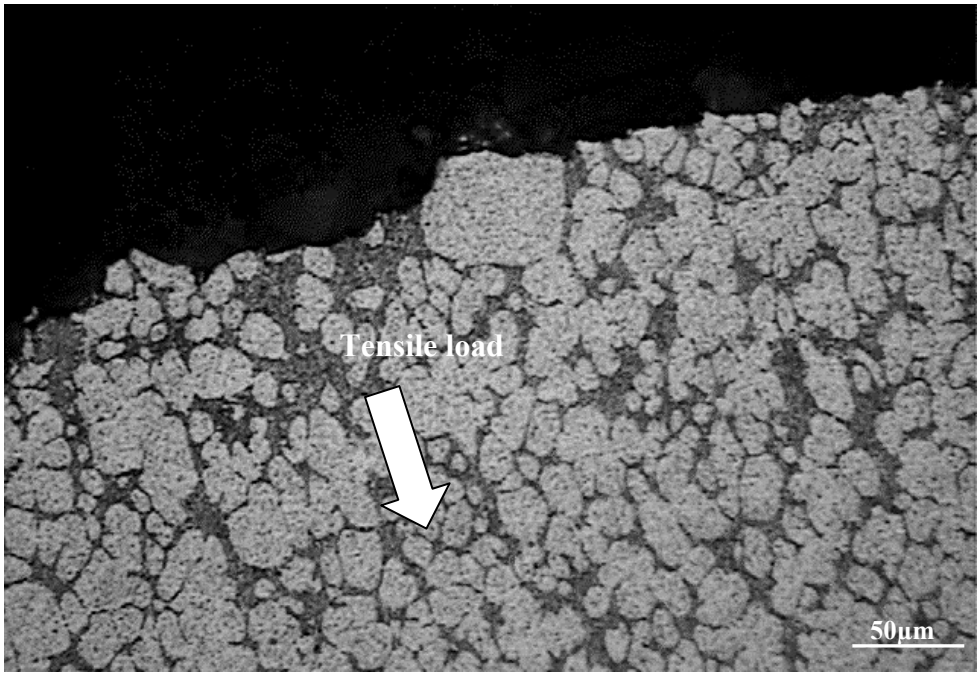

Figure Ap1.10 Optical Micrograph shows the longitudinal section of the fractured casting treated at 180˚C for 120 minutes.

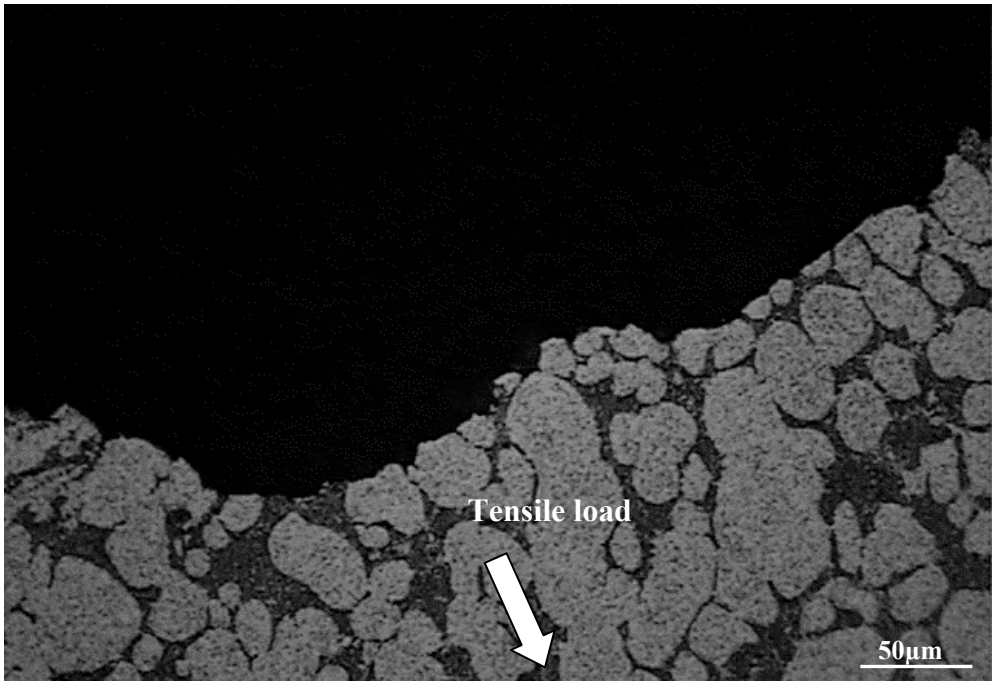

Figure Ap1.11 Optical Micrograph shows the longitudinal section of the fractured casting treated at 250˚C for 120 minutes.

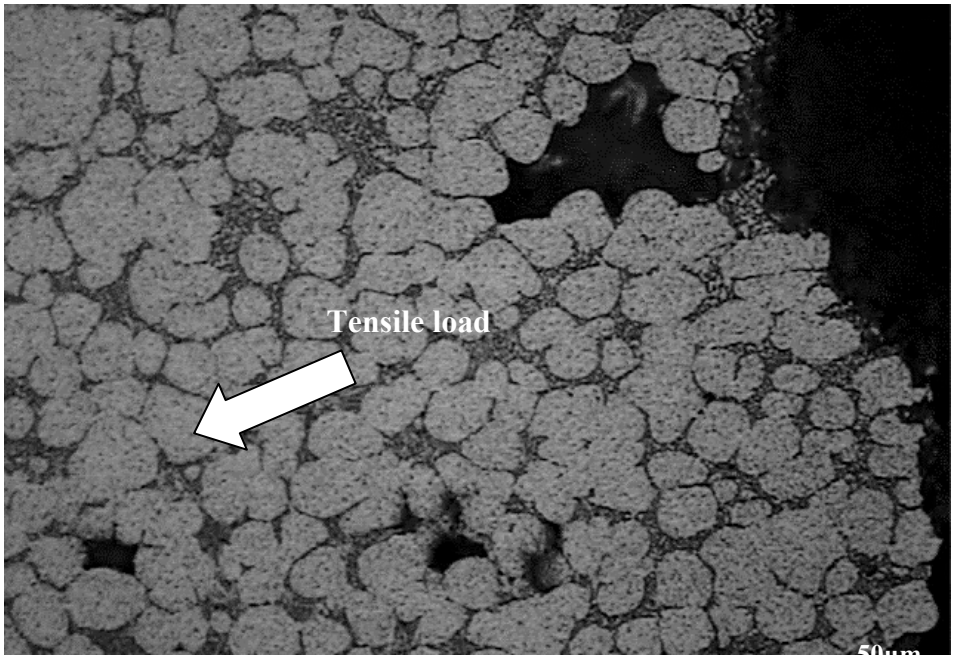

Figure Ap1.12 Optical Micrograph shows the longitudinal section of the fractured casting treated at 300˚C for 120 minutes.

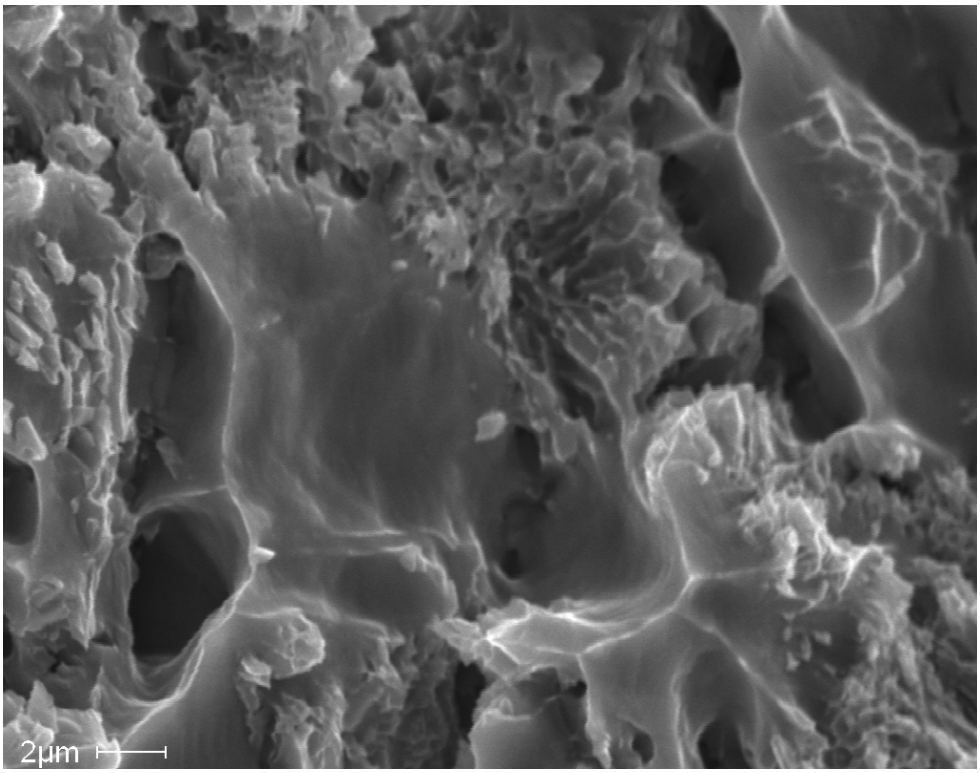

Figure Ap1.13 SEM micrograph showing the fracture surface of a sample heat treated at 120˚C for 120 minutes.

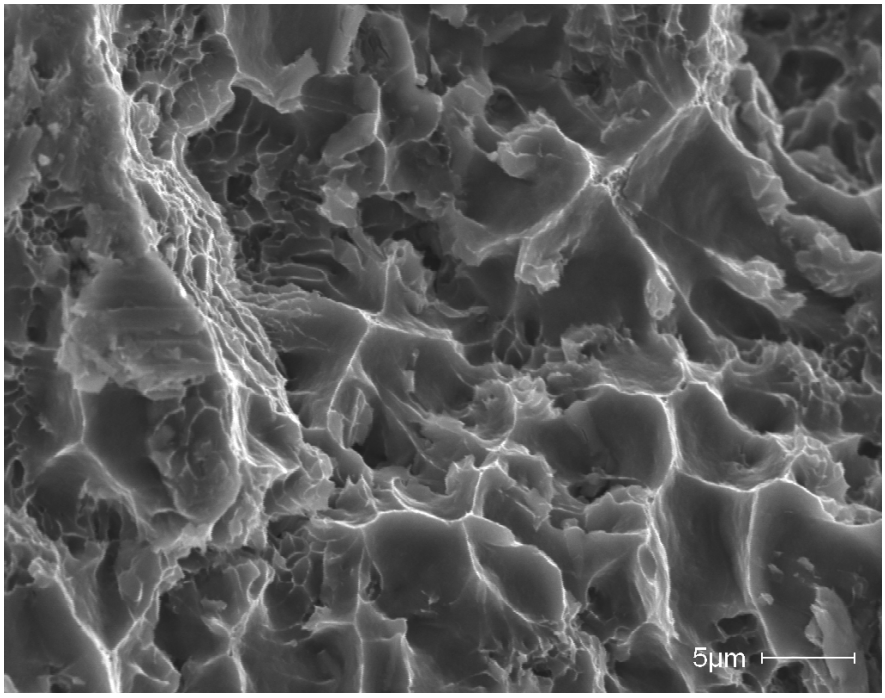

Figure Ap1.14 SEM micrograph showing the fracture surface of a sample heat treated at 250˚C for 120 minutes.

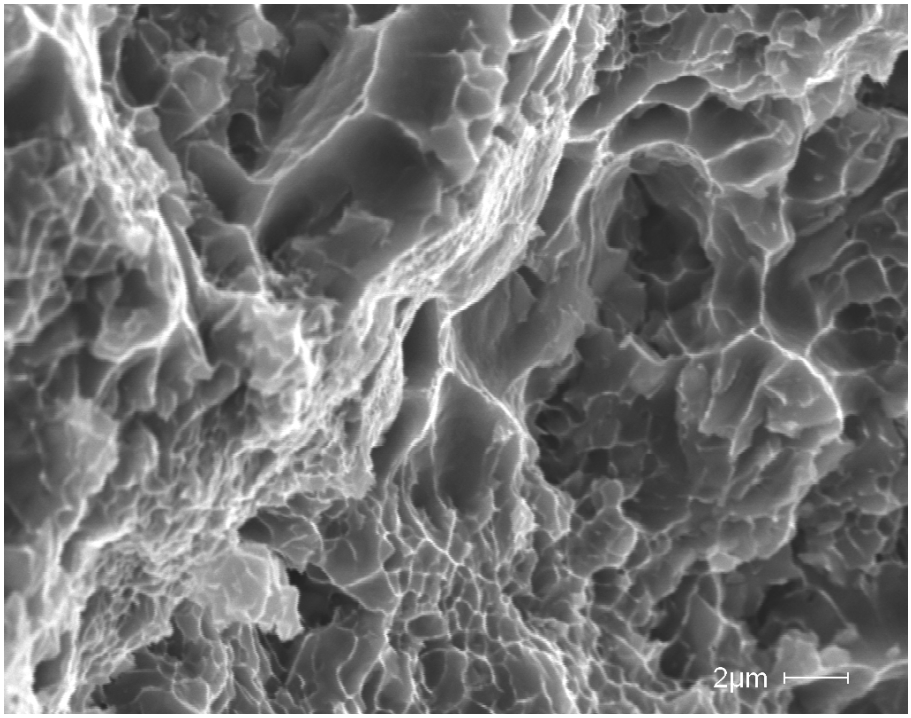

Figure Ap1.15 SEM micrograph showing the fracture surface of a sample heat treated at 300˚C for 120 minutes.

APPENDIX II

TENSILE CURVES FOR AS-CAST AND DIFFERENT THERMAL TREATMENTS

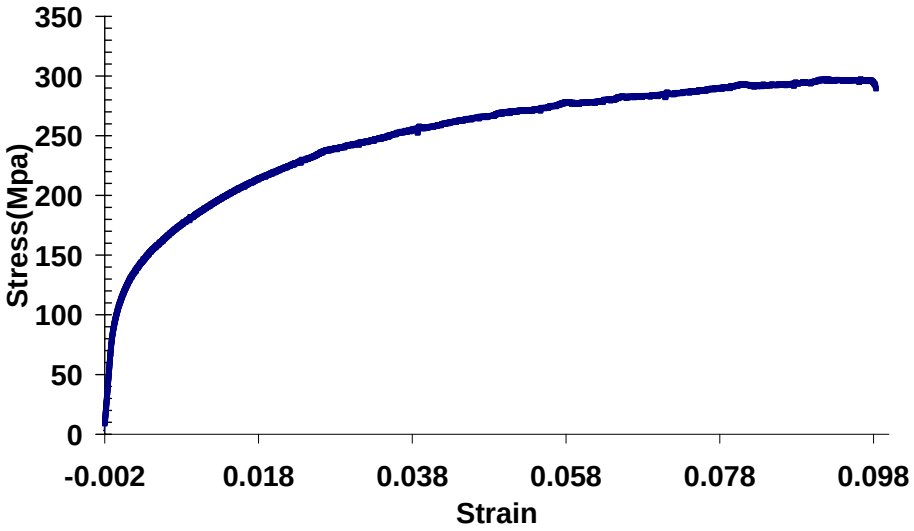

Figure Ap2.1 True stress-strain curve for the as-cast sample.

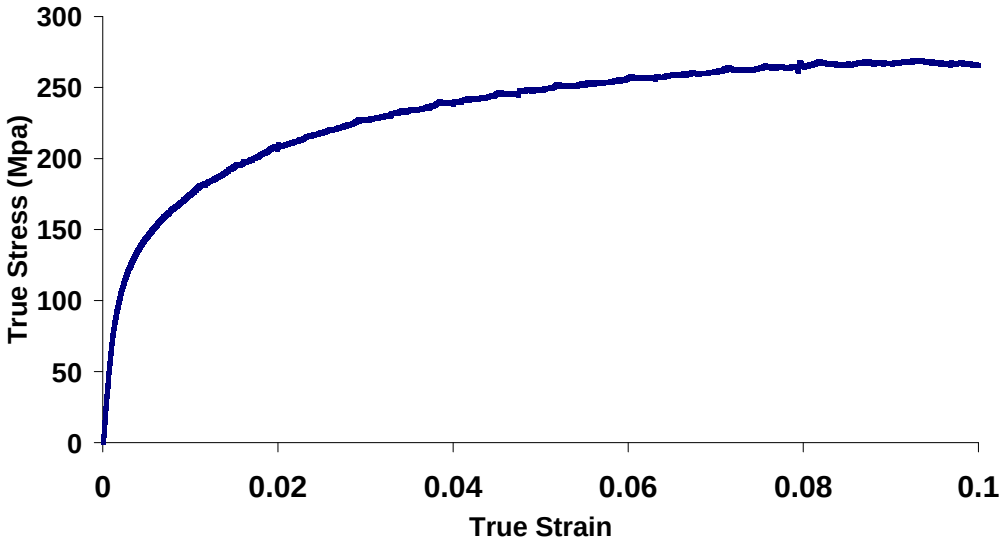

Figure Ap2.2 True stress-strain curve for a sample treated at 120˚C for 120 minutes.

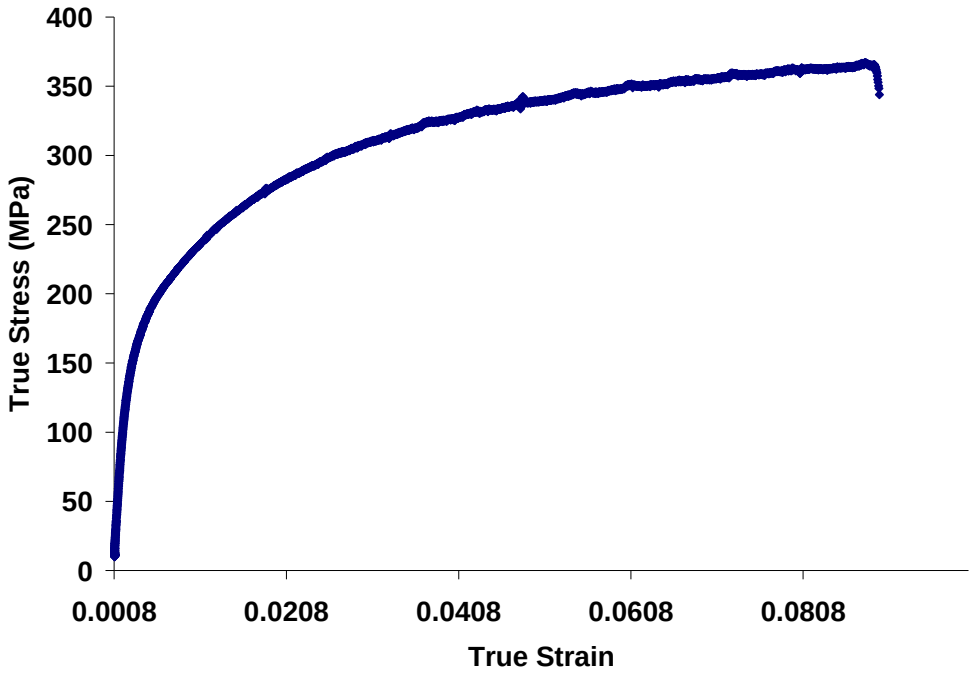

Figure Ap2.3 True stress-strain curve for a sample treated at 150˚C for 120 minutes.

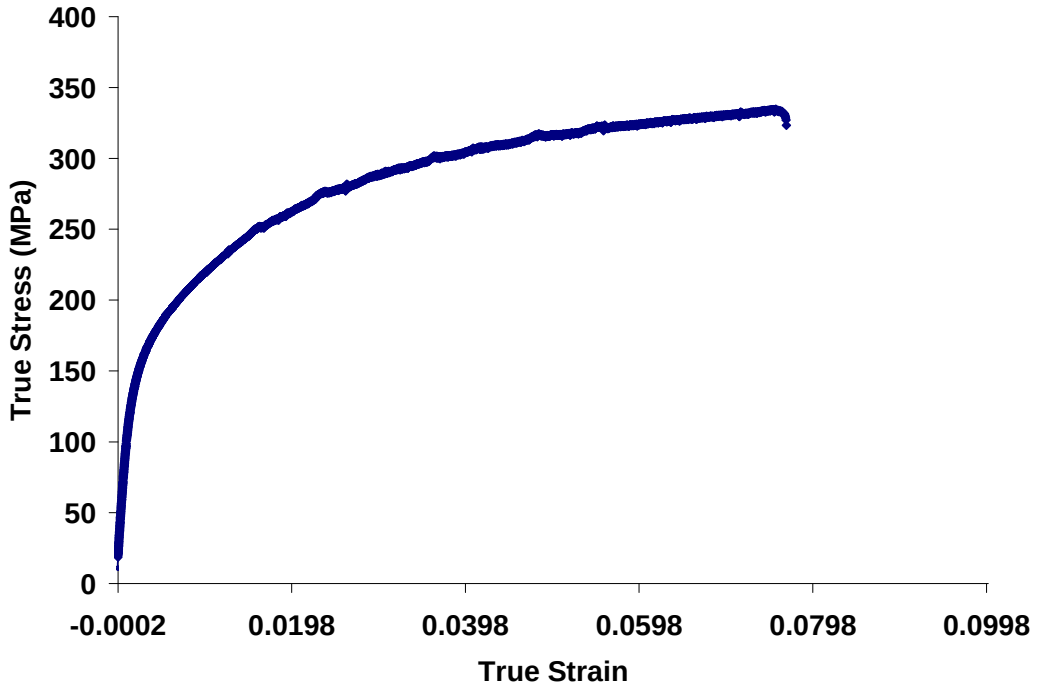

Figure Ap2.4 True stress-strain curve for a sample treated at 180˚C for 120 minutes.

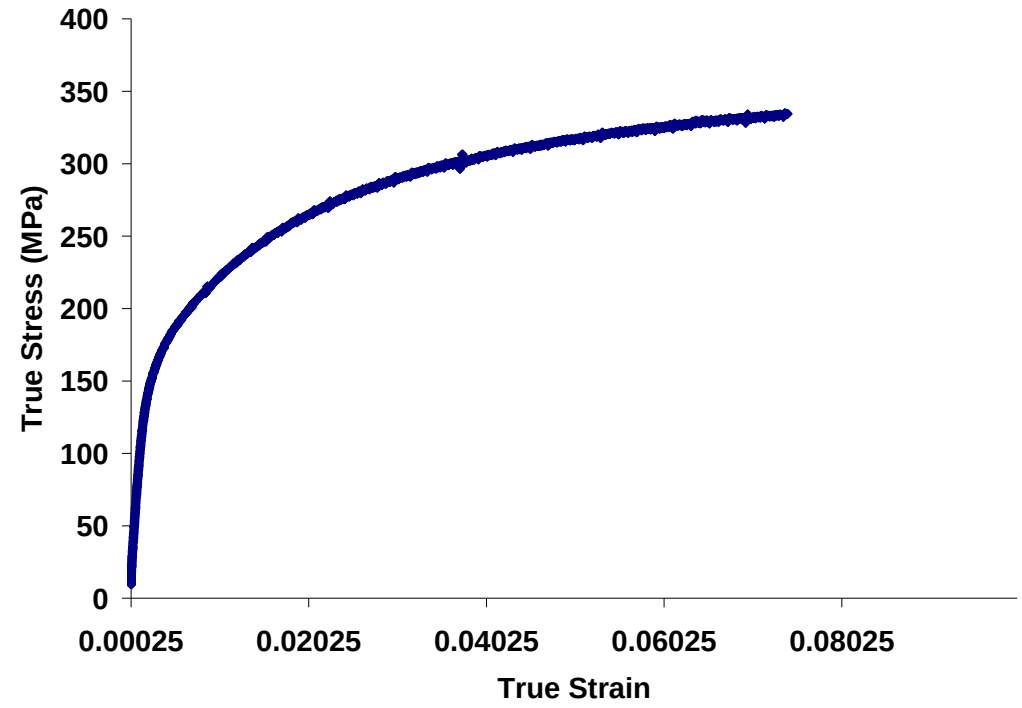

Figure Ap2.5 True stress-strain curve for a sample treated at 200˚C for 120 minutes.

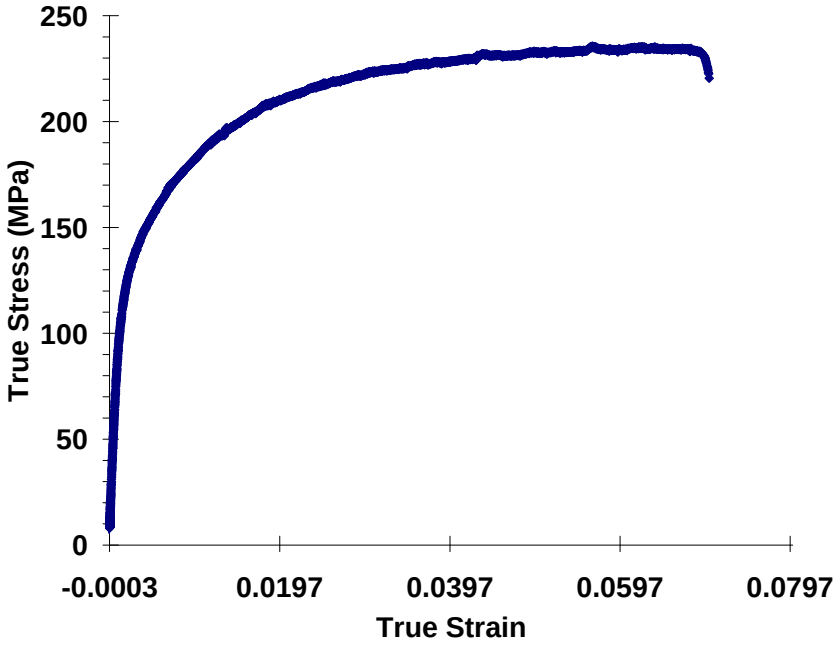

Figure Ap2.6 True stress-strain curve for a sample treated at 250˚C for 120 minutes.

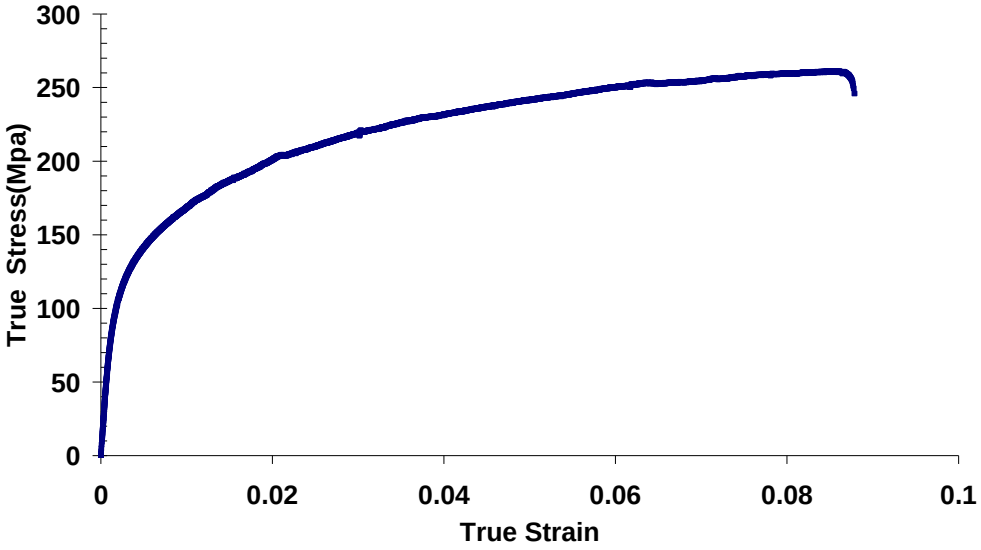

Figure Ap2.7 True stress-strain curve for a sample treated at 300˚C for 120 minutes.

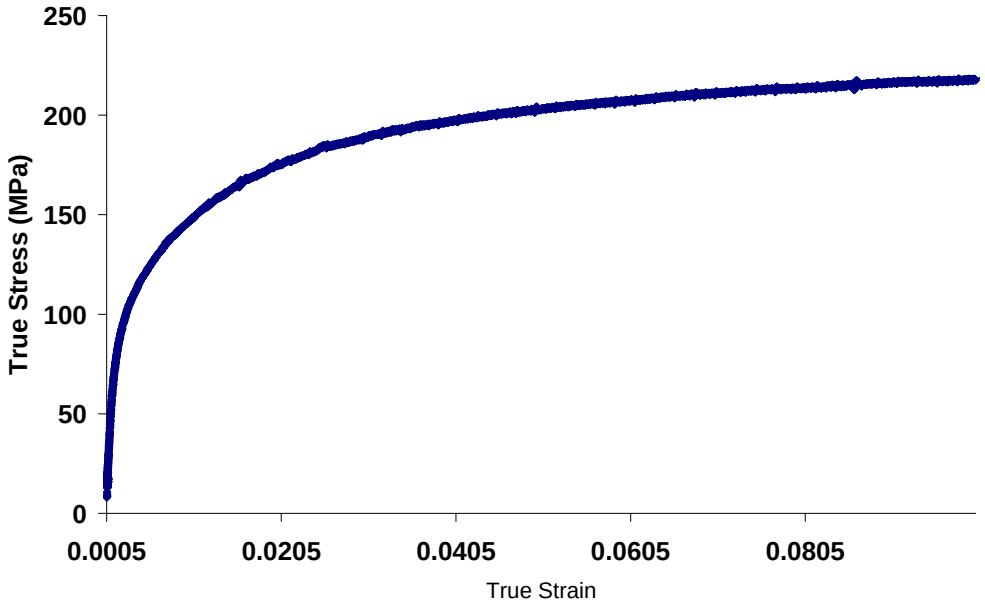

Figure Ap2.8 True stress-strain curve for a sample treated at 350˚C for 120 minutes.

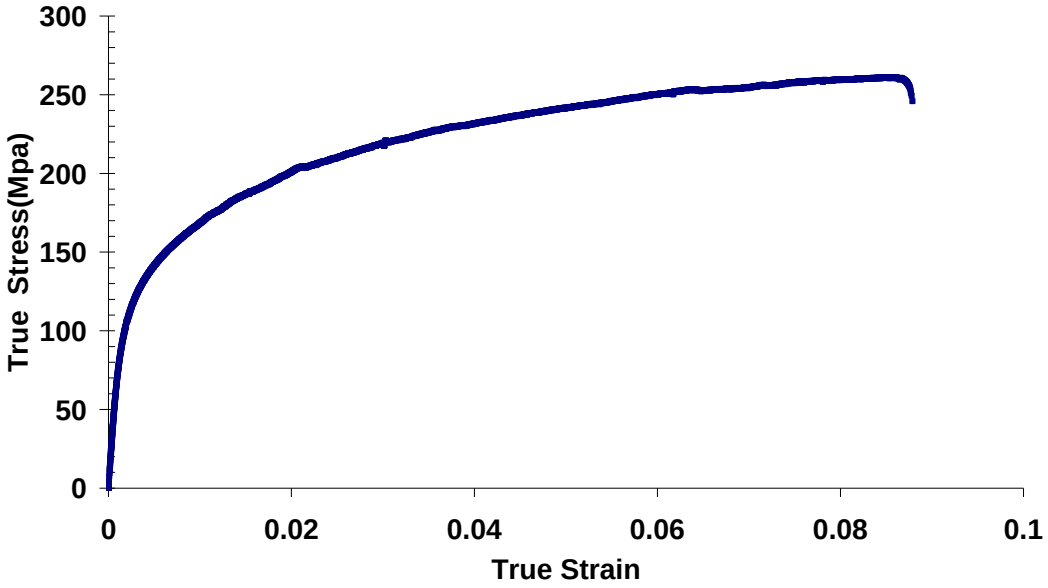

Figure Ap2.9 True stress-strain curve for a sample treated at 200˚C for 30 minutes.

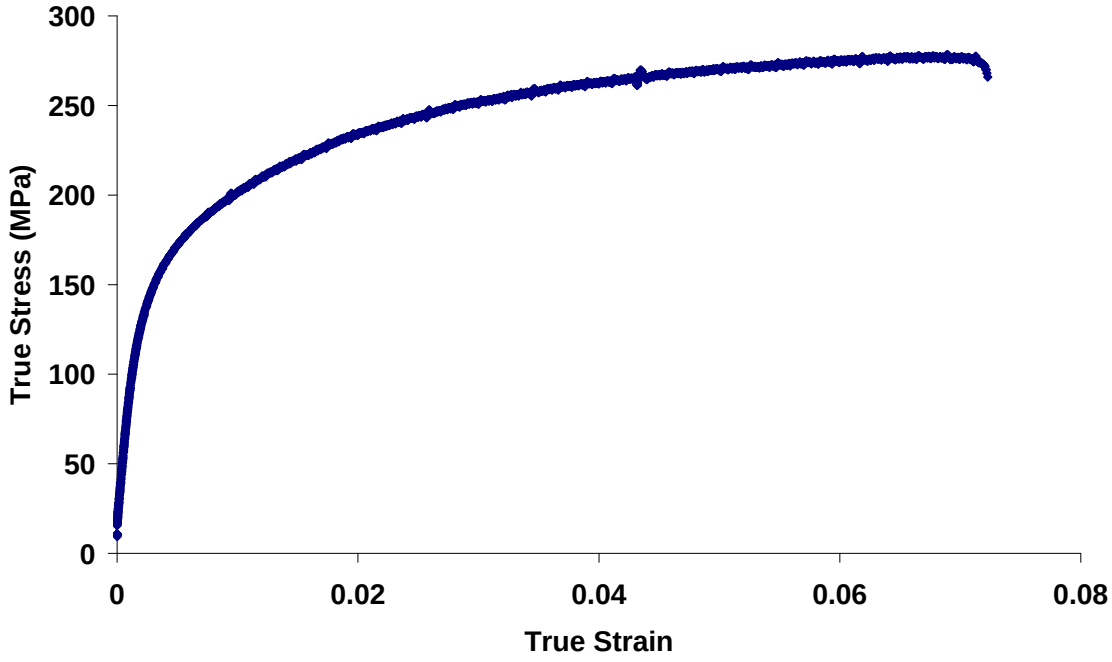

Figure Ap2.10 True stress-strain curve for a sample treated at 200˚C for 60 minutes.

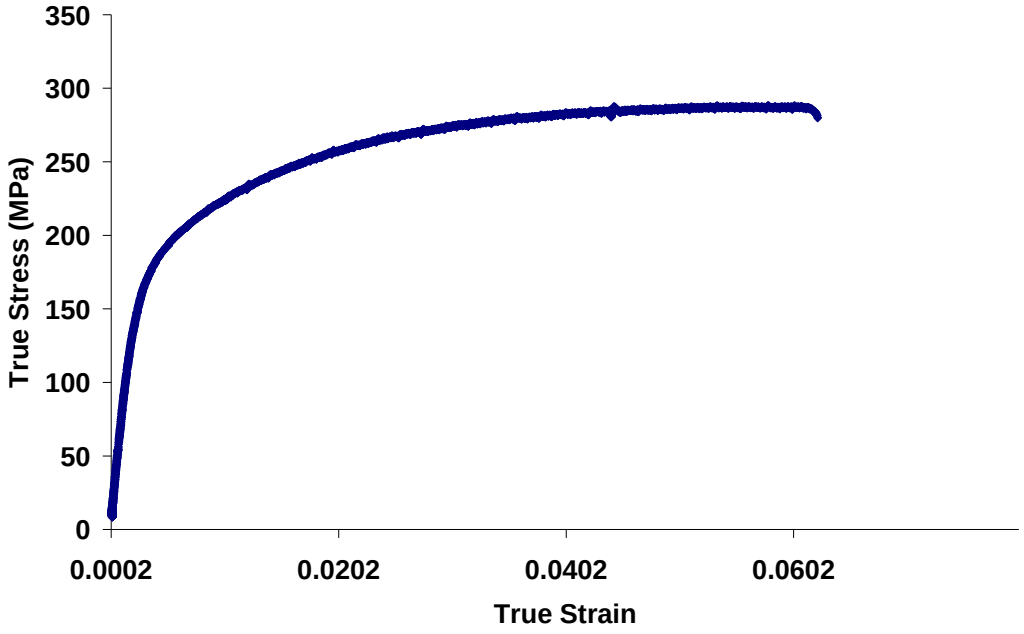

Figure Ap2.11 True stress-strain curve for a sample treated at 200˚C for 90 minutes.

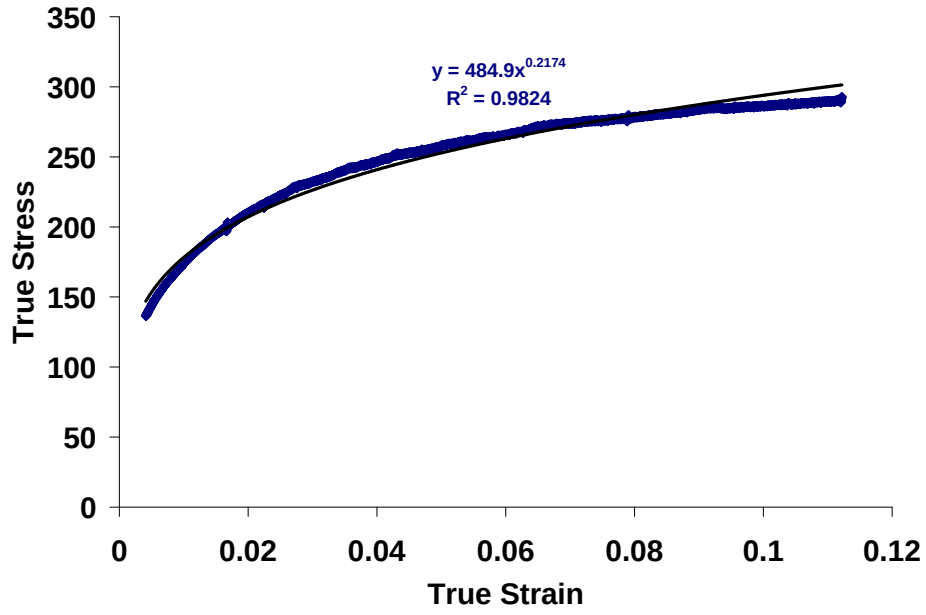

Figure Ap2.12 Power curve on plastic region at 120˚C for 120 minutes.

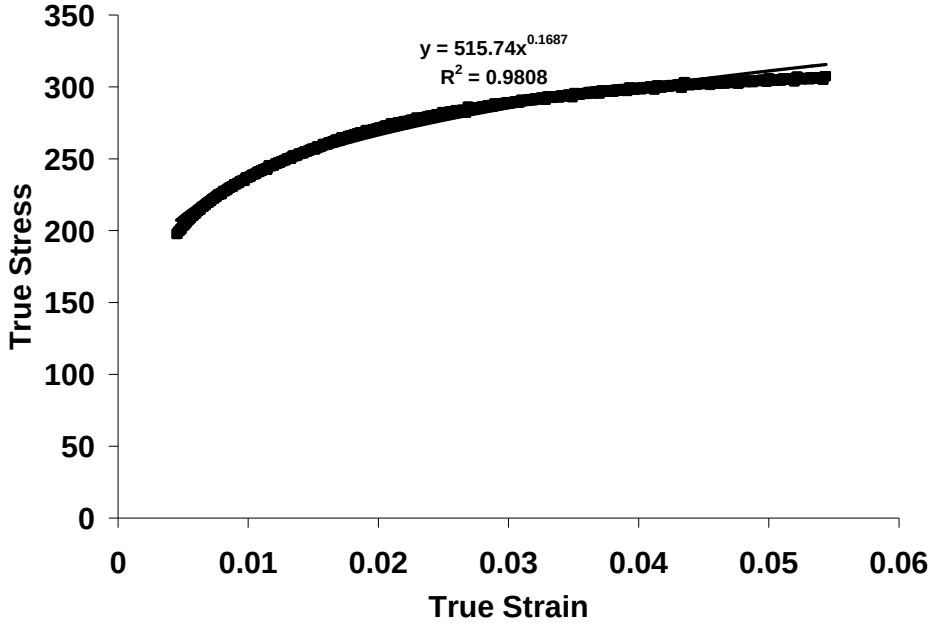

Figure Ap2.13 Power curve on plastic region at 180˚C for 120 minutes.

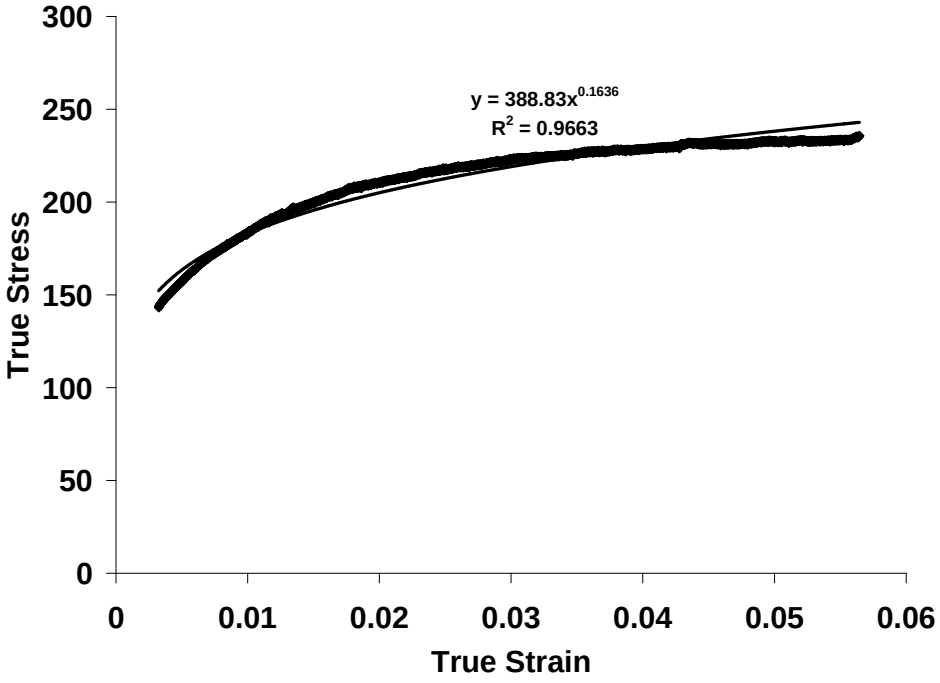

Figure Ap2.14 Power curve on plastic region at 250˚C for 120 minutes.

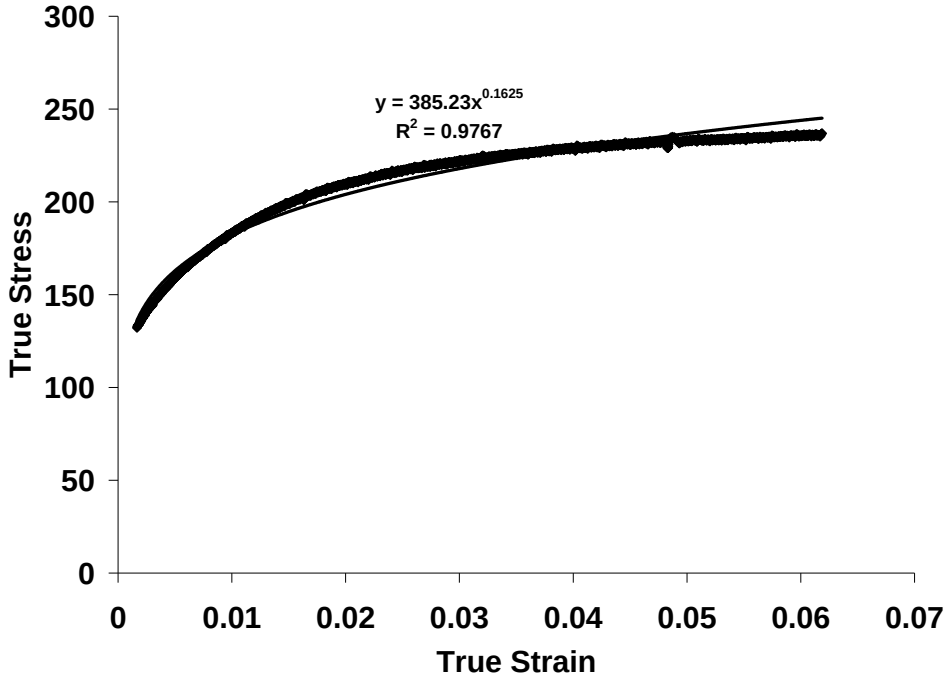

Figure Ap2.15 Power curve on plastic region at 300˚C for 120 minutes.

APPENDIX-III

TABLE OF DATA

Table Ap3.1 Sample specifications for as-cast condition

Condition	Name of the Specimen	Gauge Length (mm)	Average width (mm)	Average Thickness (mm)	Average cross-sectional Area (mm^2)
As Cast	A_4	28.42	6.19	1.89	11.6991
	B_1	27.94	6.1	1.89	11.529
	B_3	27.55	6.06	1.98	11.9988
	C_3	28.87	6.14	1.91	11.7274
	C_4	28.57	6.13	1.94	11.8922

Table Ap3.2 Sample specifications for 120˚C treatment (for 120 minutes)

Condition	Name of the Specimen	Gauge Length (mm)	Average width (mm)	Average Thickness (mm)	Average cross-sectional Area (mm^2)
120° C Heat Treated	A_2	28.76	6.17	1.95	12.0315
	B_2	27.94	6.25	1.83	11.4375
	C_2	28.20	6.44	1.73	11.1412

Table Ap3.3 Sample specifications for 180˚C treatment (for 120 minutes)

Condition	Sample Name	Gauge Length (mm)	Average width (mm)	Average Thickness (mm)	Average cross-sectional Area (mm^2)
180˚c Heat Treated	D_1	32.36	5.95	1.93	11.48
	D_1	32.38	5.88	1.90	11.17
	D_2	31.07	5.87	1.92	11.27
	D_3	28.61	5.95	1.92	11.47
	D_3	29.72	5.84	1.91	11.15
	F_4	28.99	6.02	1.90	11.43
	F_4	29.72	6.00	1.93	11.58

Table Ap3.4 Sample specifications for 200˚C treatment (for 120 minutes)

Condition	Sample Name	Gauge Length (mm)	Average width (mm)	Average Thickness (mm)	Average cross-sectional Area (mm^2)
200˚c Heat Treated	F_1	30.62	6.10	1.91	11.65
	F_1	31.12	5.98	1.93	11.54
	F_2	31.1	5.94	1.91	11.34
	F_3	28.66	5.95	1.96	11.66
	F_3	29.46	5.93	1.97	11.68
	G_4	29.6	5.85	1.92	11.23
	G_4	28.46	5.92	1.95	11.54

Table Ap3.5 Sample specifications for 250˚C treatment (for 120 minutes)

Condition	Sample Name	Gauge Length (mm)	Average width (mm)	Average Thickness (mm)	Average cross-sectional Area (mm^2)
250˚c Heat Treated	G_1	31.09	6.01	1.95	11.71
	G_1	29.61	5.95	1.91	11.36
	G_2	30.70	5.95	1.92	11.42
	G_3	28.12	5.88	1.91	11.23
	G_3	30.54	5.86	1.88	11.01
	D_4	28.23	5.86	1.91	11.92

Table Ap3.6 Sample specifications for 300˚C treatment (for 120 minutes)

Condition	Sample Name	Gauge Length (mm)	Average width (mm)	Average Thickness (mm)	Average cross-sectional Area (mm^2)
300c Heat Treated	H_1	31.46	5.92	1.95	11.54
	H_1´	31.75	5.84	1.96	11.44
	H_2	29.46	5.91	1.95	11.52
	H_3	28.87	5.95	1.89	11.24
	H_3´	28.86	5.92	1.87	11.07
	H_4	29.46	5.91	1.90	11.22

Table Ap3.7 Sample specifications for 350˚C treatment (for 120 minutes)

Condition	Name of the Specimen	Gauge Length (mm)	Average width (mm)	Average Thickness (mm)	Average Cross-Sectional Area (mm^2)
350° C Heat Treated	A_1	28.06	6.12	1.89	11.5668
	A_3	27.70	6.25	1.95	12.19
	B_4	28.01	6.08	1.94	11.7952
	C_1	28.97	6.01	1.97	11.8397

Table Ap3.8 Sample specifications for 350˚C treatment (for 120 minutes)

Condition	Name of the Specimen	Gauge Length (mm)	Average width (mm)	Average Thickness (mm)	Average Cross-Sectional Area (mm^2)
200° C Heat Treated (30 minutes)	P4	33.21	5.83	1.66	9.67
	D5	27.07	5.95	1.89	11.24
	G5	27.04	5.91	1.91	11.28
	H5	27.29	5.96	1.93	11.50
	H05	26.37	5.96	1.95	11.62

Table Ap3.9 Sample specifications for 200˚C (60 minutes)

Condition	Name of the Specimen	Gauge Length (mm)	Average width (mm)	Average Thickness (mm)	Average Cross-Sectional Area (mm^2)
200° C Heat Treated (60 minutes)	P4	35.25	6.07	1.92	11.65
	F5	27.24	5.94	1.94	11.52
	F05	26.94	5.96	1.94	11.56
	G5	28.75	5.98	1.95	11.66

Table Ap3.10 Sample specifications for 200˚C (90 minutes)

Condition	Name of the Specimen	Gauge Length (mm)	Average width (mm)	Average Thickness (mm)	Average Cross-Sectional Area (mm^2)
200° C Heat Treated (90minutes)	I1	28.99	6.34	1.86	11.79
	J1	27.51	6.41	1.92	12.30
	J4	27.52	6.14	1.86	11.42
	P4	33.46	6.13	1.87	11.46
	D5	26.3	5.91	1.95	11.52

Table Ap3.11 Tensile properties in the as-cast samples

Treatment	Sample Name	Yield Strength (Mpa)	UTS (Mpa)	Elongation %
As Cast	A4	135.5	263.00	11.51
	B1	150.58	271.51	11.15
	B3	128.3	264.10	11.61
	C3	142.12	259.85	11.43
	C4	131.83	239.91	8.6

Table Ap3.12 Tensile properties in the samples heat treated at 120˚C for 120 minutes

Treatment	Sample Name	Yield Strength (Mpa)	UTS (Mpa)	Elongation %
120° C Heat Treated	A2	135.50	261.86	11.4
	B2	132.56	247.03	10.2
	C2	136.60	249.02	9.45

Table Ap3.13 Tensile properties in the samples heat treated at 180˚C for 120 minutes

Treatment	Sample Name	Yield Strength (Mpa)	UTS (Mpa)	Elongation %
180° C Heat Treated	D_1	197.0	304.47	7.07
	D_1	187.16	242.19	3.66
	D_2	182.5	276.01	6.87
	D_3	183.5	196.88	3.61
	D_3	164	170.44	3.46
	F_4	197.5	307.4	8.14

Table Ap3.14 Tensile properties in the samples heat treated at 200˚C for 120 minutes

Treatment	Sample Name	Yield Strength (Mpa)	UTS (Mpa)	Elongation %
200° C Heat Treated	F_{i1}	181.5	225.92	4.45
	F_1	198.5	289.19	5.81
	F_2	187	280.96	7.21
	F_{i3}	183	225.53	4.61
	F_3	193.5	288.76	7.01
	G_{i4}	201	294.23	7.03
	G_4	190	283.75	6.83

Table Ap3.15 Tensile properties in the samples heat treated at 250˚C for 120 minutes

Treatment	Sample Name	Yield Strength (Mpa)	UTS (Mpa)	Elongation %
250° C Heat Treated	G_{i1}	160	253.5	6.71
	G_1	151.5	204.58	3.45
	G_2	143.5	235.7	8.76
	G_{i3}	158.5	205.57	4.81
	G_3	172.5	263.15	7.64
	D_4	158.5	212.82	2.12

Table Ap3.16 Tensile properties in the samples heat treated at 300˚C for 120 minutes

Treatment	Sample Name	Yield Strength (Mpa)	UTS (Mpa)	Elongation %
300° C Heat Treated	H_{i1}	150.4	223.53	8.4
	H_1	154.5	132.31	2.56
	H03	152.7	135.1031	8.2
	H_4	146.2	236.91	9.55

Table Ap3.17 Tensile properties in the samples heat treated at 350˚C for 120 minutes

Treatment	Sample Name	Yield Strength (Mpa)	UTS (Mpa)	Elongation %
350° C Heat Treated	A1	127.53	209.64	10.5
	A3	114.24	213.8	9.7
	B4	117.6	221.23	10.01
	C1	95.74	161.78	5.3

Table Ap3.18 Tensile properties in the samples heat treated at 200˚C for 30 minutes

Treatment	Sample Name	Yield Strength (Mpa)	UTS (Mpa)	Elongation %
200° C Heat Treated (30minutes)	D5	160.2	277.35	9.67
	G5	163.4	242.59	8.72
	H5	157.3	271.80	9.83
	H05	161.6	255.9	9.54

Table Ap3.19 Tensile properties in the samples heat treated at 200˚C for 60 minutes

Treatment	Sample Name	Yield Strength (Mpa)	UTS (Mpa)	Elongation %
200° C Heat Treated (60minutes)	F5	162.4	264.93	8.3
	F05	163.1	261.7782	7.1
	G5	170.3	264.6631	7.4
	P4	180.5	275.008	8.2

Table Ap3.20 Tensile properties in the samples heat treated at 200˚C for 90 minutes

Treatment	Sample Name	Yield Strength (Mpa)	UTS (Mpa)	Elongation %
200° C Heat Treated (90minutes)	I1	203.13	300.0751	4.9
	J1	194.2	293.932	6.78
	J4	195.61	286.873	7.46
	P4	193.34	276.518	7.34
	D5	187.12	278.6796	3.6

VITA AUCTORIS

NAME: KAZI FOYEZ AHMMED

COUNTRY OF BIRTH: BANGLADESH

DATE OF BIRTH: 1982

EDUCATION: Bangladesh University of Engineering and Technology,
Dhaka, Bangladesh
Department of Materials and Metallurgical Engineering
2000-2006, B.Sc.
University of Windsor, Windsor, On
Department of Mechanical, Automotive and Materials
Engineering
2008-2009, M.Sc.